Fisheries New Zealand
Tini a Tangaroa

Underwater sound propagation modelling to illustrate potential noise exposure to Maui dolphins from seismic surveys and vessel traffic on West Coast North Island, New Zealand.

New Zealand Aquatic Environment and Biodiversity Report No. 217

C. McPherson
Z. Li
J. Quijano

ISSN 1179-6480 (online)
ISBN 978-0-9951257-9-7 (online)

June 2019

New Zealand Government

Requests for further copies should be directed to:

Publications Logistics Officer
Ministry for Primary Industries
PO Box 2526
WELLINGTON 6140

Email: brand@mpi.govt.nz
Telephone: 0800 00 83 33
Facsimile: 04-894 0300

This publication is also available on the Ministry for Primary Industries websites at:
http://www.mpi.govt.nz/news-and-resources/publications
http://fs.fish.govt.nz go to Document library/Research reports

TABLE OF CONTENTS

1. EXECUTIVE SUMMARY

McPherson, C.; Zizheng, L.; Quijano, J. (2019). Underwater sound propagation modelling to illustrate potential noise exposure to Maui dolphins from seismic surveys and vessel traffic on West Coast North Island, New Zealand.

***New Zealand Aquatic Environment and Biodiversity Report No. 217*. 62 p.**

The purpose of this study was to provide an indicative assessment of vessel traffic and seismic survey related noise off the West Coast North Island (WCNI) of New Zealand. The study considered an area of interest of 267 540 km^2 (343 km × 780 km), divided into 3 km grid squares, off the West Coast North Island of New Zealand. Information was extracted from a high-resolution Automated Identification System (AIS) dataset for the year of July 2014 to June 2015 within this area of interest. Fifteen vessel categories were defined: Bulker, Containership, Tug, Tanker, Vehicle Carrier, Fishing, Cruise, Ferry, and Government/Research (including seismic survey vessels), Naval, Passenger (<100 m), High-speed craft, Recreational, and Floating Production Storage and Offloading (FPSO) facility, Jackup platform and Other. For each category, the vessel density and speed were mapped for the full year, i.e., summer (November – April) and winter (May – October).

Vessel traffic noise was assessed using acoustic modelling for each of two representative months for each season, March (summer) and July (winter). JASCO's cumulative vessel noise model was used to model the sound from vessels, FPSOs, and two marine seismic surveys within the area of interest. The two seismic surveys considered were both within 100 km of the WCNI: the TGS Northwest Frontier Multiclient 2-D Marine Seismic Survey (MSS) (4400 in3 array) and the Todd Energy Trestles 3 D MSS (3460 in3 array). The study applied a realistic lower bound for sound levels to provide context for vessel and seismic survey noise contributions, referred to as the baseline quiet noise level. The comparison of modelling predictions to this baseline quiet noise level allows identification of periods when the ambient noise would be driven by non-anthropogenic sources, such as natural (wind and waves) and biological sources.

The noise model was used to create maps of the Sound Pressure Level (SPL) in 1-minute time steps and one-month equivalent continuous underwater noise levels (L_{eq}), accounting for potential baseline quiet noise levels. These maps were created for both unweighted and frequency-weighted sound levels to account for the hearing capability of Maui dolphins, which were classified as high-frequency cetaceans according to the classification adopted by NOAA (NMFS 2018). The modelled sound fields were sampled at 14 receiver locations in the regions of Kaipara, Manakau, Kawhia, New Plymouth, Cape Egmont and the South Taranaki Bight, ranging from 2 to 50 nautical miles (nmi) from shore—within or near to predicted Maui dolphin habitat. The sound levels at these locations are presented as plots of unweighted and high-frequency weighted received sound levels over each month.

The study demonstrates that traffic density north of the Taranaki region is relatively low within 12 nmi of the coast, while higher densities occur in the Taranaki and South Taranaki Bight regions. Fishing vessels exhibit a strong seasonal pattern of operations; however, most of the commercial shipping has a density that is consistent between seasons.

The propagation conditions in winter support lower rates of attenuation and increased propagation ranges and thus noise sources have a larger area of influence. The median sound levels at the receiver locations north of the Taranaki region are the same in both March and July. This indicates that the TGS MSS, which was typically at greater distances from the coast and had sparsely spaced lines, only had a limited influence on the sound fields. Localised vessel traffic had a greater influence; however, such occurrences were short in duration and distributed in time. At least 75 percent of the time, the sound levels at Kaipara, Manakau and Kawhia are predicted to be driven by either non-anthropogenic sources

such as natural (wind and waves) and biological sources, or anthropogenic sources not included in the modelling study.

The receivers located at Cape Egmont (2 nmi from shore), and in the South Taranaki Bight (12 and 50 nmi from shore) have noise floors above the baseline quiet noise level applied in this study due to the proximity of infrastructure such as Floating Production Storage and Offloading facilities (FPSOs) and jackup platforms. The high-frequency weighted median sound levels are higher at all receiver locations from Taranaki to the South Taranaki Bight in winter, which is likely to be due to the propagation conditions.

Out of the 14 receiver locations considered, the two at New Plymouth and one at Cape Egmont experience the greatest number of proximal vessels. This is apparent both in the density maps and in the time dependent receiver lots. Due to both the higher levels of shipping traffic, and the proximity of existing infrastructure, the predicted sound levels at these three locations are always greater than the baseline quiet noise level considered in the study.

The results from the study are representative of sound levels and anthropogenic activity relevant to the area of the West Coast of the North Island potentially occupied by Maui dolphins for the period July 2014 to June 2015. These results are likely to be representative of other periods with similar levels of activity from similar vessels and seismic survey sources in similar locations. The study did not consider any seismic survey activity within the West Coast North Island Marine Mammal Sanctuary, with the closest modelled impulses being approximately 12 km away near Manakau, and 14 km away near Cape Egmont. The closest distance to receivers from the two seismic surveys considered was 12.7 km (Manakau 20 nmi from shore) and 10 km (Cape Egmont, 2 nmi from shore).

Future work that could realistically be conducted could consider the influence of small vessel traffic, particularly in nearshore environments and the influence of construction activities such as pile driving. The modelling study could also be conducted for a region and across a period for which long-term acoustic recordings and weather observations from marine meteorological stations are available, which would both assist the estimation of baseline noise levels. This would also allow the monitoring study results to be used to benchmark the modelling results for the contribution of anthropogenic sources to the ambient environment (e.g. MacGillivray et al. 2014a, MacGillivray et al. 2014c, MacGillivray et al. 2018b).

The implementation of an appropriate long-term noise monitoring study would also be able to quantify the temporal presence of Maui dolphins along with their abundance. An assessment of the perception of anthropogenic sound in the region by Maui or Hector's dolphin for consideration of potential impacts such as masking (Erbe et al. 2016) would benefit from further information about the hearing capabilities of the dolphins.

2. INTRODUCTION

The project achieved the following Research Objectives:

1. Characterise seasonal (summer and winter) density of vessels using AIS and oil and gas seismic survey locations in 2014–15 within 100 km of the area of the West Coast of the North Island potentially occupied by Maui dolphins.
2. Produce time-averaged sound footprints for all vessel traffic and marine seismic surveys at a resolution of 3 km grid squares for two one-month periods (March and July), presenting the results as both unweighted and frequency-weighted sound levels to account for the hearing capability of Maui dolphins.
3. Estimate sound levels at defined receiver points corresponding with locations potentially occupied by Maui dolphins, at a frequency band relevant to this species, for the two one-month periods.

3. METHODS

3.1 STUDY AREA AND RECEIVER LOCATIONS

The study area of interest (Figure 1) has an area of 267 540 km^2 (343 km × 780 km) and encompasses an area larger than that defined by Research Objective 1, which only required consideration of areas within 100 km of the West Coast of the North Island. To consider the presence of vessels within the study area, vessel density and speed information was obtained for multiple commercial, government, and recreational vessel categories in the New Zealand Exclusive Economic Zone, derived from a high-resolution Automated Identification System (AIS) dataset for the year July 2014 to June 2015. The AIS dataset contains time-stamped information on vessel type, speed, and location, from which vessel track information was inferred (Appendix D). Each vessel category was considered separately, and the spatio-temporal vessel information was used to create gridded maps of vessel density and speed for three periods: summer, winter and the full year.

Two seismic surveys occurred within 100 km of the West Coast during the study period and were included in this study; the TGS Northwest Frontier Multiclient 2-D Marine Seismic Survey (MSS) (4400 in^3 seismic airgun array) and the Todd Energy Trestles 3 D MSS (3460 in^3 seismic airgun array).

Noise modelling was conducted in the study area highlighted in Figure 1. Modelling sound field sampling locations, or receivers, were positioned offshore from Kaipara, Manakau, Kawhia, New Plymouth, Cape Egmont and in the South Taranaki Bight (STB) (Table 1). A number of receivers were positioned close to the boundary of the West Coast North Island Marine Mammal Sanctuary, including at New Plymouth 2 and 12 nmi from shore, Manakau 12 nmi and Kaipara 12 nmi from shore.

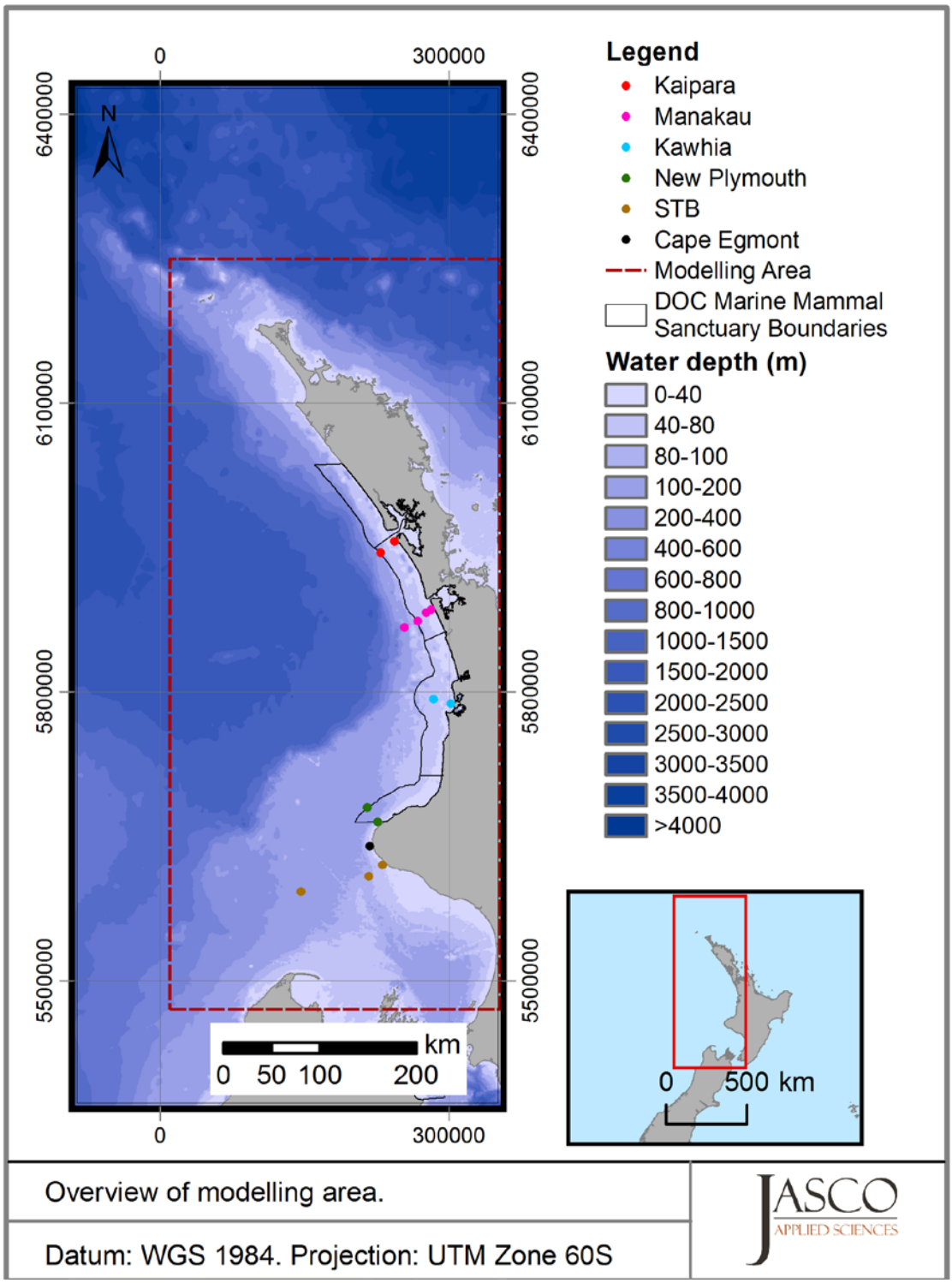

Figure 1: Map of modelling study boundary (red) including defined receiver points for sampling of the modelled sound fields.

Table 1: Locations of defined receiver points (UTM Zone 60 south).

Location	Distance from shore (nmi)	Latitude (°S)	Longitude (°E)	Easting (m)	Northing (m)
Kaipara	12	-36.6080	173.9680	228809.15	5944330.71
	2	-36.5030	174.1370	243581.71	5956446.34
	20	-37.3120	174.2190	253546.35	5866888.42
Manakau	12	-37.2540	174.3770	267372.48	5873725.30
	5	-37.1767	174.4826	276512.64	5882558.91
	2	-37.1520	174.5370	281270.55	5885425.29
Kawhia	12	-37.9910	174.5390	283888.12	5792325.67
	2	-38.0350	174.7430	301923.19	5787897.17
New Plymouth	12	-38.9850	173.7080	214846.75	5679731.15
	2	-39.1220	173.8300	225947.38	5664898.53
STB	2	-39.5239	173.8691	230873.70	5620395.46
	12	-39.6265	173.6992	216686.56	5608491.04
	50	-39.7450	172.8714	146220.00	5592390.00
Cape Egmont	2	-39.3449	173.7264	217880.00	5639840.00

3.2 BIOLOGICAL THRESHOLDS

The potential for anthropogenic sounds to impact marine mammals is largely dependent on whether the sound occurs at frequencies that an animal can hear well, unless the received sound pressure level is so high that it can cause physical tissue damage regardless of its frequency content. Auditory weighting functions have been proposed for marine mammal species, specifically associated with Temporary and Permanent Threshold Shift (TTS and PTS, respectively) thresholds expressed in metrics which consider what is known about marine mammal hearing (e.g., SPL and SEL) (Southall et al. 2007, Finneran 2016). Marine mammal auditory weighting functions published by Finneran (2016) are included in the Technical Guidance published by the United States National Ocean and Atmospheric Administration (NOAA) and National Marine Fisheries Service (NMFS) (NMFS 2018), for use in conjunction with corresponding TTS or PTS (injury) onset acoustic criteria. The NOAA Technical Guidance for assessing the effects of anthropogenic sound on the hearing of marine mammal species presents auditory weighting functions for marine mammals (Appendix F.3) and thresholds at which individual marine mammals are predicted to experience changes in their hearing sensitivity for acute, incidental exposure to all underwater anthropogenic sound sources.

The application of marine mammal auditory weighting functions emphasises the importance of making measurements and characterising sound sources in terms of their overlap with biologically-important frequencies (e.g., frequencies used for soundscape perception, orientation and navigation, communication or the detection of predators or prey), and not only the frequencies of interest or concern for the completion of the sound-producing activity (i.e., context of sound source; NMFS 2018).

The NMFS Technical Guidance (NMFS 2018) classifies both Maui (and Hector's) dolphins as high-frequency cetaceans. The high-frequency cetacean auditory weighting function is therefore applied in this study to provide an indication of sound levels relevant to Maui (and Hector's) dolphins. In addition, unweighted results are presented for context.

3.3 NOISE MODELLING

JASCO's cumulative vessel noise model was used to simulate underwater sound levels generated by the ensemble of vessels reporting AIS positions. The model combines information from several sources—including vessel tracking data (Appendix D), noise emission data (Appendix C), bathymetry, sediment geoacoustics, water sound speed and ambient noise data (Appendix B)—to predict marine environmental noise from ship traffic and seismic surveys (Figure 2). Terminology is described in Appendix F, including acoustic metrics (Appendix F.2) and marine mammal frequency weighting (Appendix F.3). Vessel sound emissions are determined by referencing a database of source levels (according to vessel type and speed). The transmission of sound from each vessel is determined according to a database of pre-computed transmission loss curves for the study area (Appendix B). The model was run in time-lapse mode for 1-minute time steps, and generated sequences of 2-dimensional maps, or "snapshots", of the dynamic sound field, at a depth of 10 m, yielding Sound Pressure Level (SPL) as a function of easting, northing, frequency, and time.

Modelling did not account for small vessels without AIS transponders, vessels at idle or under dynamic positioning, echosounders or sonar, or construction activities such as pile driving. The months selected to represent through the modelling in summer (November – April) and winter (May – October) were March (summer) and July (winter). March was selected in consultation with the Ministry for Primary Industries (MPI) due to the presence of two seismic surveys, and July was considered to be representative of typical vessel activity during winter.

The model used a computational grid (easting and northing) to represent the study area, where each grid cell had dimensions 3 × 3 km. The steps in the model calculation were as follows:

1. For each 1-minute time step, the model computed the location of each vessel and assigned it to the appropriate grid cell.
2. The noise emitted by each vessel was calculated according to its category-specific source level and speed (Appendix C).
3. Source levels and directivity of airgun arrays for tracks corresponding to seismic surveys were predicted using JASCO's Airgun Array Source Model (AASM), which accounts for array layout, volume, tow depth, the firing pressure of each airgun, and interactions between different airguns in the array. Seismic arrays in this work were modelled over AASM's full frequency range, up to 25 kHz. Details of the model are described in Appendix E.
4. The propagation of vessel noise to surrounding grid cells was calculated from sound transmission curves (Appendix B), which were based on water depth, water column properties, and seabed composition (Appendix A). This assessment focussed on Maui dolphins, which are High Frequency cetaceans, therefore the modelling range from each source was 100 km.
5. The noise contributions from all vessels were summed together to calculate the cumulative noise in each grid cell.
6. A baseline quiet noise level derived from the National Institute of Water and Atmosphere (NIWA) Cook Strait Acoustic Monitoring Programme (Appendix A), was added to the computational grid.
7. A map of 1/3 octave band cumulative SPL at 10 m depth was generated for the current time step; the model then advanced to the next time step (calculation step 1) until finished. To represent the noise relevant to high-frequency (HF) cetaceans, maps of HF-weighted SPL, using the weighting from the United States National Marine Fisheries Services (NMFS) (2018) (Figure F 1) were also generated.
8. The sound fields were sampled at 14 defined receiver locations to assist with understanding the temporal variation of sound levels throughout the representative summer and winter months at locations potentially occupied by Maui dolphins. These model outputs were presented as plots of unweighted and HF-weighted sound levels over time.

All model calculations are frequency-dependent. For this study, the modelled frequency range encompassed the dominant frequency range for the anthropogenic sources considered in this study, and a significant portion of the hearing range of low-, mid- and high-frequency cetaceans (9 Hz to 70 800

Hz; Appendix F.3). More details about the development of the cumulative vessel noise model are provided in Section 2.1 of MacGillivray et al. (2018a).

The SPL results were also used to calculate one-month equivalent continuous underwater noise levels (L_{eq}) for March and July. Energy equivalent SPL (L_{eq}; dB re 1 µPa) reflects the average SPL of an acoustic signal over long periods of time (F 7). The L_{eq} metric is useful for presenting geographic distributions of mean noise levels.

A realistic lower bound for sound levels is required to provide context for vessel and seismic survey noise contributions. Adding non-anthropogenic ambient noise sources to the model, such as wind, rain and biological sources, and accounting for their actual time-varying contributions would require detailed information that was unavailable for this study (e.g., meteorological data on a finely sampled grid, locations of snapping shrimp habitat, marine fauna calling densities, etc.), which was limited to modelling vessels and seismic surveys. Therefore, a baseline quiet noise level was determined using the 5th percentile from the long-term Cook Strait acoustic monitoring project led by NIWA (Appendix A). The comparison of modelling predictions to the baseline quiet noise level allows it to be determined when the ambient noise would be driven by non-anthropogenic sources during calm weather conditions.

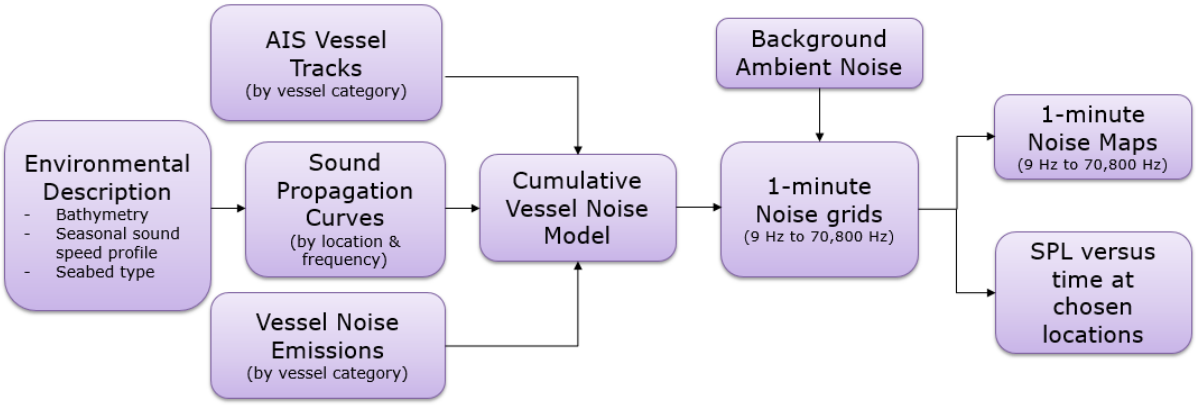

Figure 2: High-level flow chart showing inputs and outputs of the cumulative vessel noise model (time-lapse mode).

4. RESULTS

Vessel density and speed grid maps for each vessel category were created for the entire year, along with summer and winter season (see Appendix G). Due to the significant number of maps produced, selected examples only are presented in the report. These examples are of fishing vessels (Figure 3), government and research category vessels (Figure 4), and bulker category vessels (Figure 5).

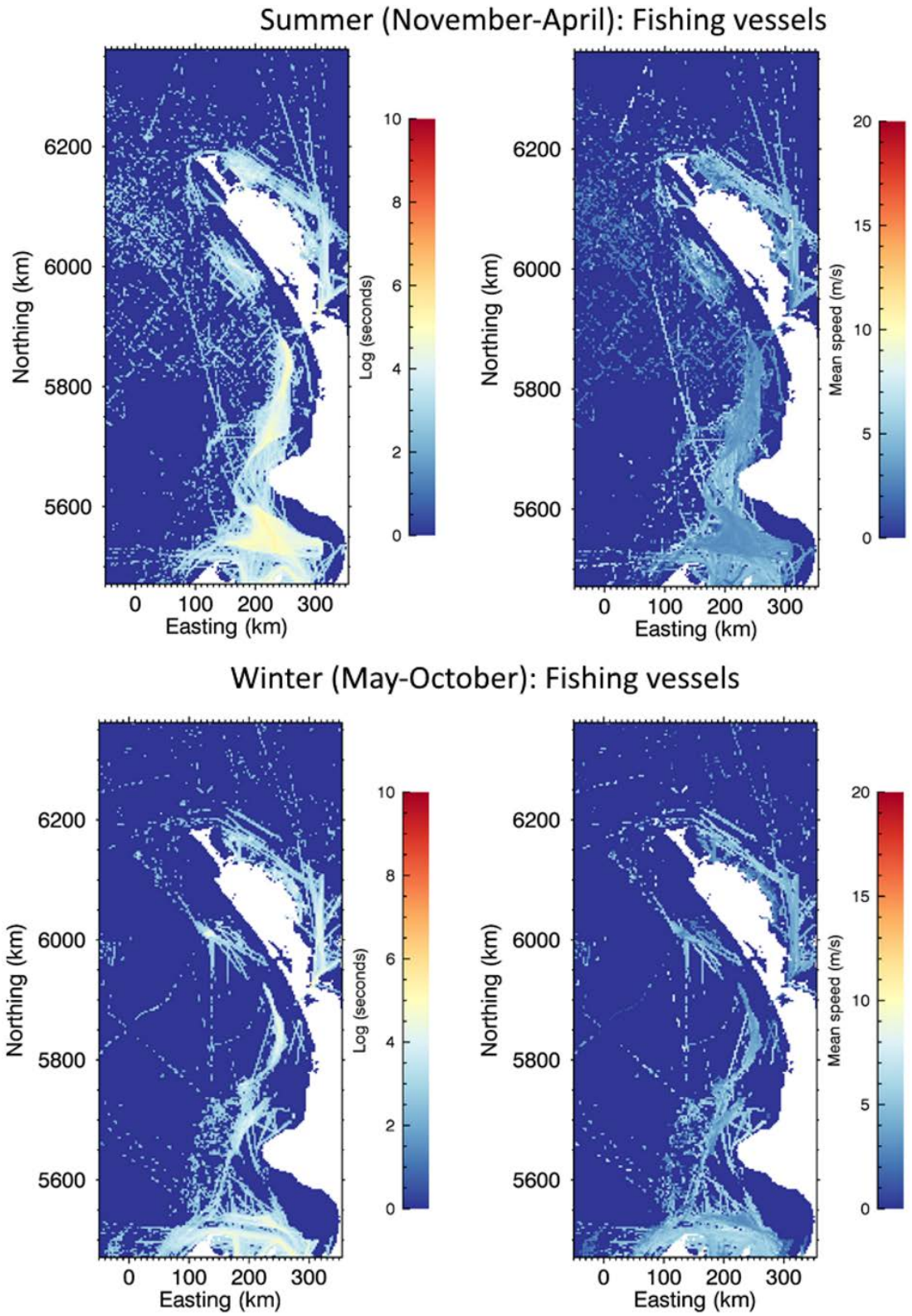

Figure 3: Fishing vessels: total vessel time (traffic density grid) and average vessel speed (traffic speed grid) during summer and winter seasons.

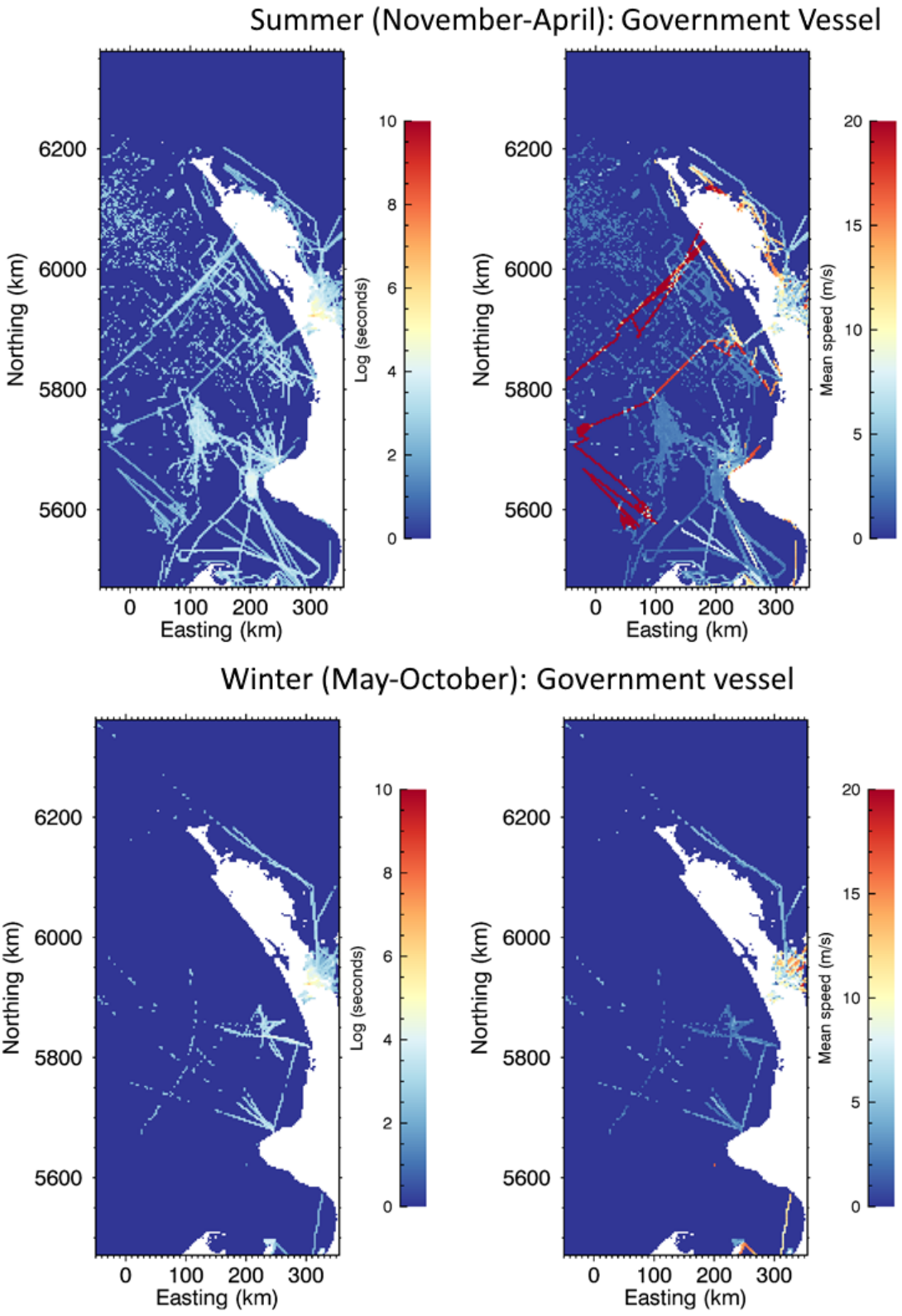

Figure4: Government and research category vessels: total vessel time (traffic density grid) and average vessel speed (traffic speed grid) during summer and winter seasons.

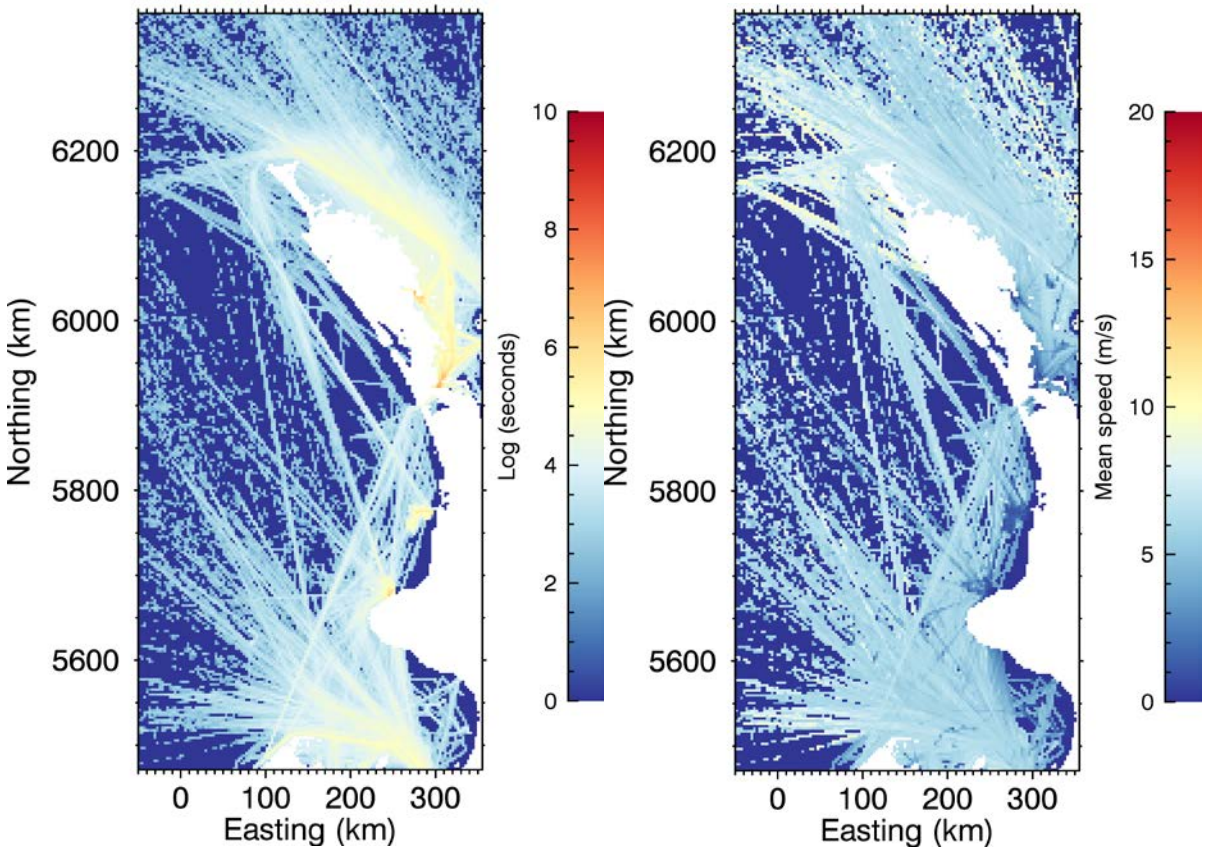

Figure 5: Bulker vessel category: total vessel time (traffic density grid) and average vessel speed (traffic speed grid) for the full year.

For each season, a set of time-dependent sound pressure level (SPL) grids were generated that represented 1-minute snapshots of vessel traffic noise over the entire months of March and July. The SPL and HF-weighted SPL snapshots from the model simulations were rendered as animations (see Appendix G) to show the time evolution of the vessel traffic noise in the study area.

To provide context to the results, the approximate distance from Todd Energy Trestles 3 D MSS to nearby receivers was as follows (listed by receiver and distance) Cape Egmont receiver: 10 km, STB 12 nmi receiver: 21 km, STB 2 nmi receiver: 23 km, and New Plymouth 2 nmi receiver (at the boundary of the WCNI Marine Mammal Sanctuary): 23 km. The approximate distance from the survey to the closest boundary of the WCNI Marine Mammal Sanctuary is 14 km. The distance from the nearest impulses from the TGS Northwest Frontier Multiclient 2-D MSS to receivers was Manakau 20 nmi receiver: 12.7 km, Manakau 12 nmi receiver (at the boundary of the WCNI Marine Mammal Sanctuary): 26 km. The closest modelled impulse to the boundary of the WCNI Marine Mammal Sanctuary is 12 km, just south of Manakau.

Figure 6 shows a single 1-minute snapshot, as of 05:34:00, June 6, with the unweighted and HF-weighted SPL. In addition to several vessels on transit at the north east coast and in the STB, two prominent features can be observed corresponding to the FPSOs UMUROA and RAROA modelled under dynamic positioning operations (Figure C 2). Noise contributions corresponding to the MAUIA, MAUIB, and KUPE platforms are less prominent. The noise footprint of the FPSOs are also prominent in the HF-weighted snapshot due to the high frequency components of their spectra.

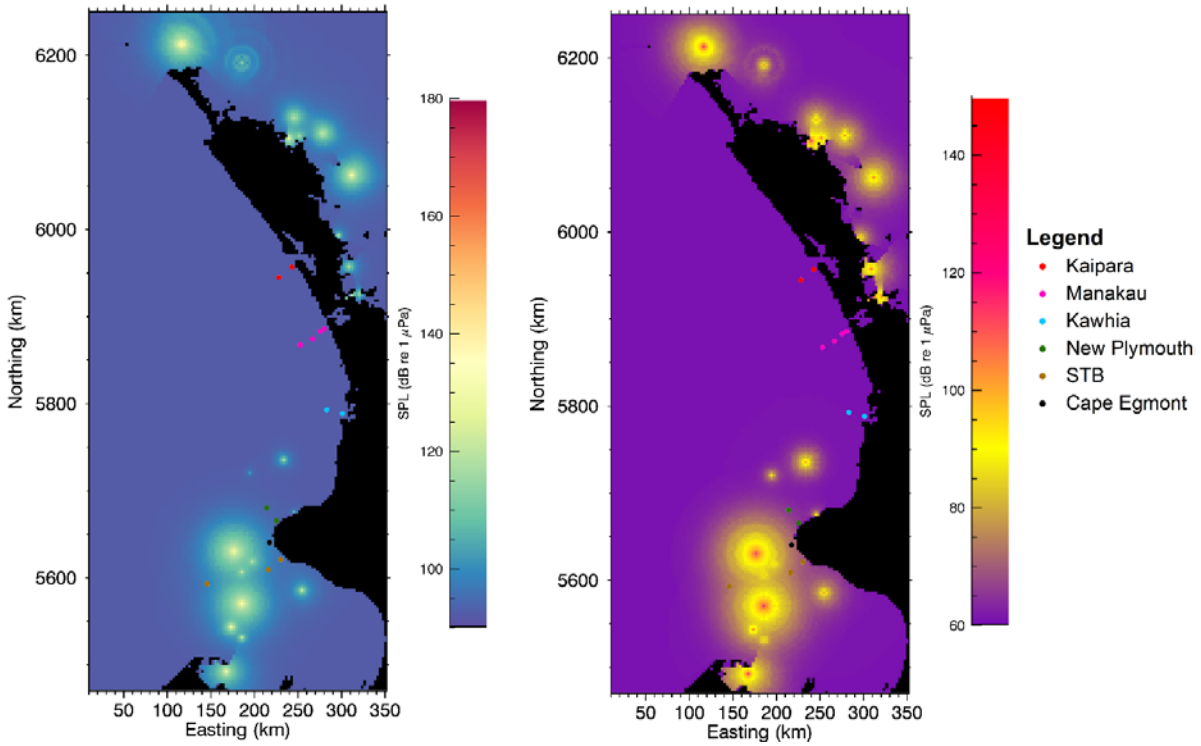

Figure 6: Time snapshots of unweighted SPL (left) and HF-weighted SPL (right) for March 6 (NZST 05:34:00), showing the contribution of multiple vessels, jackup platforms, and FPSOs (locations shown in Figure C2) to the noise footprint.

Figure 7 is a similar example corresponding to March 5 (time 05:19:00), which in addition to vessel noise also shows the influence of seismic airgun impulses from the TGS Northwest Frontier Multiclient 2-D Marine Seismic Survey (MSS) (4400 in^3 array) and the Todd Energy Trestles 3 D MSS (3460 in^3 array). The TGS survey impulse at 5850 km northing is the most prominent feature, with a loud noise footprint due to factors such as a larger array (4400 in^3) operating at deeper water (zone 8, 1750 m nominal water depth) compared to the Trestles survey (3460 in^3 array in 150 m water depth). The airgun directionality for both surveys can be observed in the broadband SPL footprint. Note that the noise from the FPSOs in the broadband SPL panel is masked by the Todd Trestles survey impulse (at about 5640 km Northing). However, due to filtering out of the dominant low-frequency energy characteristic of the seismic impulses (Appendix E.2), the contribution from all platforms, FPSOs, and seismic surveys can be identified in the HF-weighted SPL panel of the figure.

The seasonal dependence of the noise footprint is illustrated by comparing Figures 6 and 7 (March) with Figure 8 (July) for stationary references such as the FPSOs. As shown in Figure B 2, vessel noise can propagate farther in winter, thereby resulting in larger noise footprints. This type of comparison is only useful to compare individual events, however, understanding of the combined noise footprint requires consideration of the complex interactions between environment, vessel traffic, vessel mean speed, and the seasonal variability of these factors.

For example, individual events related to fishing traffic are expected to be louder in winter compared to summer due to the transmission loss environment. However, fishing vessel events are more frequent (and may have a higher noise footprint) in the study area during summer, as illustrated in Figure 3, although this only considers vessels with AIS transponders. This is also the case for government and research vessels, which includes vessels engaged in seismic exploration, with little activity during winter, as shown in Figure 4.

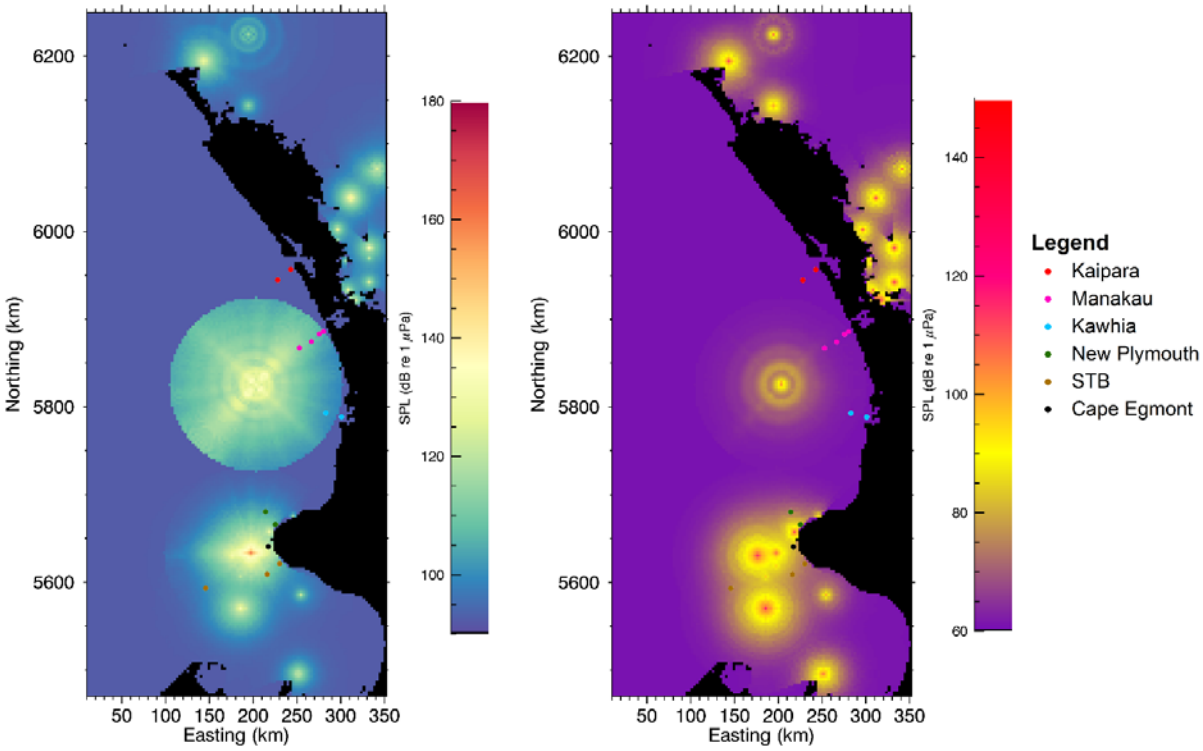

Figure 7: Time snapshots of broadband SPL (left) and HF-weighted SPL (right) for March 5 (time 05:19:00), showing the contribution of concurrent seismic surveys, multiple vessels, jackup platforms, and FPSOs to the noise footprint.

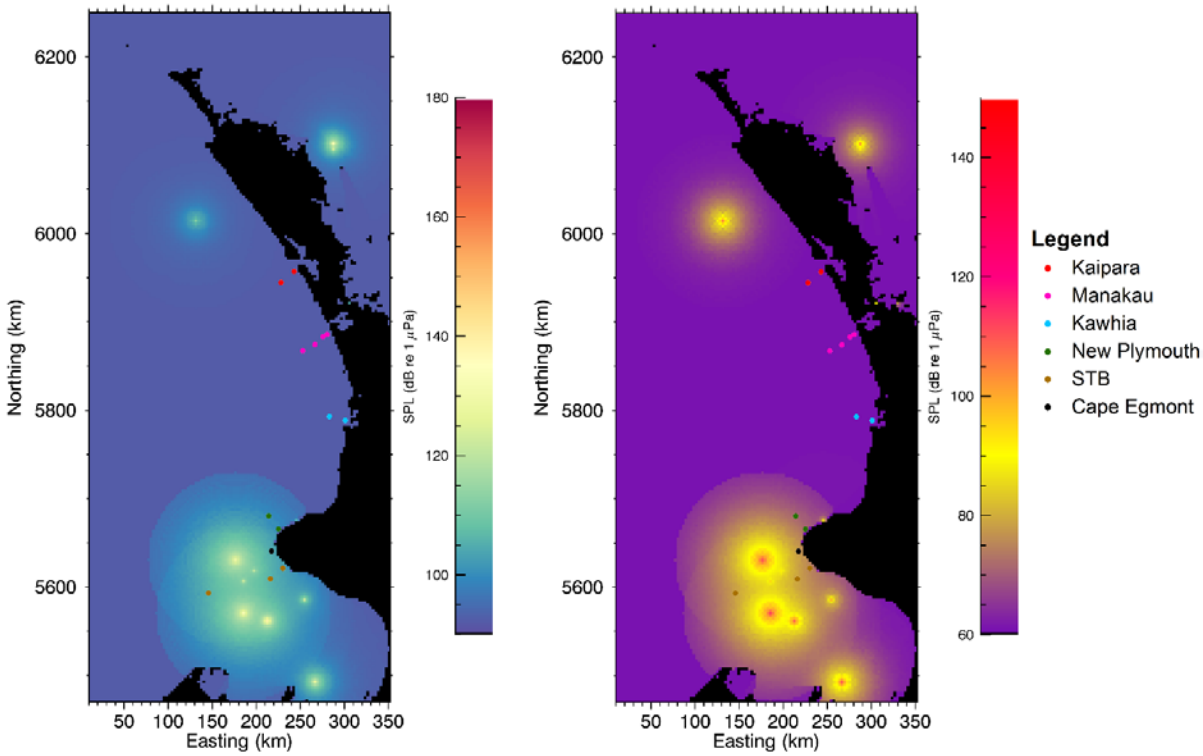

Figure 8: Time snapshots of broadband SPL (left) and HF-weighted SPL (right) for July 12 (time 10:25:00), showing the contribution of multiple vessels, jackup platforms, and FPSOs to the noise footprint. As a reference for noise footprint seasonal dependence, compare the noise footprint extent of the FPSOs to those from March shown in Figure 6.

One-month equivalent continuous underwater noise levels (L_{eq}) are presented for March (broadband: Figure 9; HF-weighted: Figure 10) and July (broadband: Figure 11; HF-weighted: Figure 12) For March, noise from the TGS MSS (located between 5800–6150 km northing offshore) and the Todd

Energy Trestles 3 D MSS (about5640 km northing and 200 km easting, off Cape Egmont) dominated the broadband L_{eq} off the North Island's west coast; however, their contribution is less evident and more localised in the HF-weighted L_{eq} map, for which noise from the FPSOs (modelled under dynamic positioning) becomes dominant. In the absence of seismic surveys throughout July, noise from the FPSOs (modelled under dynamic positioning) is dominant in the broadband L_{eq} and the HF-weighted L_{eq}.

The vessel traffic levels are higher south of Waiiti, with New Plymouth having the highest levels along the entire coast. However, within 12 nmi of the west coast north of Waiiti, the coastal vessel traffic was generally low and concentrated near the harbours of Manakau and Kawhia. When there is no seismic survey activity, such as in July, the monthly L_{eq} along this stretch of the coastline is close to the baseline quiet level used in the modelling, which indicates negligible contributions from vessels. The vessel traffic density is higher from New Plymouth south, both across to the South Island and into the South Taranaki Bight, and thus the monthly L_{eq} is also higher, both for broadband and HF-weighted. The overall traffic level and monthly L_{eq} is lower in June.

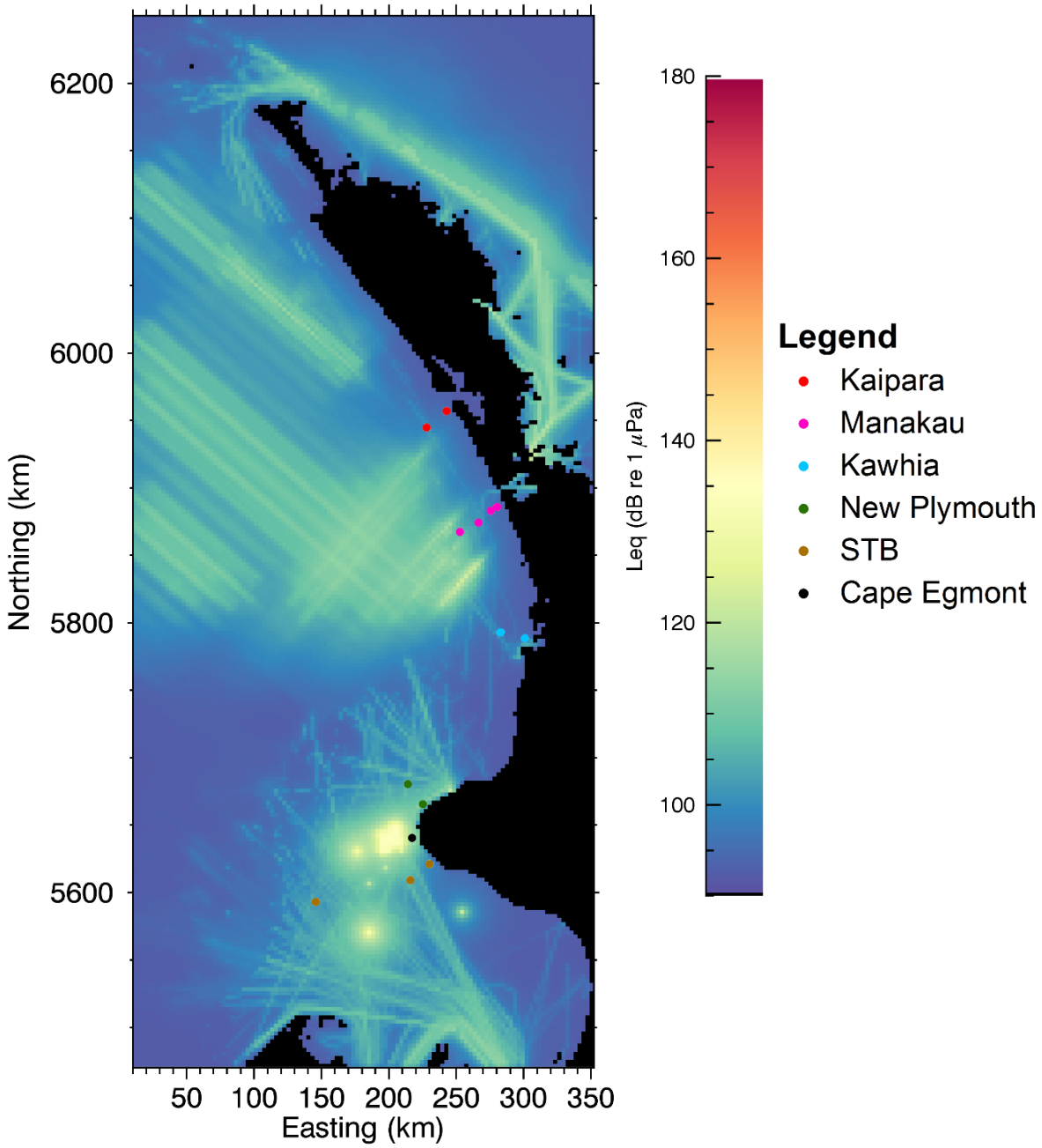

Figure 9: One-month equivalent continuous underwater noise levels (L_{eq}) for March: Broadband SPL.

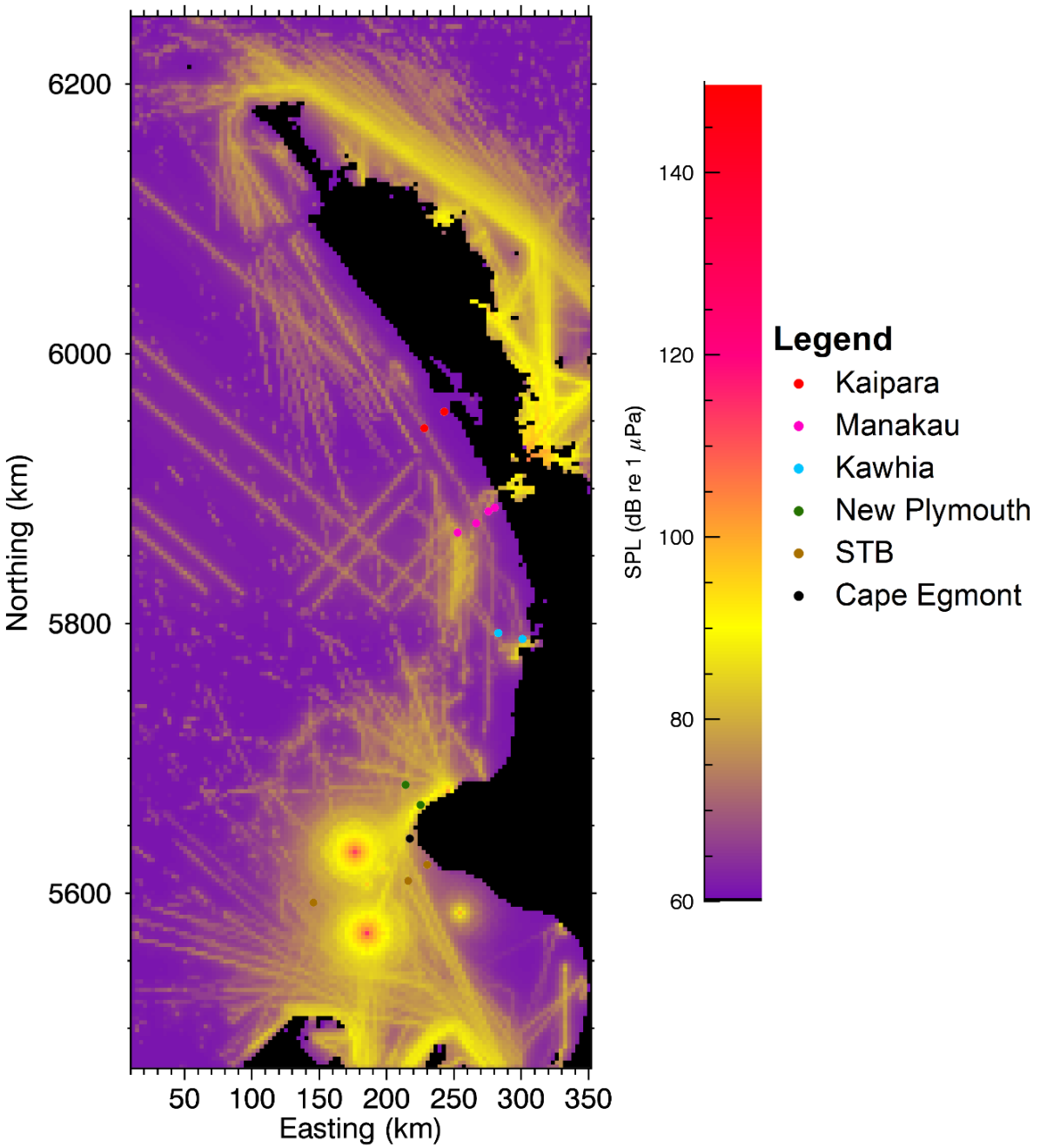

Figure 10: One-month equivalent continuous underwater noise levels (L_{eq}) for March: HF-weighted SPL.

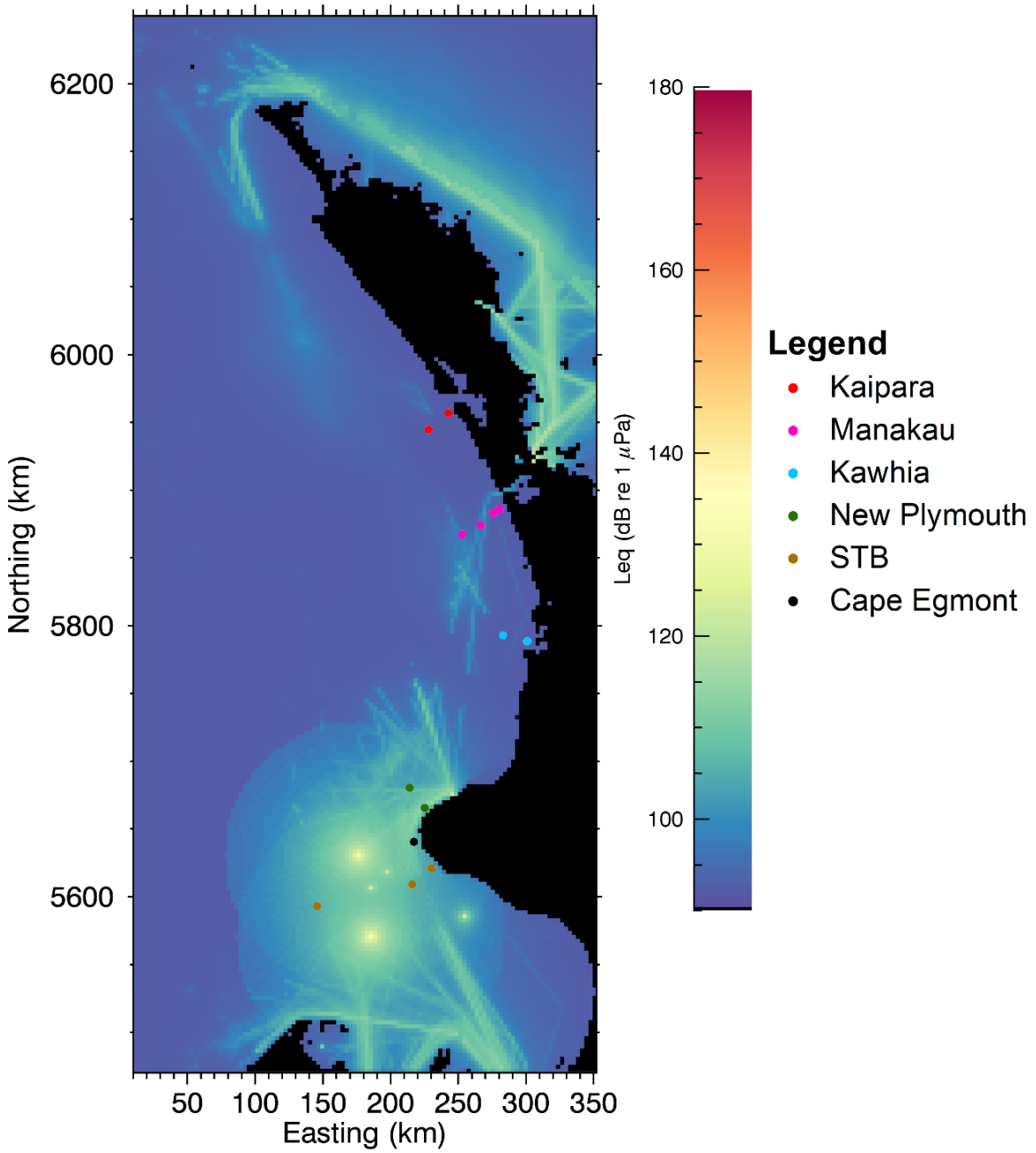

Figure 11: One-month equivalent continuous underwater noise levels (L_{eq}) for July: Broadband SPL.

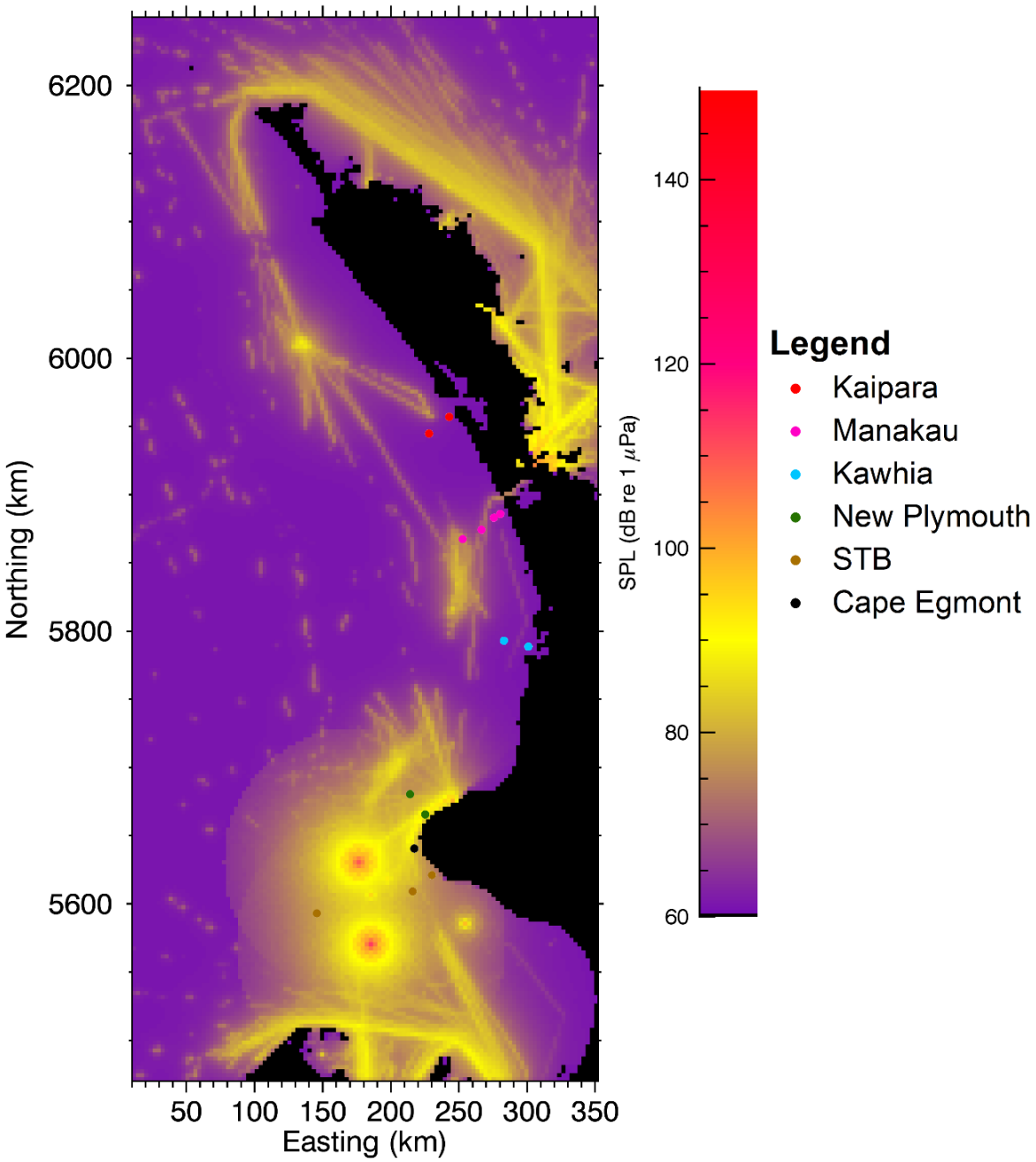

Figure 12: One-month equivalent continuous underwater noise levels (L_{eq}) for July: HF-weighted SPL.

To assist with understanding the temporal variation of sound levels throughout the representative summer and winter months modelled at locations potentially occupied by Maui dolphins, fourteen receiver locations were defined in consultation with MPI. The receivers can be grouped based on their proximity to five regions: Kaipara, Manukau, Kawhia, New Plymouth, Cape Egmont, and the STB (Figure 1; Table 1). The results are presented as both unweighted and high-frequency weighted sound levels, and the data used to create the plots has been provided to Fisheries New Zealand (see Appendix G).

The variation in SPL over time for each of the regions in March is shown in Figures 13–17, ordered north to south. Two 24 hour periods of interest in March are shown for specific regions to place the contribution from seismic surveys in context. Sound levels for March 4 are shown in Figures 18 and 19 for receivers at Kaipara and New Plymouth/Cape Egmont, for demonstration of sound levels due to the two modelled seismic surveys, along with a one-minute snapshot from the day (Figure 20). Sound levels

at Manukau on March 11 are also shown in Figure 21, to illustrate sound levels due to the TGS MSS, along with a one-minute snapshot from the day (Figure 22). The sudden increase and decrease in the sound levels during the seismic surveys is due to the airgun array only being active during the ramp-up process and while on the acquisition line.

The variation in SPL over time for each of the regions in July are shown in Figures 23–27, ordered north to south.

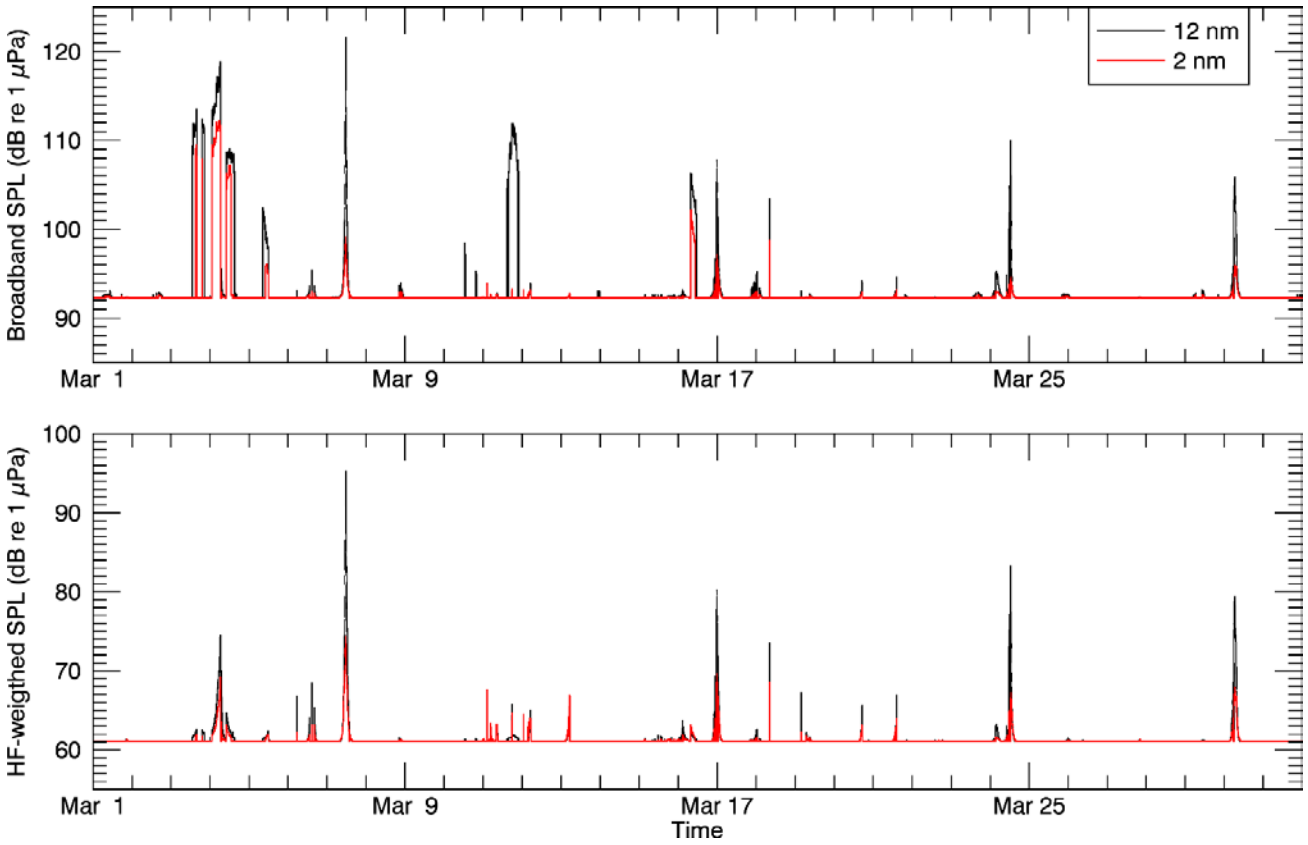

Figure 13: Kaipara, March: SPL variation over time, broadband SPL (top) and HF-weighted SPL (bottom). Locations provided in Figure 1 and Table 1.

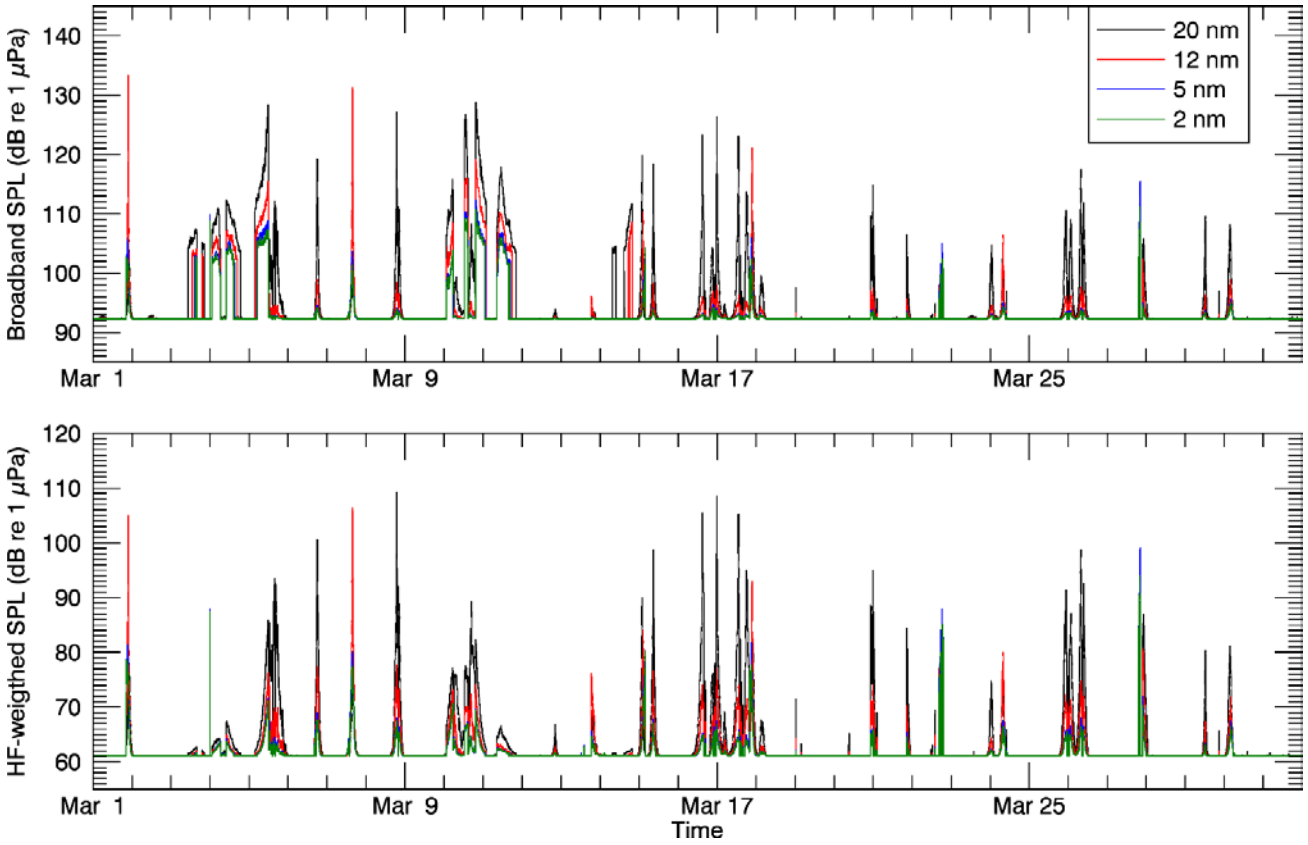

Figure 14: Manukau, March: SPL variation over time, broadband SPL (top) and HF-weighted SPL (bottom). Locations provided in Figure 1 and Table 1.

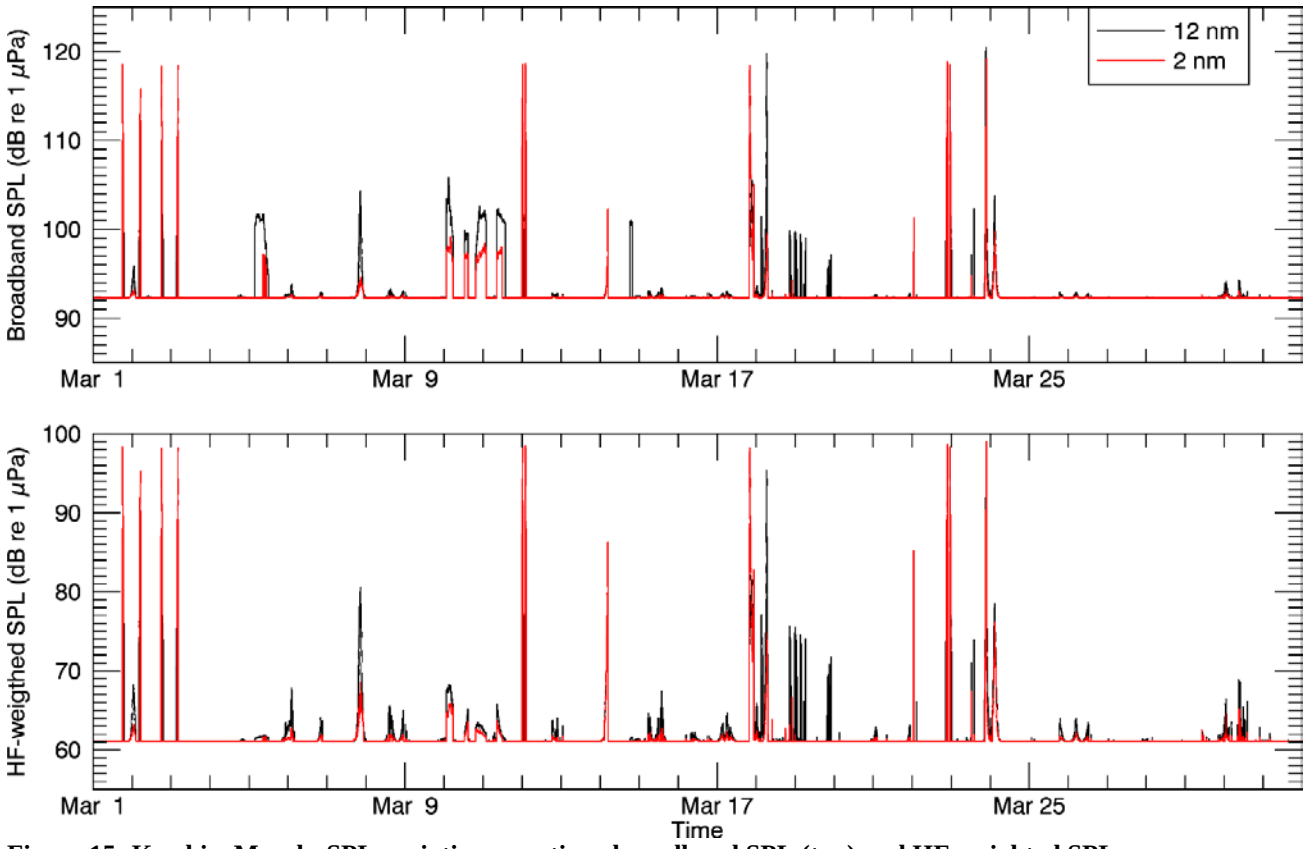

Figure 15: Kawhia, March: SPL variation over time, broadband SPL (top) and HF-weighted SPL (bottom). Locations provided in Figure 1 and Table 1.

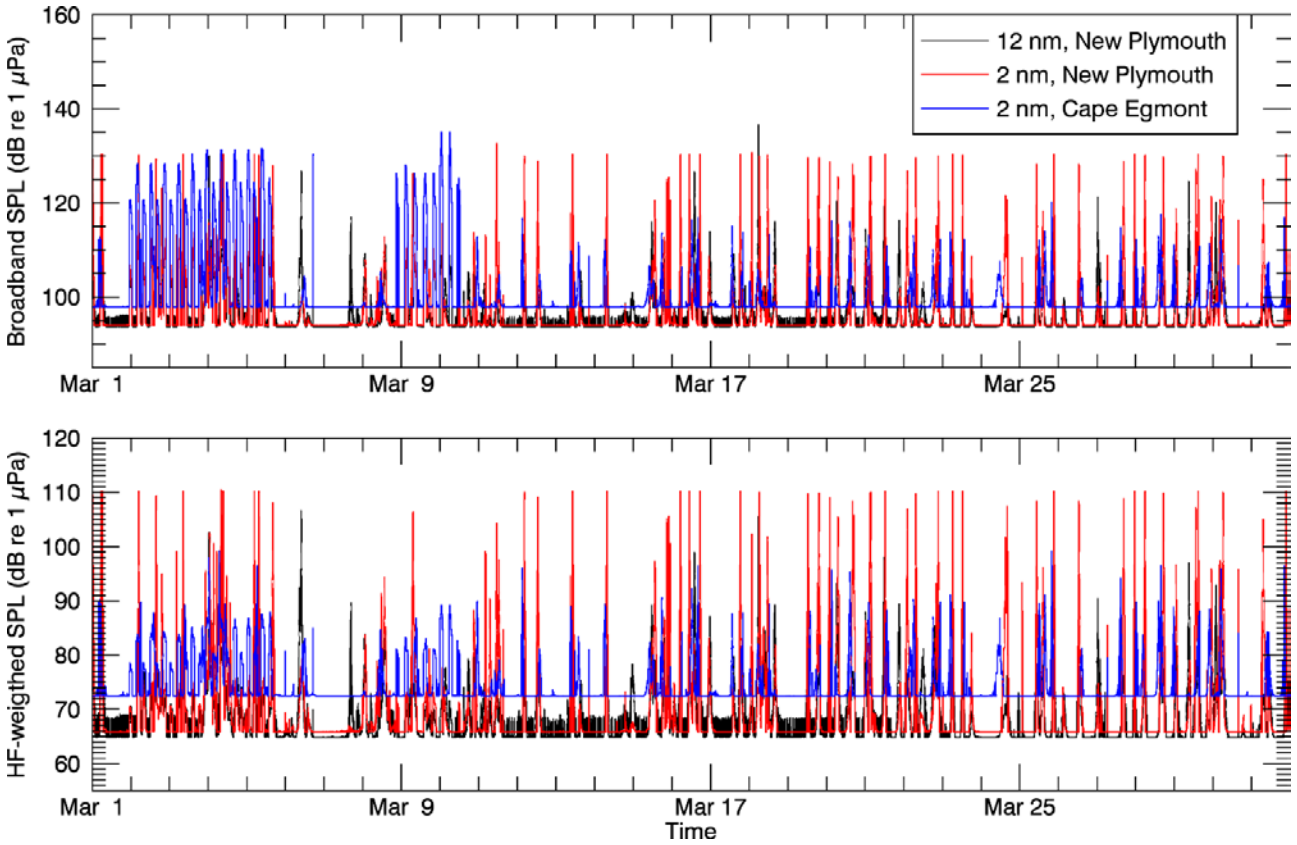

Figure 16: New Plymouth and Cape Egmont, March: SPL variation over time, broadband SPL (top) and HF-weighted SPL (bottom). Locations provided in Figure 1 and Table 1.

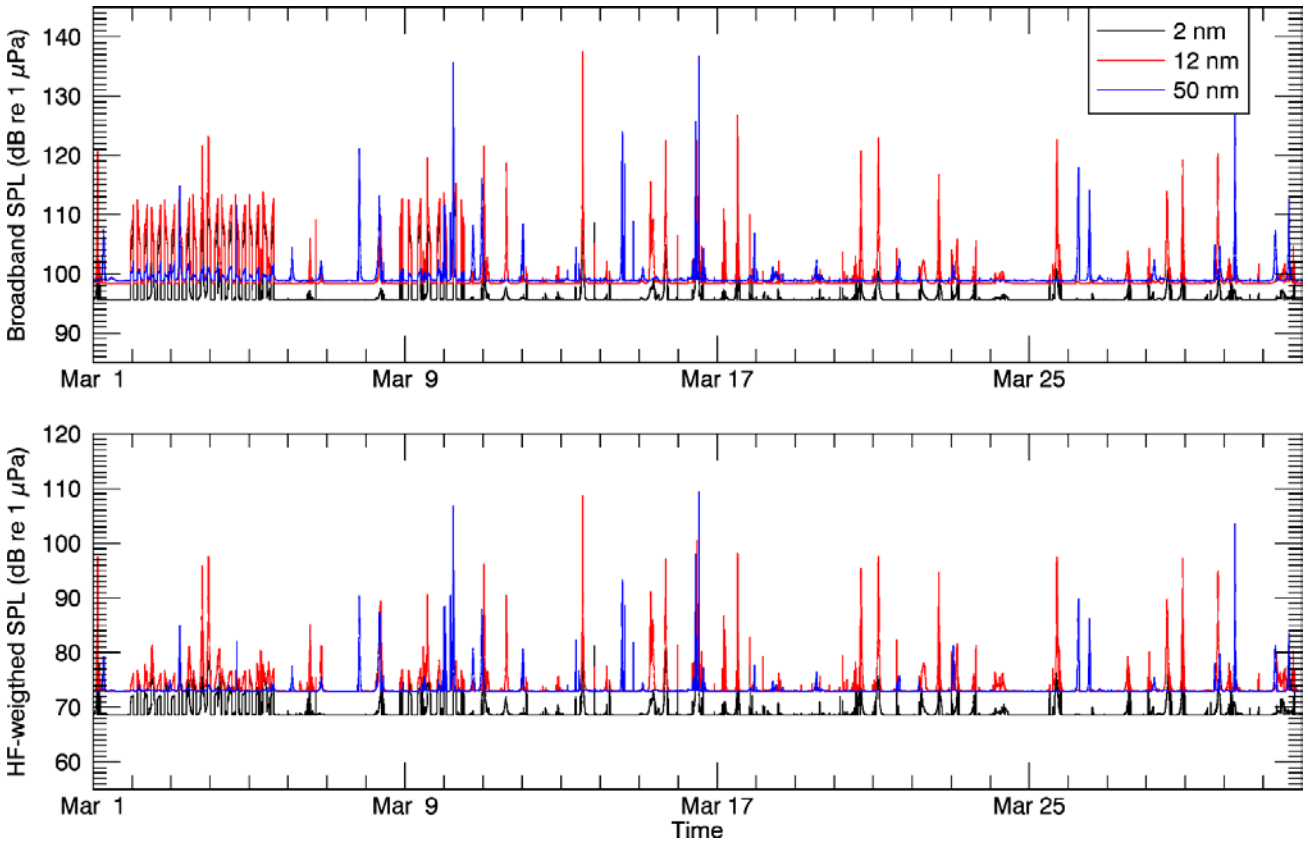

Figure 17: STB, March: SPL variation over time, broadband SPL (top) and HF-weighted SPL (bottom). Locations provided in Figure 1 and Table 1.

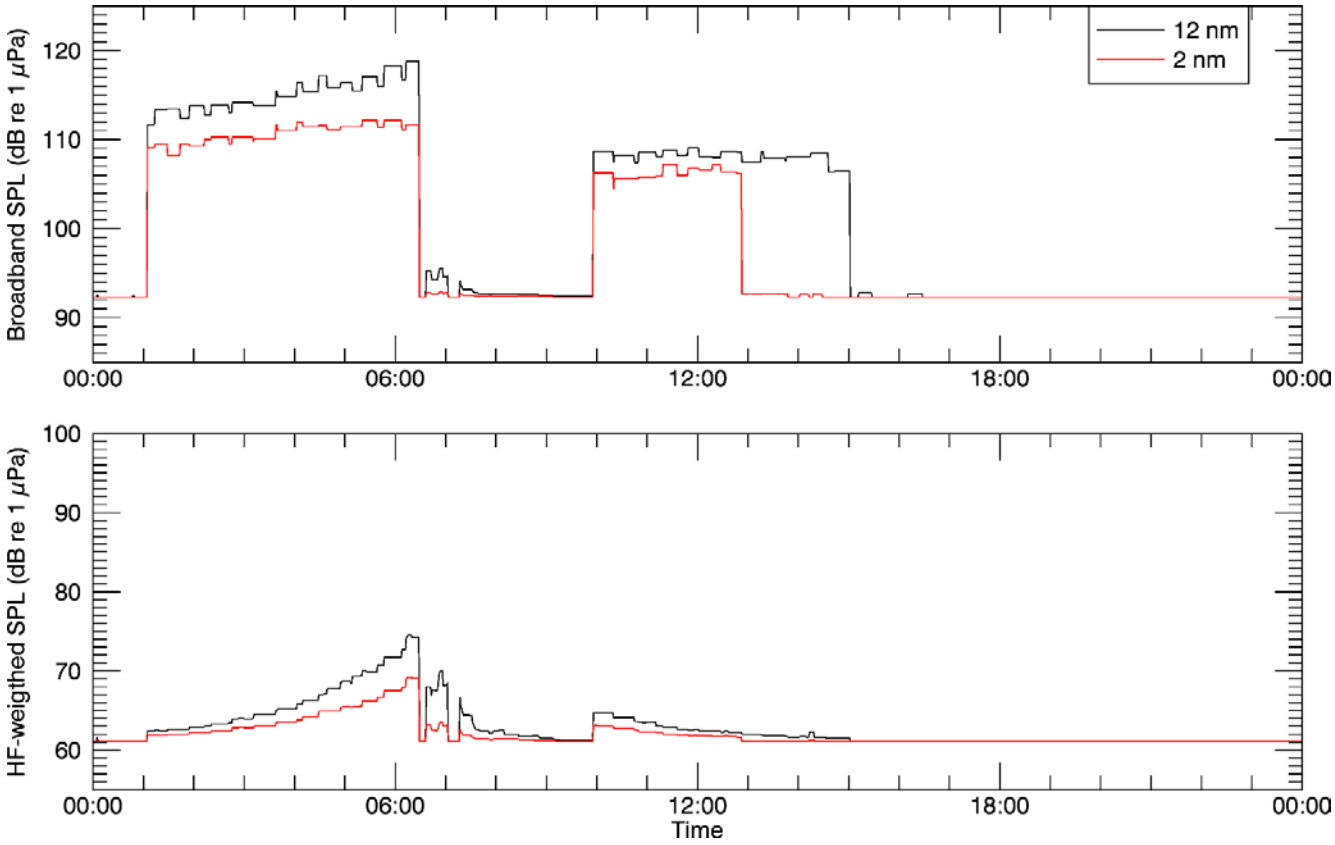

Figure 18: Kaipara, March 4: SPL variation over a 24 h period, broadband SPL (top) and HF-weighted SPL (bottom). Locations provided in Figure 1 and Table 1.

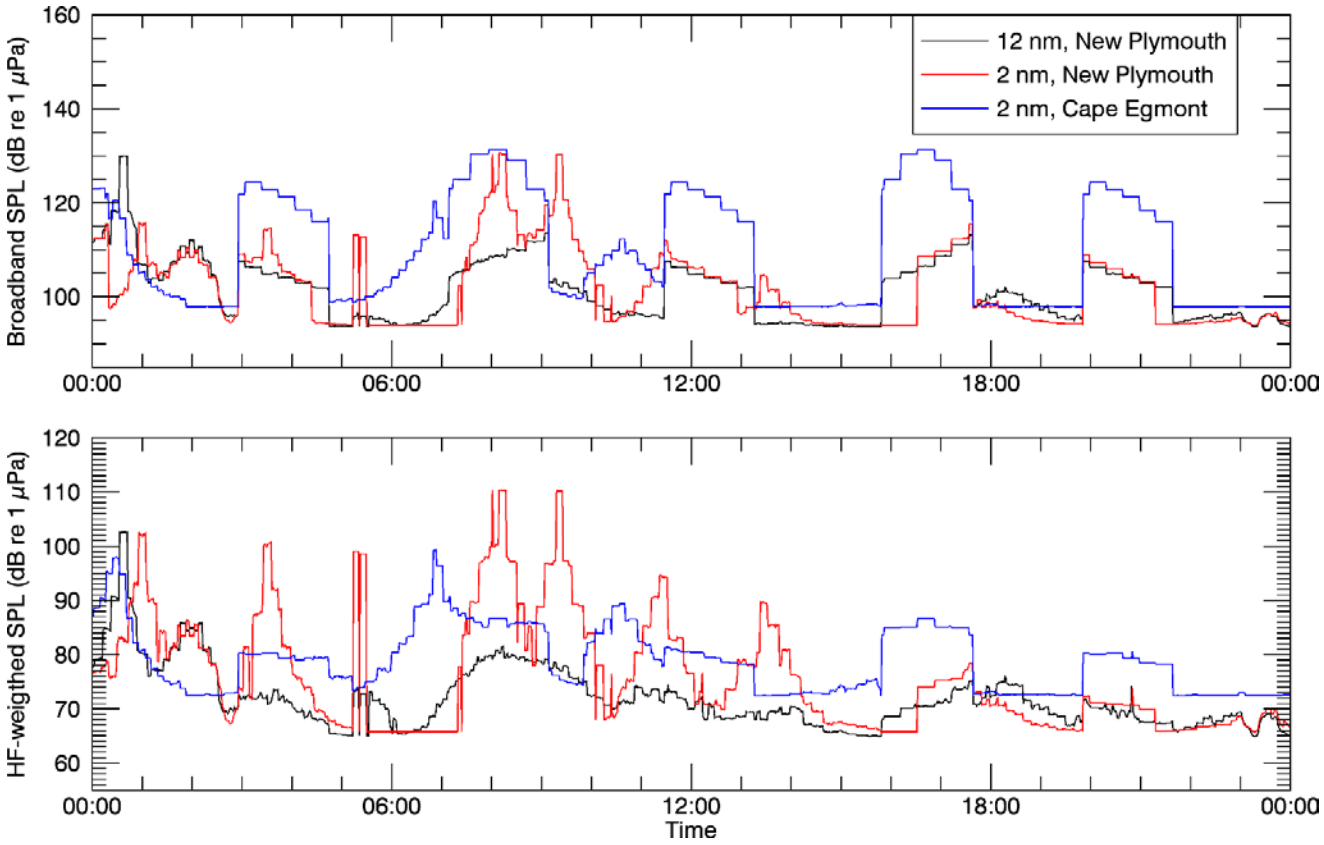

Figure 19: New Plymouth and Cape Egmont, March 4: SPL variation over a 24 h period, broadband SPL (top) and HF-weighted SPL (bottom). Locations provided in Figure 1 and Table 1.

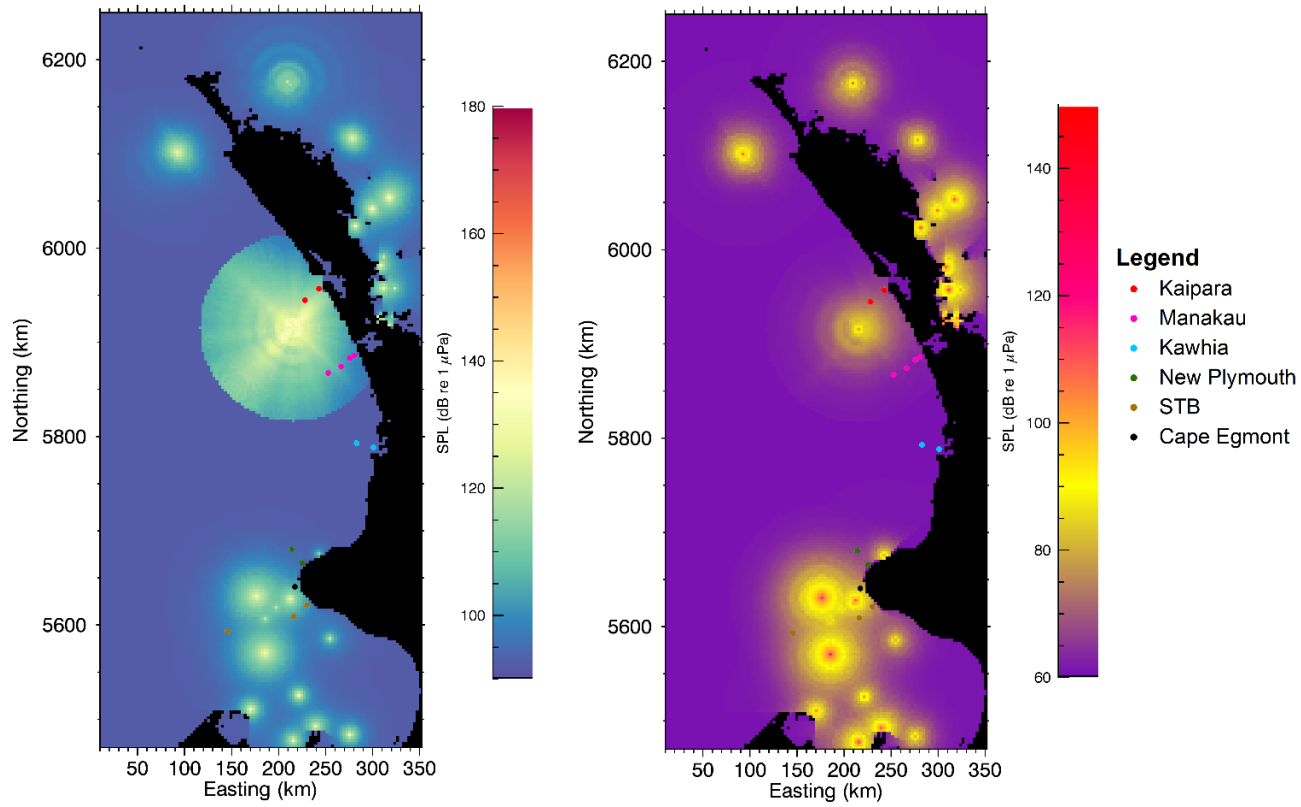

Figure 20: Time snapshots of broadband SPL (left) and HF-weighted SPL (right) for March 4 (time 06:00:00), to provide context for Figures 18 and 19 showing the proximity of the TGS MSS to the receivers at Kaipara and the Todd Energy Trestles MSS to New Plymouth and Cape Egmont.

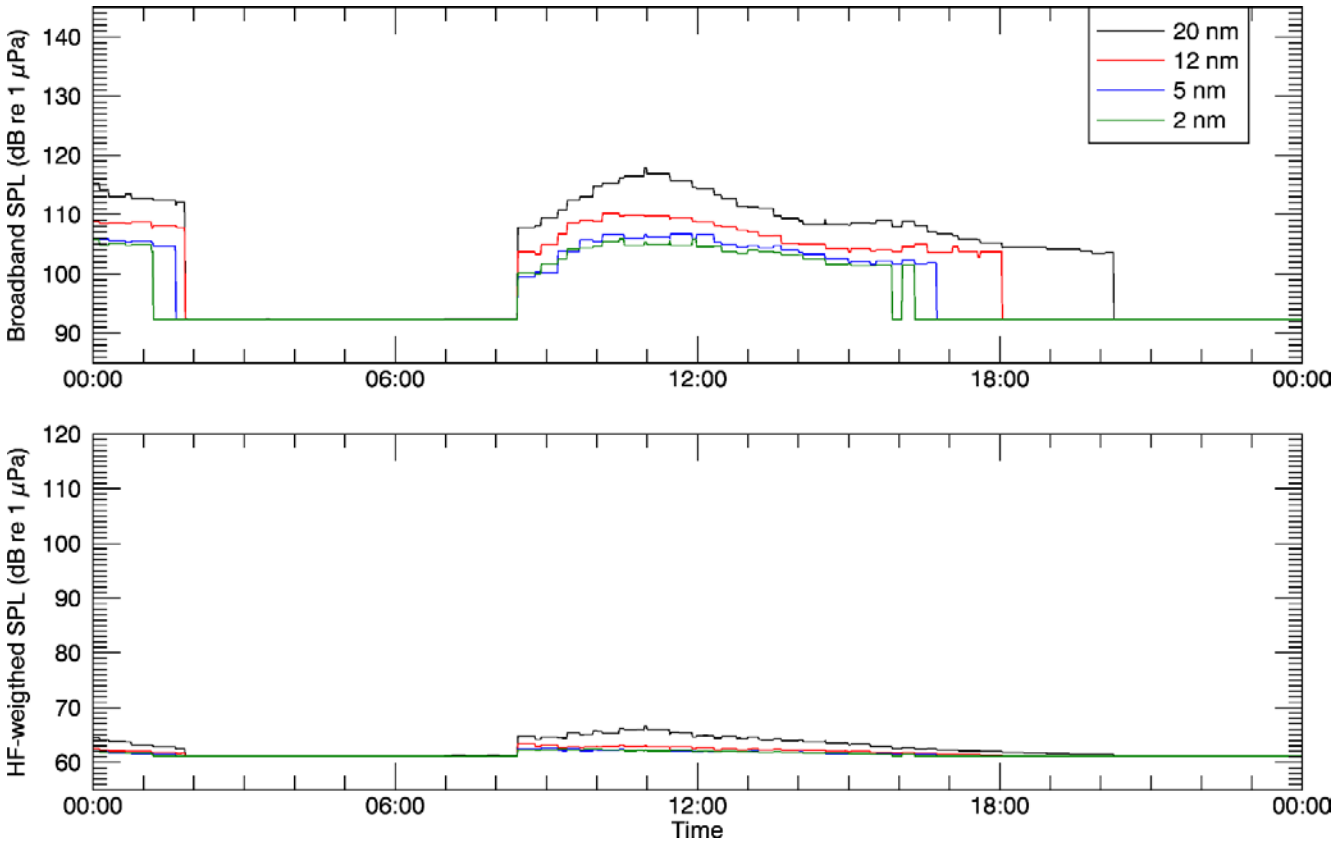

Figure 21: Manakau, March 11: SPL variation over a 24 h period, broadband SPL (top) and HF-weighted SPL (bottom). Locations provided in Figure 1 and Table 1.

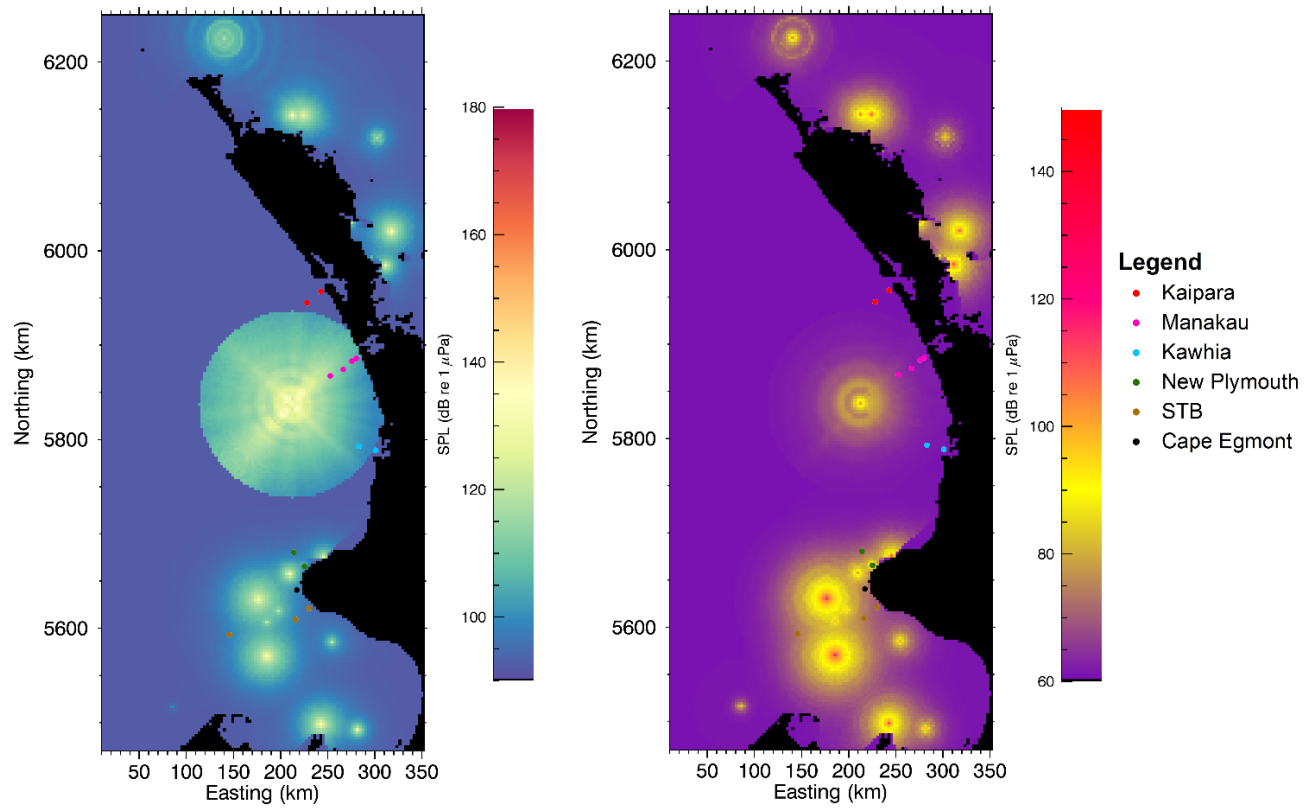

Figure22: Time snapshots of broadband SPL (left) and HF-weighted SPL (right) for March 11 (time 12:00:00), to provide context for Figure 21, showing the proximity of the TGS MSS to the receivers at Manakau.

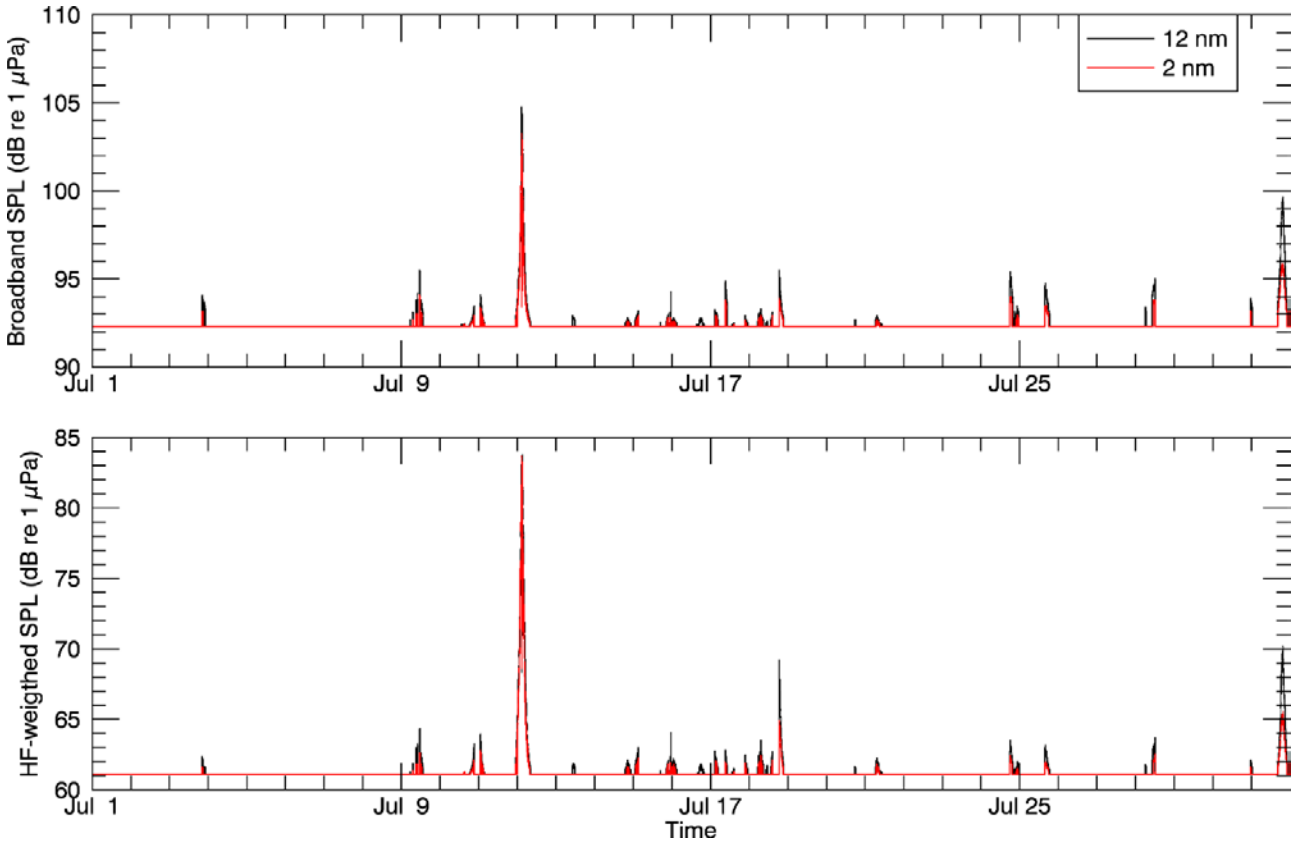

Figure23: Kaipara, July: SPL variation over time, broadband SPL (top) and HF-weighted SPL (bottom). Locations provided in Figure 1 and Table 1.

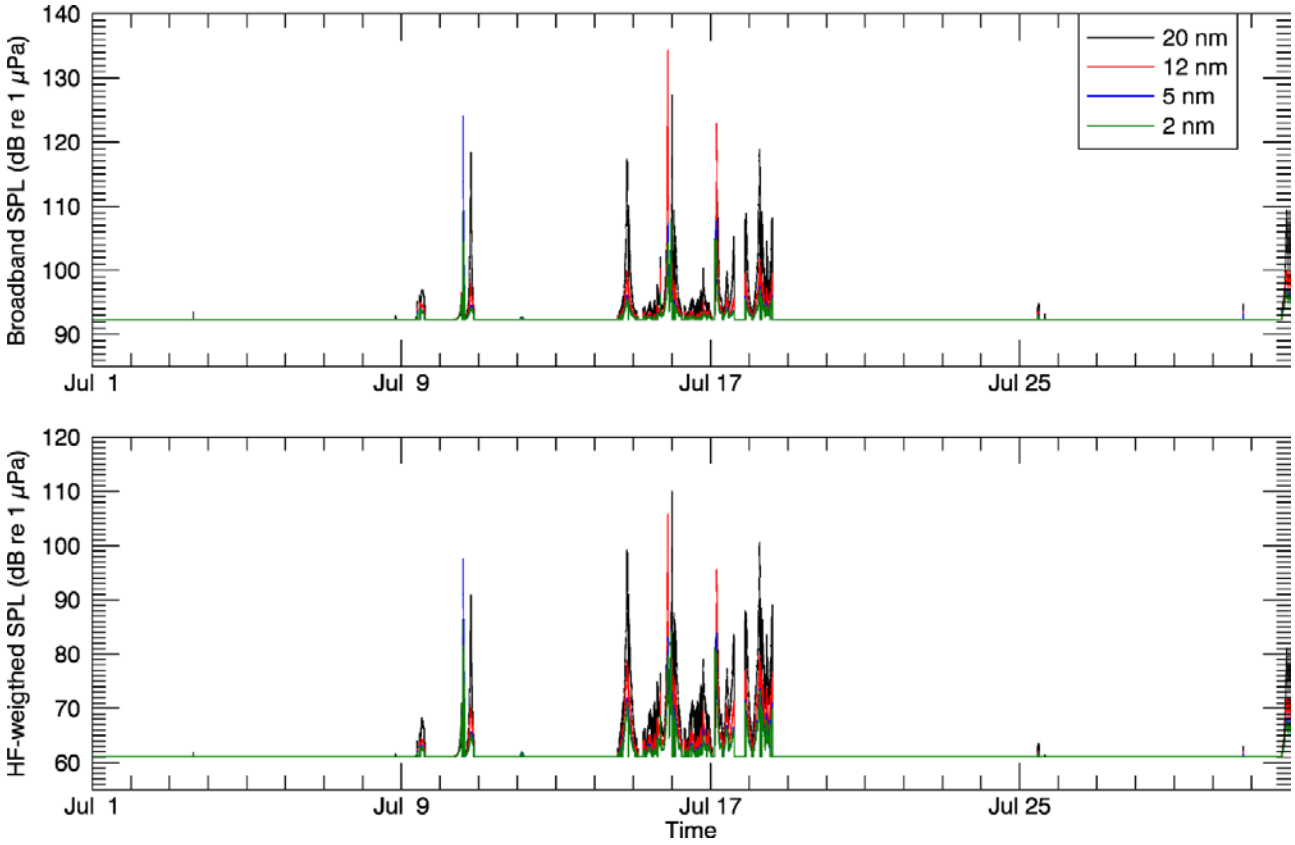

Figure 24: Manukau, July: SPL variation over time, broadband SPL (top) and HF-weighted SPL (bottom). Locations provided in Figure 1 and Table 1.

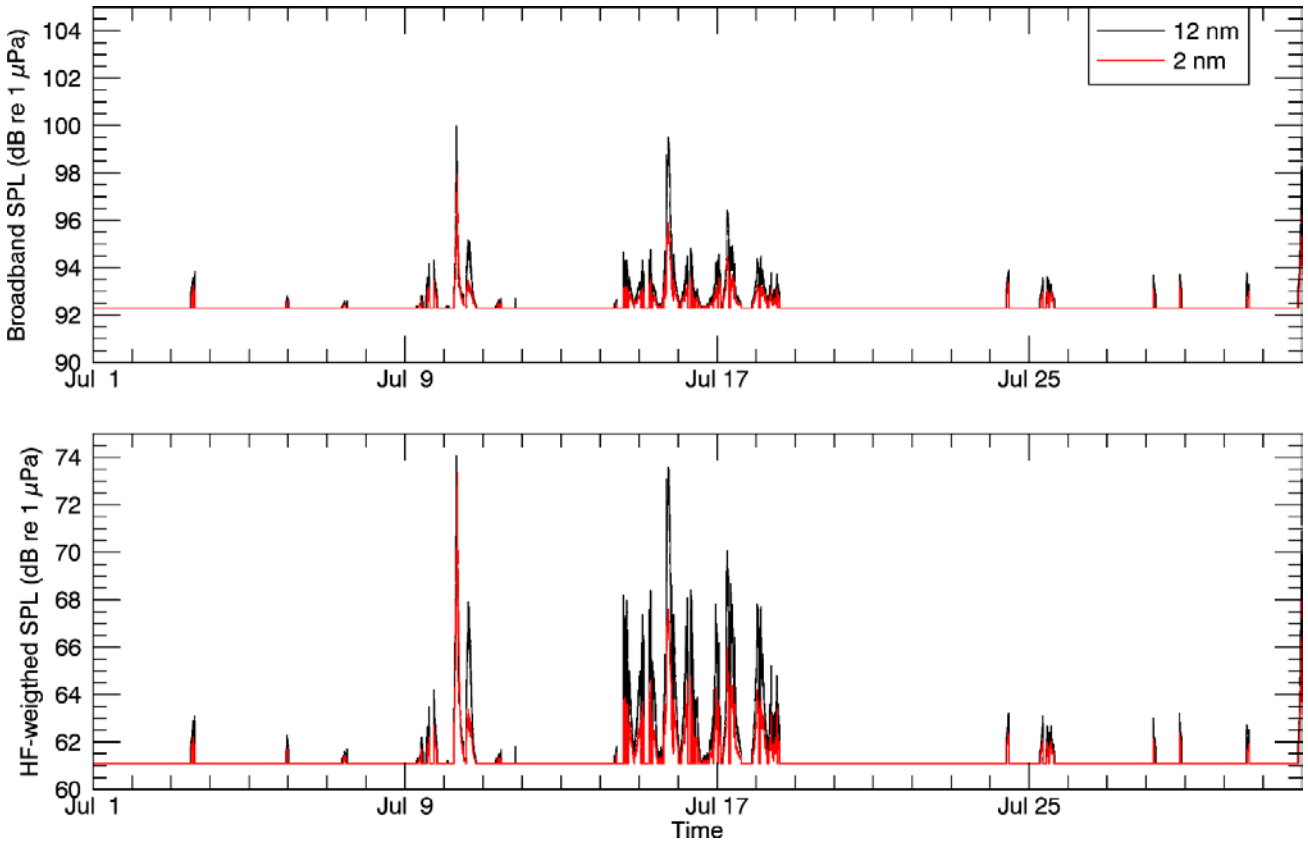

Figure 25: Kawhia, July: SPL variation over time, broadband SPL (top) and HF-weighted SPL (bottom). Locations provided in Figure 1 and Table 1.

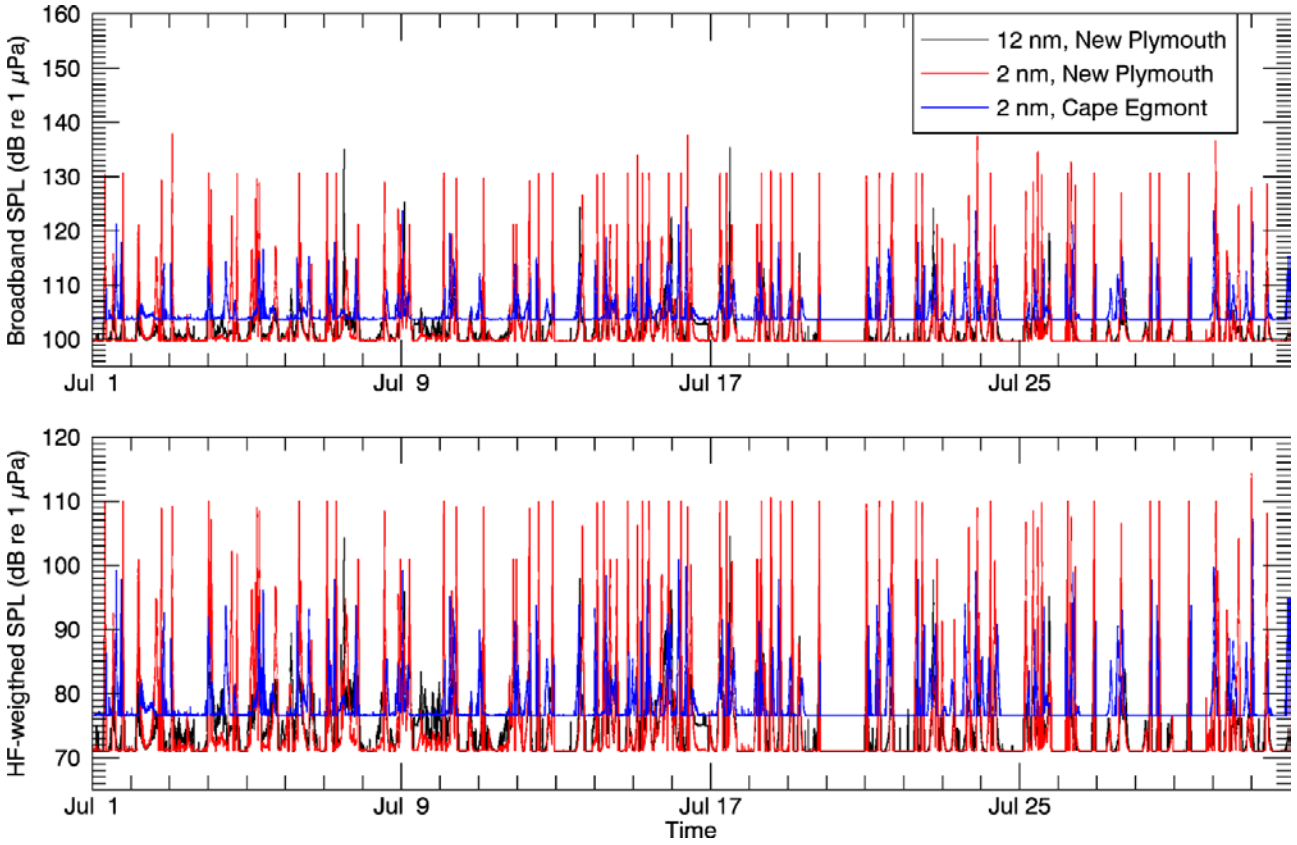

Figure 26: New Plymouth and Cape Egmont, July: SPL variation over time, broadband SPL (top) and HF-weighted SPL (bottom). Locations provided in Figure 1 and Table 1.

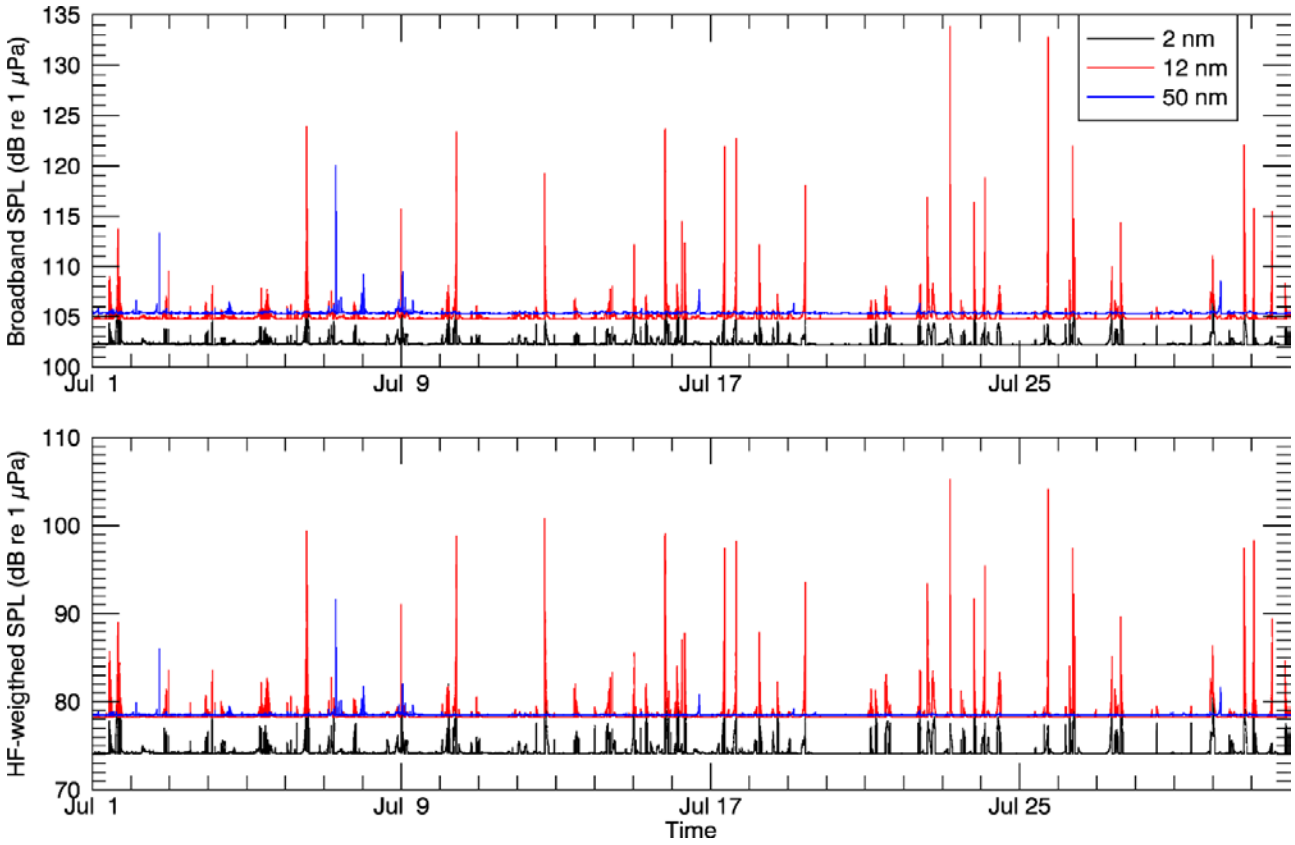

Figure 27: STB, July: SPL variation over time, broadband SPL (top) and HF-weighted SPL (bottom). Locations provided in Figure 1 and Table 1.

Summary statistics are provided for broadband SPL (unweighted) and HF-weighted for March (Tables 2 and 3) and June (Tables 4 and 5). The ambient broadband SPL (10–70 800 Hz) used in the modelling based upon the L_5 from measurements in the STB is 92.3 dB re 1 µPa, while the HF-weighted ambient SPL is 61.1 dB re 1 µPa (Appendix A.4). When the sound levels are equivalent to the baseline quiet noise level, this is when the soundscape, or ambient noise, would be driven by non-anthropogenic sources, such as natural (wind and waves) and biological sources. The percentiles represent the time periods for which the sound levels presented in the tables are exceeded.

Table 2: March: Summary of broadband SPL statistics. SPL units: dB re 1 µPa. Grey cells indicate the percentiles equal to the baseline quiet noise level.

Location	Distance from shore (nmi)	Percentile					Mean	Maximum
		5th	25th	50th	75th	95th		
Kaipara	12	92.30	92.30	92.30	92.30	95.30	93.06	121.60
	2	92.30	92.30	92.30	92.30	92.70	92.57	112.20
Manakau	20	92.30	92.30	92.30	92.60	109.60	94.81	128.80
	12	92.30	92.30	92.30	92.40	104.50	93.63	133.30
	5	92.30	92.30	92.30	92.30	101.70	93.13	115.50
	2	92.30	92.30	92.30	92.30	100.30	93.03	111.30
Kawhia	12	92.30	92.30	92.30	92.30	99.10	92.89	120.50
	2	92.30	92.30	92.30	92.30	92.90	92.62	119.30
New Plymouth	12	93.60	93.60	94.80	98.50	106.60	96.80	136.60
	2	93.90	93.90	93.90	96.90	112.50	97.41	132.80
STB	2	95.60	95.60	95.60	95.80	105.60	96.68	112.70
	12	98.40	98.40	98.40	98.80	108.70	99.78	137.50
	50	98.80	98.80	98.90	99.00	100.90	99.31	136.90
Cape Egmont	2	97.90	97.90	97.90	98.30	120.60	100.70	135.00

Table 3: March: Summary of statistics for HF-weighted SPL. SPL units: dB re 1 µPa. Grey cells indicate the percentiles equal to the baseline quiet noise level.

Location	Distance from shore (nmi)	Percentile					Mean	Maximum
		5th	25th	50th	75th	95th		
Kaipara	12	61.10	61.10	61.10	61.10	61.90	61.35	95.30
	2	61.10	61.10	61.10	61.10	61.50	61.23	74.40
Manakau	20	61.10	61.10	61.10	61.60	76.40	63.28	109.30
	12	61.10	61.10	61.10	61.20	69.30	62.22	106.40
	5	61.10	61.10	61.10	61.10	64.80	61.73	99.20
	2	61.10	61.10	61.10	61.10	64.30	61.66	94.20
Kawhia	12	61.10	61.10	61.10	61.10	64.50	61.78	95.40
	2	61.10	61.10	61.10	61.10	62.10	61.57	99.10
New Plymouth	12	64.80	64.90	67.00	70.90	77.50	68.65	106.70
	2	65.80	65.80	65.80	70.30	89.50	70.07	110.40
STB	2	68.60	68.60	68.60	68.90	73.80	69.38	87.00
	12	72.90	72.90	73.00	73.30	77.60	73.85	108.70
	50	72.90	72.90	72.90	73.00	74.10	73.24	109.50
Cape Egmont	2	72.40	72.40	72.40	73.10	84.40	74.35	99.30

Table 4: July: Summary of broadband SPL statistics. SPL units: dB re 1 µPa. Grey cells indicate the percentiles equal to the baseline quiet noise level.

Location	Distance from shore (nmi)	Percentile					Mean	Maximum
		5th	25th	50th	75th	95th		
Kaipara	12	92.30	92.30	92.30	92.30	92.80	92.39	104.80
	2	92.30	92.30	92.30	92.30	92.50	92.34	103.30
Manakau	20	92.30	92.30	92.30	92.30	96.40	92.90	127.40
	12	92.30	92.30	92.30	92.30	94.40	92.61	134.40
	5	92.30	92.30	92.30	92.30	93.50	92.49	124.10
	2	92.30	92.30	92.30	92.30	93.40	92.46	109.20
Kawhia	12	92.30	92.30	92.30	92.30	93.40	92.44	102.80
	2	92.30	92.30	92.30	92.30	92.90	92.36	98.00
New Plymouth	12	99.70	99.70	100.70	103.10	106.50	101.76	135.50
	2	99.70	99.70	99.90	102.40	116.80	102.69	138.00
STB	2	102.20	102.20	102.30	102.30	103.60	102.45	109.10
	12	104.80	104.80	104.80	105.00	105.90	105.05	133.90
	50	105.30	105.30	105.40	105.40	105.50	105.39	120.10
Cape Egmont	2	103.70	103.70	103.80	104.50	110.30	104.81	124.50

Table 5: July: Summary of statistics for HF-weighted SPL. SPL units: dB re 1 µPa. Grey cells indicate the percentiles equal to the baseline quiet noise level.

Location	Distance from shore (nmi)	Percentile					Mean	Maximum
		5th	25th	50th	75th	95th		
Kaipara	12	61.10	61.10	61.10	61.10	61.80	61.28	83.80
	2	61.10	61.10	61.10	61.10	61.30	61.21	83.70
Manakau	20	61.10	61.10	61.10	61.10	71.00	62.33	109.90
	12	61.10	61.10	61.10	61.10	66.60	61.82	105.70
	5	61.10	61.10	61.10	61.10	64.10	61.56	97.70
	2	61.10	61.10	61.10	61.10	63.80	61.52	86.30
Kawhia	12	61.10	61.10	61.10	61.10	63.90	61.48	76.30
	2	61.10	61.10	61.10	61.10	62.40	61.28	73.40
New Plymouth	12	71.00	71.00	73.20	77.20	81.70	74.49	104.60
	2	71.10	71.10	71.20	75.80	95.50	75.48	114.30
STB	2	74.10	74.10	74.10	74.20	76.50	74.42	88.90
	12	78.20	78.20	78.20	78.30	79.60	78.54	105.30
	50	78.50	78.50	78.50	78.50	78.60	78.53	91.70
Cape Egmont	2	76.60	76.60	76.60	77.80	86.60	78.26	107.30

5. DISCUSSION

Vessel information extracted from the AIS dataset for the year of July 2014 to June 2015 within the study area was used to determine density and speed grids by vessel category for the full year, along with summer and winter seasons separately.

Within the study area, the cumulative noise model was used to model the sound from vessels and the two marine seismic surveys which occurred during the representative summer and winter months of March and July. This modelling created maps of the sound field in 1-minute time steps for each month, yielding maps of Sound Pressure Level (SPL) as a function of easting, northing, frequency, and time. Maps were then created of both unweighted and frequency weighted sound levels to account for the hearing capability of Maui dolphins, which are classified as high-frequency cetaceans by NOAA (NMFS 2018).

These modelled sound fields were sampled at 14 receiver locations defined in consultation with MPI, and the results are presented as plots of unweighted and HF-weighted received sound levels over each month.

5.1 STUDY LIMITATIONS

The modelling did not consider small vessels without AIS transponders, vessels operating under alternative states, echosounders or sonar, or construction activities such as pile driving, and variable ambient noise levels. These sources were not included due to an inability to source reliable information which would allow them to be modelled with any certainty. Each of these sources is addressed below.

- Noise produced by most small vessels is not included, because they do not appear in the AIS dataset. If a dataset like AIS data did exist for the small vessel traffic, it would be possible to consider them, however this exercise would only be of value in confined areas such as harbours. The scale of the modelling would require increased environmental parameter certainty and due to the complexity of obtaining reliable information to inform this modelling, acoustic monitoring is likely to be a more effective method for examining their contribution.
- Sound emissions for vessels were modelled based on the speed of the vessel, using scaling of source levels to account for the effect of higher or lower speeds. However vessels sometimes operate under entirely different states from their typical operations. For example vessels, particularly research or oil and gas vessels, may operate in states such as drifting under idle or using dynamic positioning. A vessel under idle and drifting will not produce noise due to cavitation, while vessels under dynamic positioning can emit different noise levels depending upon the weather, currents, and operational requirements. Since it is unlikely that detailed operational state information can be obtained, modelling sound emissions based on speed is considered to be reasonable.
- The contribution from echosounders and sonars in Maui dolphin habitat could be approximated qualitatively by considering vessel category density in areas of interest and the likely footprints from the typical echosounders and sonars that are likely to be mounted on such vessels. However, this depends on sufficient information on vessel sonars being available to perform such an analysis, which is not known. These sources (apart from naval sonars) are highly directional, with the highest levels in the vertical direction, and high frequency, and thus have a limited horizontal footprint.
- Construction activities could be considered if information was available, however these would have to be on a case by case basis. Pile driving can occur as part of offshore platform installation, drill rig anchor installation, or coastal harbour development. It is unlikely that such information is available from the period considered.

- Baseline noise levels were determined by weather conditions during the study period. The use of ambient monitoring data from the STB to create a baseline quiet noise level providing a realistic lower bound to the ambient noise predictions is appropriate to ensure that unrealistic sound levels are not modelled. However, ideally measurement data coupled with time-dependent data on wind speeds and weather from across the modelling region could have been used to create a more realistic baseline noise level accounting for biological and natural noise sources. An example of accounting for time-fluctuating wind noise is provided in MacGillivray et al. (2014c). However, there was insufficient data or time available for this area to do this analysis for this study.

The modelling results described in this report are representative of the year from July 2014 through to June 2015. While comparisons can be made to other periods of time, there will be differences due to changes in the details and locations of the noise sources. The locations of commercial shipping lanes and infrastructure such as existing FPSOs and jackup platforms are unlikely to change in the short term, however seismic surveys depend upon the location of interest for the survey and therefore will change from year to year. If particular vessel operations (such as offshore construction) or seismic surveys occur closer to Maui dolphin habitat, or to the receiver locations considered in this study, the sound levels at these locations could be higher than is estimated in this study. The effect of the addition of new industrial infrastructure, such as additional FPSOs, jackup rigs or seabed mining operations is also not represented in this modelling study.

5.2 SUMMARY OF RESULTS

The density and speed grids derived from the AIS data show that during the 2014–15 period vessel traffic density was low within 12 nmi of the west coast north of Waiiti. The main traffic in this area was concentrated near the harbours of Manakau and Kawhia. The amount of traffic increased moving from Waiiti to New Plymouth. There were also differences in traffic in terms of density and location between summer and winter –traffic levels in winter were lower, although the differences are less for the categories of vessels which comprise most of the commercial shipping, such as bulkers, container ships, tankers and vehicle carriers. There was a significant different in the density of fishing vessels between summer and winter. In winter the traffic density in the area of interest was lower, but there were also significantly lower densities off the West Coast of the North Island, and therefore less noise from this category in this area.

The propagation conditions in winter support longer range propagation and lower rates of attenuation, thus equivalent noise sources can have a larger footprint at this time. The difference between the levels at the relevant receiver locations between March 2015 and July 2014 is however minimal, with no change in the medians. This is because there is less vessel traffic, and no winter seismic surveys north of the Taranaki close to the areas of relevance to the Maui dolphins. In this area, the study considered sound field sampling locations at Kaipara, Manakau and Kawhia. Of these three locations, the 95th percentile of the HF-weighted SPL was different by more than 1 dB at only two locations, Manakau 20 and 12 nmi, with the differences being 5.4 and 2.7 dB respectively. This is likely to be in part due to the proximity of the TGS Northwest Frontier Multiclient 2-D MSS, with the closest impulses being 12.7 km and 26 km from the two locations respectively. These results align with components of airgun arrays impulses relevant to high-frequency cetaceans being able to propagate over these distances, as has been reported in other studies (e.g. Martin et al. 2017).

There is a greater difference between the maximum levels, with the maximum being 25.7 dB at the Kawhia 2 nmi site, which is likely to be due to an individual sound source passing in close proximity (as shown in Figure 15). The similarity between the percentiles for HF-weighted SPL at these northern sites indicates that the relatively sparse line spacing of the TGS Northwest Frontier Multiclient 2-D MSS only influenced the sound field during March to a limited extent. Examples of this can be seen when the TGS MSS approaches Kaipara on March 4 (Figures 18 and 20), however while the unweighted SPL increases by approximately 26 dB at the closest point of approach, the HF-weighted SPL only increases by approximately 15 dB (Figure 18). The same survey approached Manakau on March 11 (Figure 21), and the increase in the HF-weighted SPL is less than approximately 5 dB. However, at

least 75 percent of the time, the sound levels at Kaipara, Manakau and Kawhia are predicted to be driven by either non-anthropogenic sources such as natural (wind and waves) and biological sources, or anthropogenic sources not included in the modelling study.

The receivers located at Cape Egmont (2 nmi), and in the STB (12 and 50 nmi) have noise floors above the baseline quiet noise level used for the study. This is due to the proximity of infrastructure such as FPSOs and jackup platforms and their constant contribution to the soundscape. The receiver locations from New Plymouth south all have higher HF-weighted sound levels in winter, apart from the maximum level at STB 12 and 50 nmi locations, which could be driven by individual sources. The traffic density at these locations is primarily from industrial sources. During the study period there was virtually no government / research tracks in this area during winter (Figure 4). The traffic density in this region does not change significantly between seasons. Therefore, the longer-range sound propagation and lower attenuation in winter is likely to be a significant factor in the higher sound levels during the winter season. The closest seismic survey modelled to these receivers was the Todd Trestles 3-D MSS which occurred in early March. The influence on the received levels can be seen in Figures 16 and 17 between March 2–5 and March 9–10, with the plots showing the changing sound levels as the airgun array is active along lines and inactive during turns (Figure 19). The survey has the greatest influence on the levels at Cape Egmont, with the maximum unweighted and HF-weighted SPL being approximately 130 dB re 1 µPa and 90 dB re 1 µPa respectively. Vessel traffic resulted in higher levels at all receiver locations in this region. The receivers at New Plymouth and Cape Egmont experience the greatest number of proximal vessels, and thus the predicted levels are always greater than the baseline quiet noise level considered in the study.

5.3 BIOLOGICAL THRESHOLDS

To determine the perception of sounds by marine fauna, including Maui dolphins, it is essential to consider the species'/subject's absolute hearing sensitivity and, in addition, the critical ratio and critical bandwidth of its hearing system (Erbe et al. 2016). However, such data is not available for Maui dolphins and, moreover, this was beyond the scope of work of this modelling study; instead, a comparison of modelled sound levels with ambient sound levels has been conducted to clearly identify locations at which sound levels are higher.

Numerous studies on marine mammal behavioural responses to sound exposure have not provided enough information to determine an appropriate metric for assessing behavioural reactions. However, it is recognised that the context in which the sound is received affects the nature and extent of responses to a stimulus (Southall et al. 2007, Ellison & Frankel 2012). Because of the complexity and variability of marine mammal behavioural responses to acoustic exposure, the scientific debate is still ongoing and NMFS has not yet released technical guidance on behaviour thresholds for use in calculating animal exposures (NMFS 2018).

Some behavioural effect assessment approaches (Wood et al. 2012, BOEM 2017) use frequency-weighted SPL as considered in this study, with recent applications updated to account for more recent frequency weighting. This applies the auditory weighting functions beyond simply the intent of assessing the risk of noise induced hearing loss. The sound level statistics provided for broadband (unweighted) and HF-weighted SPL for March (Tables 2 and 3) and June (Tables 4 and 5) can be compared to such behavioural effect assessment approaches. While HF-weighted results are provided, the broadband unweighted results for the sources considered in this study (lower frequency sources) are comparable to results expected if low-frequency cetacean weighting (NMFS 2018) is applied. Ideally, this approach would also consider the actual hearing capabilities of the species of interest, such as Maui dolphins or relevant mysticetes, however this information is currently not available.

5.4 RECOMMENDATIONS FOR FUTURE WORK

Recommendations for future work that would assist in an increased understanding of Maui dolphins, the environment they live in, and their reactions to anthropogenic noise and potential impacts could include:

- Long-term noise monitoring in selected habitats within the home range of Hector's or Maui dolphins would provide information about their presence and abundance, as well as relevant information for more detailed noise modelling. AIS data and other data sources on vessel movements and industrial activities could be integrated making it possible to quantify or even identify the types of vessels.
- Measurement of hearing sensitivity in Hector's or Maui Dolphins; as no data exist on their hearing sensitivity, frequency of best hearing and overall frequency range of their hearing. These measurements could be done using Auditory Evoked Potential techniques on live-stranded animals or alternatively captive Commersons's dolphins could be used as a surrogate species.
- An auditory masking study would reveal the potential influence of vessel noise and other sound sources on the perception of important acoustic stimuli for these animals.
- A TTS study on a Hector's or Maui Dolphins surrogate species in a controlled setting (for example *C. commersonii*, in captivity) would allow the assessment of their sensitivity to man-made noise and inform underwater noise regulation.
- A Behavioural Response Study (BRS) on Hector's dolphins with sound sources including continuous (different vessel types) and impulsive sources (playback).
- Satellite telemetry on Hector's or Maui Dolphins to investigate their behaviour, home range and reactions to disturbances; ideally, using acoustic tags which would make it possible to establish a precise correlation of sound exposure and behavioural reactions.
- The effectiveness of fisheries bycatch mitigation using acoustic techniques, such as passive acoustic tracking of dolphins to assess effectiveness and appropriateness of bycatch mitigation pingers.

6. ACKNOWLEDGMENTS

This project was funded under Ministry for Primary Industries project SEA2017-27.

7. REFERENCES

[BOEM] Bureau of Ocean Energy Management. (2017). Gulf of Mexico OCS Proposed Geological and Geophysical Activities. Western, Central, and Eastern Planning Areas. Final Programmatic Environmental Impact Statement. Volume IV: Appendices M and N. Document Number 2017-051. Prepared by CSA Ocean Sciences, Stuart, FL. 702 p. https://www.boem.gov/BOEM-2017-051-v4/.

[ISO] International Organization for Standardization. (2006). *ISO 80000-3:2006. Quantities and units -- Part 3: Space and time*. https://www.iso.org/standard/31888.html.

[ISO] International Organization for Standardization. (2017). *ISO/DIS 18405.2:2017. Underwater acoustics—Terminology*. Geneva. https://www.iso.org/standard/62406.html.

[NIOSH] National Institute for Occupational Safety and Health. (1998). *Criteria for a recommended standard: Occupational noise exposure*. Document Number 98-126. U.S. Department of Health and Human Services, NIOSH, Cincinnati, OH. 122 p.

[NMFS] National Marine Fisheries Service. (2018). 2018 Revision to: Technical Guidance for Assessing the Effects of Anthropogenic Sound on Marine Mammal Hearing (Version 2.0): Underwater Thresholds for Onset of Permanent and Temporary Threshold Shifts. U.S. Department of

Commerce, NOAA. NOAA Technical Memorandum NMFS-OPR-59. 167 p. https://www.fisheries.noaa.gov/webdam/download/75962998.

[NOAA] National Oceanic and Atmospheric Administration. (2013). Draft guidance for assessing the effects of anthropogenic sound on marine mammals: Acoustic threshold levels for onset of permanent and temporary threshold shifts, December 2013, Silver Spring, MA: NMFS Office of Protected Resources, p. 76. http://www.nmfs.noaa.gov/pr/acoustics/draft_acoustic_guidance_2013.pdf.

[NOAA] National Oceanic and Atmospheric Administration. (2015). Draft guidance for assessing the effects of anthropogenic sound on marine mammal hearing: Underwater acoustic threshold levels for onset of permanent and temporary threshold shifts, July 2015, 180 p. Silver Spring, Maryland: NMFS Office of Protected Resources. http://www.nmfs.noaa.gov/pr/acoustics/draft%20acoustic%20guidance%20July%202015.pdf.

[REM] Resource and Environmental Management Limited. (2015). *Trestles 3D Seismic Survey: Marine Mammal Impact Assessment*. Report for Todd Energy Limited, Nelson. https://www.doc.govt.nz/Documents/conservation/marine-and-coastal/mmia/todd-energy-trestles-3d-seismic-survey-mmia-taranaki.pdf.

ANSI S12.7-1986. R2006. *American National Standard Methods for Measurements of Impulsive Noise*. American National Standards Institute, New York.

ANSI S1.1-1994. R2004. *American National Standard Acoustical Terminology*. American National Standards Institute, New York.

ANSI/ASA S1.13-2005. R2010. *American National Standard Measurement of Sound Pressure Levels in Air*. American National Standards Institute and Acoustical Society of America, New York.

ANSI/ASA S3.20-1995. R2008. *American National Standard Bioacoustical Terminology*. American National Standards Institute and Acoustical Society of America, New York.

ANSI/ASA S12.64/Part 1. R2009. American National Standard Quantities and Procedures for Description and Measurement of Underwater Sound from Ships Part 1: General Requirements. American National Standards Institute and Acoustical Society of America, New York.

Becker, J.J.; Sandwell, D.T.; Smith, W.H.F.; Braud, J.; Binder, B.; Depner, J.; Fabre, D.; Factor, J.; Ingalls, S. et al. (2009). Global Bathymetry and Elevation Data at 30 Arc Seconds Resolution: SRTM30_PLUS. *Marine Geodesy* 32(4): 355–371.

Buckingham, M.J. (2005). Compressional and shear wave properties of marine sediments: Comparisons between theory and data. *Journal of the Acoustical Society of America* 117(1): 137–152. http://dx.doi.org/10.1121/1.1810231.

Carnes, M.R. (2009). *Description and Evaluation of GDEM-V 3.0*. Document Number NRL Memorandum Report 7330-09-9165. U.S. Naval Research Laboratory, Stennis Space Center, MS. 21 pp.

Collins, M.D. (1993). A split-step Padé solution for the parabolic equation method. *Journal of the Acoustical Society of America* 93(4): 1736–1742. https://doi.org/10.1121/1.406739.

Collins, M.D.; Cederberg, R.J.; King, D.B.; Chin-Bing, S. (1996). Comparison of algorithms for solving parabolic wave equations. *Journal of the Acoustical Society of America* 100(1): 178–182. https://doi.org/10.1121/1.415921.

Coppens, A.B. (1981). Simple equations for the speed of sound in Neptunian waters. *Journal of the Acoustical Society of America* 69(3): 862–863. http://dx.doi.org/10.1121/1.385486.

Delarue, J.; Mouy, X.; McPherson, C. (2017). *Acoustic Monitoring in the Cook Strait Region: February 2017 to September 2017, Results Delivery Summary*. Document 01513, Version 1.0. Technical report by JASCO Applied Sciences for NIWA.

Dragoset, W.H. 1984. A comprehensive method for evaluating the design of airguns and airgun arrays. *Proceedings, 16th Annual Offshore Technology Conference* Volume 3, 7-9 May 1984. OTC 4747, Houston, TX. pp 75–84.

Ellison, W.T.; Frankel, A.S. (2012). A common sense approach to source metrics. *In* Popper, A.N. and A.D. Hawkins (eds.). *The Effects of Noise on Aquatic Life*. Springer, New York. pp 433–438.

Erbe, C. 2002. Underwater noise of whale-watching boats and potential effects on killer whales (*Orcinus orca*), based on an acoustic impact model. *Marine Mammal Science* 18(2): 394-418. https://dx.doi.org/10.1111/j.1748-7692.2002.tb01045.x.

Erbe, C.; Reichmuth, C.; Cunningham, K.; Lucke, K.; Dooling, R. (2016). Communication masking in marine mammals: A review and research strategy. *Marine Pollution Bulletin* 103(1): 15–38. https://doi.org/10.1016/j.marpolbul.2015.12.007.

Finneran, J.J. (2015). Auditory weighting functions and TTS/PTS exposure functions for cetaceans and marine carnivores. Technical report by SSC Pacific, San Diego, CA.

Finneran, J.J. (2016). *Auditory weighting functions and TTS/PTS exposure functions for marine mammals exposed to underwater noise*. Technical Report for Space and Naval Warfare Systems Center Pacific, San Diego, CA. 49 p. http://www.dtic.mil/dtic/tr/fulltext/u2/1026445.pdf.

François, R.E.; Garrison, G.R. (1982a). Sound absorption based on ocean measurements: Part II: Boric acid contribution and equation for total absorption. *Journal of the Acoustical Society of America* 72(6): 1879–1890. https://doi.org/10.1121/1.388673.

François, R.E.; Garrison, G.R. (1982b). Sound absorption based on ocean measurements: Part I: Pure water and magnesium sulfate contributions. *Journal of the Acoustical Society of America* 72(3): 896–907. https://doi.org/10.1121/1.388170.

Hamilton, E.L. (1980). Geoacoustic modeling of the sea floor. *Journal of the Acoustical Society of America* 68(5): 1313–1340. https://doi.org/10.1121/1.385100.

Hannay, D.E.; Mouy, X.; Li, Z. (2016). An automated real-time vessel sound measurement system for calculating monopole source levels using a modified version of ANSI/ASA S12.64-2009. *Canadian Acoustics* 44(3). https://jcaa.caa-aca.ca/index.php/jcaa/article/view/3002.

Landro, M. 1992. Modeling of GI gun signatures. *Geophysical Prospecting* 40: 721–747. https://doi.org/10.1111/j.1365-2478.1992.tb00549.x

Laws, R.M., L. Hatton, and M. Haartsen. 1990. Computer modeling of clustered airguns. *First Break* 8(9): 331–338.

Lurton, X. 2002. An Introduction to Underwater Acoustics: Principles and Applications. Springer, Chichester, UK. 347 pp.

MacGillivray, A.O.; Li, Z.; Warner, G.; O'Neill, C. (2014a). *APPENDIX 9.8-B Regional Commercial Vessel Traffic Underwater Noise Exposure Study*. Roberts Bank Terminal 2 Technical Report—Underwater Noise Construction Activities and Terminal Vessel Operations Noise Modelling Study. Technical report prepared by JASCO Applied Sciences for Port Metro Vancouver. 80 pp. http://www.ceaa-acee.gc.ca/050/documents/p80054/101367E.pdf.

MacGillivray, A.O., Z. Li, G. Warner, and C. O'Neill. 2014b. Regional Commercial Vessel Traffic Underwater Noise Exposure Study. *In Roberts Bank Terminal 2 Project Environmental Impact Statement*. Volume 2, Appendix 9.8-B. Canadian Environmental Assessment Agency Registry Reference Number 80054. http://www.ceaa-acee.gc.ca/050/documents/p80054/101367E.pdf.

MacGillivray, A.O., McPherson, C.R.; McPherson, G.; Izett, J.; Gosselin, J.; Zizheng, L.; Hannay, D.E. (2014c). Modelling underwater shipping noise in the Great Barrier Reef Marine Park using AIS vessel track data. *Internoise 2014*. Nov 16-19, Melbourne Australia. p. 10. http://www.acoustics.asn.au/conference_proceedings/INTERNOISE2014/papers/p671.pdf.

MacGillivray, A.O., Li, Z.; Yurk, H. (2018a). *Modelling of Cumulative Vessel Noise for Haro Strait Slowdown Trial: Final Report*. Document Number 01577. Version 2.0. Technical report by JASCO Applied Sciences for Vancouver Fraser Port Authority ECHO Program. https://www.flipsnack.com/portvancouver/echo-haro-strait-slowdown-trial-summary/full-view.html

MacGillivray, A.O.; Li, Z.; Yurk, H. (2018b). Modelling of Cumulative Vessel Noise for Haro Strait Slowdown Trial: Final Report. *In ECHO Program: Voluntary Vessel Slowdown Trial Summary Findings*. Appendix A. Vancouver Fraser Port Authority. https://www.flipsnack.com/portvancouver/echo-haro-strait-slowdown-trial-summary/full-view.html.

Martin, S.B.; Matthews, M.-N.R.; MacDonnell, J.T.; Bröker, K. (2017). Characteristics of seismic survey pulses and the ambient soundscape in Baffin Bay and Melville Bay, West Greenland. *Journal of the Acoustical Society of America* 142(6): 3331–3346. https://doi.org/10.1121/1.5014049.

Mattsson, A. and M. Jenkerson. 2008. Single Airgun and Cluster Measurement Project. Joint Industry Programme (JIP) on Exploration and Production Sound and Marine Life Proramme Review, October 28-30. International Association of Oil and Gas Producers, Houston, TX.

McPherson, C.; MacGillivray, A.; Hagar, E. (2018). *Validation of airgun array modelled source signatures*. *176th Meeting Acoustical Society of America*, 5–9 November 2018. Accepted Abstract, Victoria, BC, Canada.

McPherson, C.R., M. Wood, and R.G. Racca. 2016. Potential Impacts of Underwater Noise from Operation of the Barossa FPSO Facility on Marine Fauna, ConocoPhillips Barossa Project. Document Number 01117, Version 1.0. Technical report by JASCO Applied Sciences for Jacobs. Appendix N of Barossa Area Development Offshore Project Proposal. https://www.nopsema.gov.au/assets/OPPs/A598152-2.pdf.

McPherson, C.R.; Delarue, J.; Whitt, C.; Maxner, E.; Kowarski, K.; Mouy, X. (2017). *Acoustic Monitoring in the Cook Strait Region: June 2016 to December 2016, Summary Report*. Document Number 01391. Version 1.0. Technical report by JASCO Applied Sciences for NIWA.

Medwin, H.; Clay, C.S. (1997). *Fundamentals of Acoustical Oceanography*. Academic Press.

Probert, P.K.; Swanson, K.M. (1985). Sediment texture of the continental shelf and upper slope off the west coast of South Island, New Zealand. *New Zealand Journal of Marine and Freshwater Research* 19(4): 563–573. https://doi.org/10.1080/00288330.1985.9516119.

Quijano, J.; Hannay, D.E.; Austin, M.E. (2018). Composite Underwater Noise Footprint of a Shallow Arctic Exploration Drilling Project. *IEEE Journal Of Oceanic Engineering* doi: 10.1109/JOE.2018.2858606.

SLR Consulting NZ Limited. (2014). TGS-NOPEC Geophysical Company Northwest Frontier Multiclient 2D Marine Seismic Survey Marine Mammal Impact Assessment. 296 p.

SLR Consulting NZ Limited. (2017). *The Western Platform Multi Client 3D Seismic Survey Marine Mammal Impact Assessment*. Document Number 740.10032-R02. Version v1.0. Report for Schlumberger New Zealand Ltd, Nelson, New Zealand. https://www.doc.govt.nz/Documents/conservation/marine-and-coastal/mmia/schlumberger-2017-taranaki-basin-3dmc-seismic-survey-mmia-2017.pdf.

Southall, B.L.; Bowles, A.E.; Ellison, W.T.; Finneran, J.J.; Gentry, R.L.; Greene, C.R. Jr.; Kastak, D.; Ketten, D.R.; Miller, J.H. et al. (2007). Marine Mammal Noise Exposure Criteria: Initial Scientific Recommendations. *Aquatic Mammals* 33(4): 411–521. https://doi.org/10.1080/09524622.2008.9753846.

Teague, W.J.; Carron, M.J.; Hogan, P.J. (1990). A comparison between the Generalized Digital Environmental Model and Levitus climatologies. *Journal of Geophysical Research* 95(C5): 7167–7183.

Veirs, S., V. Veirs, and J.D. Wood. 2016. Ship noise extends to frequencies used for echolocation by endangered killer whales. *PeerJ* 4(e1657). https://doi.org/10.7717/peerj.1657.

Wenz, G.M. (1962). Acoustic Ambient Noise in the Ocean: Spectra and Sources. *Journal of the Acoustical Society of America* 34(12): 1936–1956. https://doi.org/10.1121/1.1909155.

Wood, J.; Southall, B.L.; Tollit, D.J. (2012). *PG&E offshore 3-D Seismic Survey Project Environmental Impact Report–Marine Mammal Technical Draft Report*. SMRU Ltd. 121 p. https://www.coastal.ca.gov/energy/seismic/mm-technical-report-EIR.pdf.

Zhang, Z.Y.; Tindle, C.T. (1995). Improved equivalent fluid approximations for a low shear speed ocean bottom. *Journal of the Acoustical Society of America* 98(6): 3391–3396. https://doi.org/10.1121/1.413789.

Ziolkowski, A. (1970). A method for calculating the output pressure waveform from an air gun. *Geophysical Journal of the Royal Astronomical Society* 21(2): 137–161. https://doi.org/10.1111/j.1365-246X.1970.tb01773.x.

8. APPENDIX A ENVIRONMENTAL PARAMETERS FOR ACOUSTIC MODELLING

A.1. Sediment geoacoustics

Seabed sediments for the modelling area considered in this study fall into two categories (SLR 2017): terrigenous mud in deeper waters (continental slope sediment), and terrigenous dominant fine sand with sparse coarse sand in shallow waters (continental shelf sediment). For the continental slope, sediment geoacoustic parameters (Table A-1) were obtained from regression curves corresponding to land-derived mud sediments suggested by Hamilton (1980).

Table A-1: Continental slope geoacoustic profile used as the input to the acoustic model at sites located in water depth greater than or equal to 400 m.

Material	Depth below seafloor (m)	Density (g/cm^3)	P-wave speed (m/s)	P-wave attenuation (dB/λ)	S-wave speed (m/s)	S-wave attenuation (dB/λ)
Land-derived mud	0–150	1.51–1.72	1522–1702	0.12–0.16	250	3.75
	150–300	1.72–1.89	1702–1853	0.16–0.22		
	300–600	1.89–2.16	1853–2093	0.22–0.25		
	600–1000	2.16–2.30	2093–2342	0.25–0.16		
	1000–2000	2.30–2.58	2342–3750	0.16–0.08		
Bedrock	>2000	2.58	3750	0.08		

For the continental shelf, samples collected in waters up to 200 m deep suggest fine sands with mean grain diameter of 0.125 mm (Probert & Swanson 1985). With this grain size, a sediment grain-shearing model (Buckingham 2005) was used to estimate the density, compressional-wave speed, shear-wave speed, and compressional-wave attenuation for the upper sediment layer (Table A-2).

Table A-2: Continental shelf geoacoustic profile used as the input to the acoustic model at sites located in water depth less than 400 m.

Material	Depth below seafloor (m)	Density (g/cm^3)	P-wave speed (m/s)	P-wave attenuation (dB/λ)	S-wave speed (m/s)	S-wave attenuation (dB/λ)
Land-derived fine sand	0–150	1.83	1614–2212	0.37–1.90	400	3.65
	150–300		2212–2422	1.90–2.19		
	300–600		2422–2696	2.19–2.47		
	600–1000		2696–2950	2.47–2.67		
	1000–2000		2950–3750	2.67–0.08		
Bedrock	>2000	2.58	3750	0.08		

A.2 Bathymetry

Water depths throughout the modelled area (Figure 1) were extracted from the SRTM 15+ dataset (Becker et al. 2009). Bathymetry data were extracted and re-gridded onto a Universal Transverse Mercator (UTM) coordinate projection (Zone 60 S) with a regular grid spacing of 1000 × 1000 m.

A.3 Sound speed profile

Water sound speed profiles in this work were derived from temperature and salinity profiles from the U.S. Naval Oceanographic Office's Generalized Digital Environmental Model V 3.0 (GDEM; Teague et al. 1990, Carnes 2009). GDEM provides an ocean climatology of temperature and salinity for the world's oceans on a latitude-longitude grid with 0.25° resolution, with a temporal resolution of one month, based on global historical observations from the U.S. Navy's Master Oceanographic Observational Data Set (MOODS). The temperature and salinity profiles were converted to sound speed profiles according to the equations of Coppens (1981).

The sound speed profiles for March and July were calculated at four locations: one on the continental shelf near shore, and three at progressively deeper locations farther offshore (up to 2000 m depth). The SSP for each month was obtained as an average of the sound speed at the four locations. Since the maximum water depth for the modelling area is 4380 m, the final profiles for modelling (Figure A-1) were extrapolated beyond 2000 m depth, assuming a vertical gradient of 16 m/s per km (Medwin & Clay 1997).

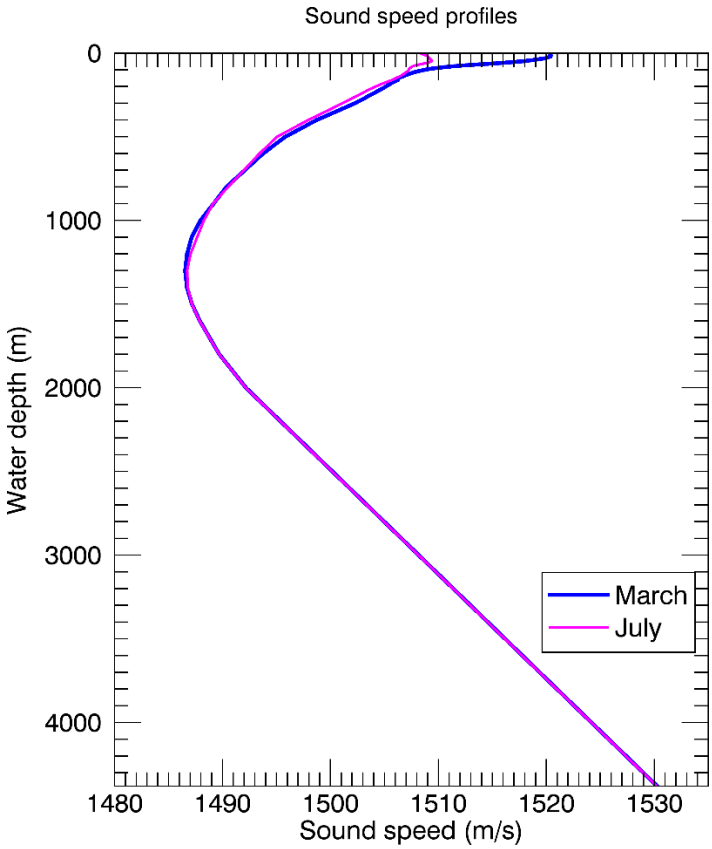

Figure A-1: March and July sound speed profiles used for the modelling. Profiles are calculated from temperature and salinity profiles from GDEM V 3.0 (Teague et al. 1990, Carnes 2009).

A.4 Background ambient noise

The NIWA Cook Strait acoustic monitoring programme occurred over two deployments, June to December 2016 and February to August 2017. Autonomous Multichannel Acoustic Recorders (AMARs) (http://www.jasco.com/amar/) were deployed at seven and six locations respectively across the Cook Strait region.

Two of these recording stations (Table A-3) were considered relevant for this project as they were located within the modelling region. Both AMARs recorded data on a duty cycle of 630 s at 16 kHz sampling rate, 125 s at 250 kHz sampling rate and 145 s sleep. The data from both recorders was processed to characterise total ocean noise and sounds from vessels, seismic surveys, and marine mammal calls, with results delivered to NIWA in the form of a detailed report for the 2016 deployment (McPherson et al. 2017) and a delivery of results for the 2017 deployment (Delarue et al. 2017).

Table A-3: Deployment details for each station.

Deployment Number	Station	Latitude	Longitude	Depth (m)	Deployment	Retrieval/ end of data
1	2	−40.41957	174.5074	110	4 Jun 2016	20 Dec 2016
2	2	-40.5259	174.7571	113	23 Feb 2017	29 Aug 2017

The ambient noise spectra from the two stations is represented in two forms in this report:

- Distribution of 1/3-octave-band SPLs (e.g., Figure A-2, top panel): These box-and-whisker plots show the average and extreme sound levels in each 1/3-octave-band.
- Power Spectral Densities (PSDs) (e.g. Figure A-2, bottom panel): The PSD plots show the statistical sound levels in 1 Hz frequency bins. The *n*th percentile level (L_n) is the level (i.e., PSD level, SPL, or SEL) which exceeds n% of the data. These levels can be directly compared to the Wenz curves. We also plot the spectral probability density (Merchant et al. 2013) to assess whether the distribution is multi-modal.

To create a baseline quiet noise level profile that could be considered conservative and does not include vessel noise and other anthropogenic sources and also represents the lower noise levels present during calm weather conditions, the 5th percentile level (L_5) from both stations was combined, with the lowest value taken at each frequency point. This approach is likely to underestimate true ambient sound levels, due to the contribution and variability of noise from natural sources such as wind and waves, however it therefore represents a quieter environment, and thus allows the assessment to be more conservative. The results for the 2016 deployment are shown in Figure A-2, and those for the 2017 deployment in Figure A-3. Although the recorders both recorded at a sampling rate of 250 kHz, characterising up to 120 kHz, to be conservative we extrapolated the ambient sound levels above 6 kHz following a linear decay based on the data from 1 kHz to 6 kHz. The resulting 1 Hz spectra was then converted to a 1/3-octave-band spectra (Figure A-4) for inclusion in the modelling. The broadband SPL (10–70 800 Hz) is 92.3 dB re 1 µPa while the HF-weighted ambient SPL is 61.1 dB re 1 µPa.

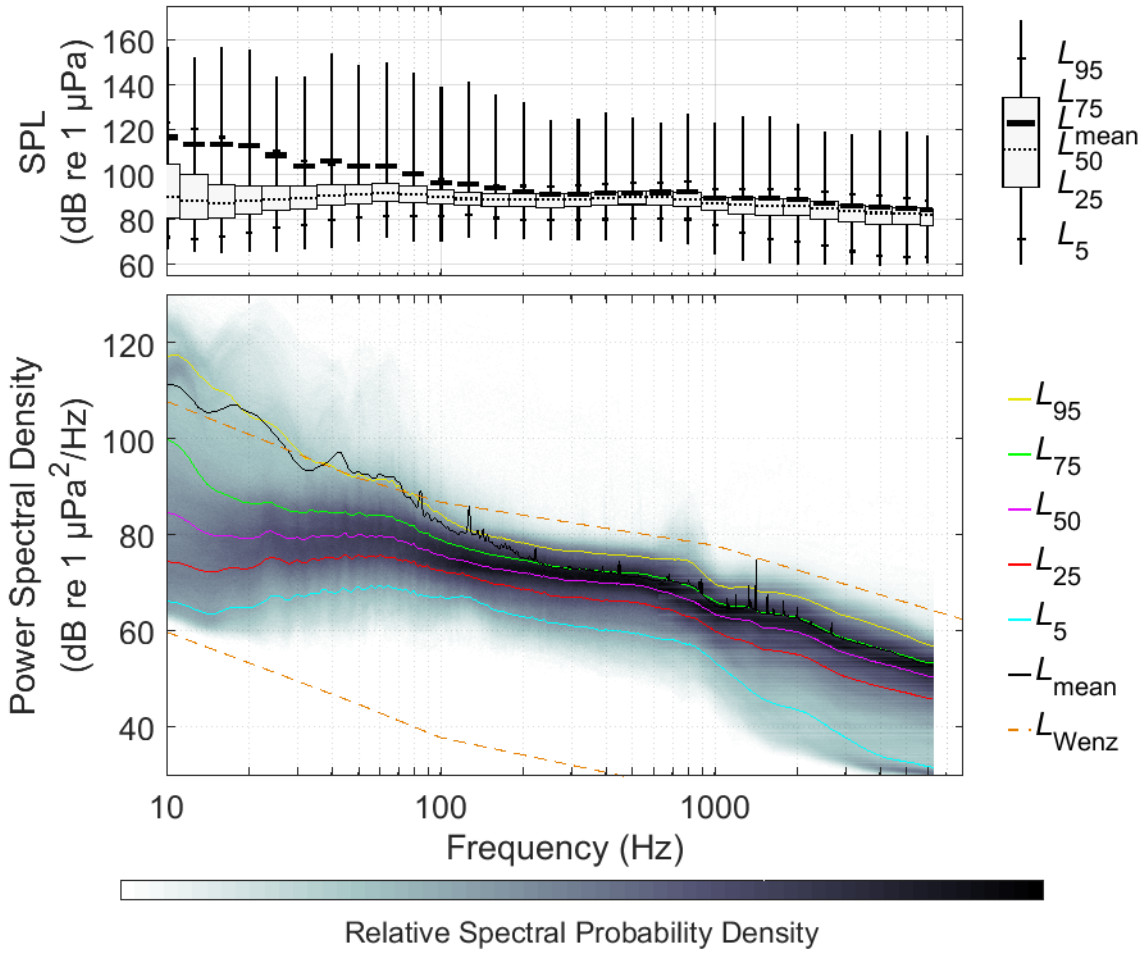

Figure A-2: Station 2, June – December 2016: Percentiles and mean of 1/3-octave-band SPL and (bottom) percentiles and probability density (grayscale) of 1-min PSD levels (McPherson et al. 2017) compared to the limits of prevailing noise (Wenz 1962).

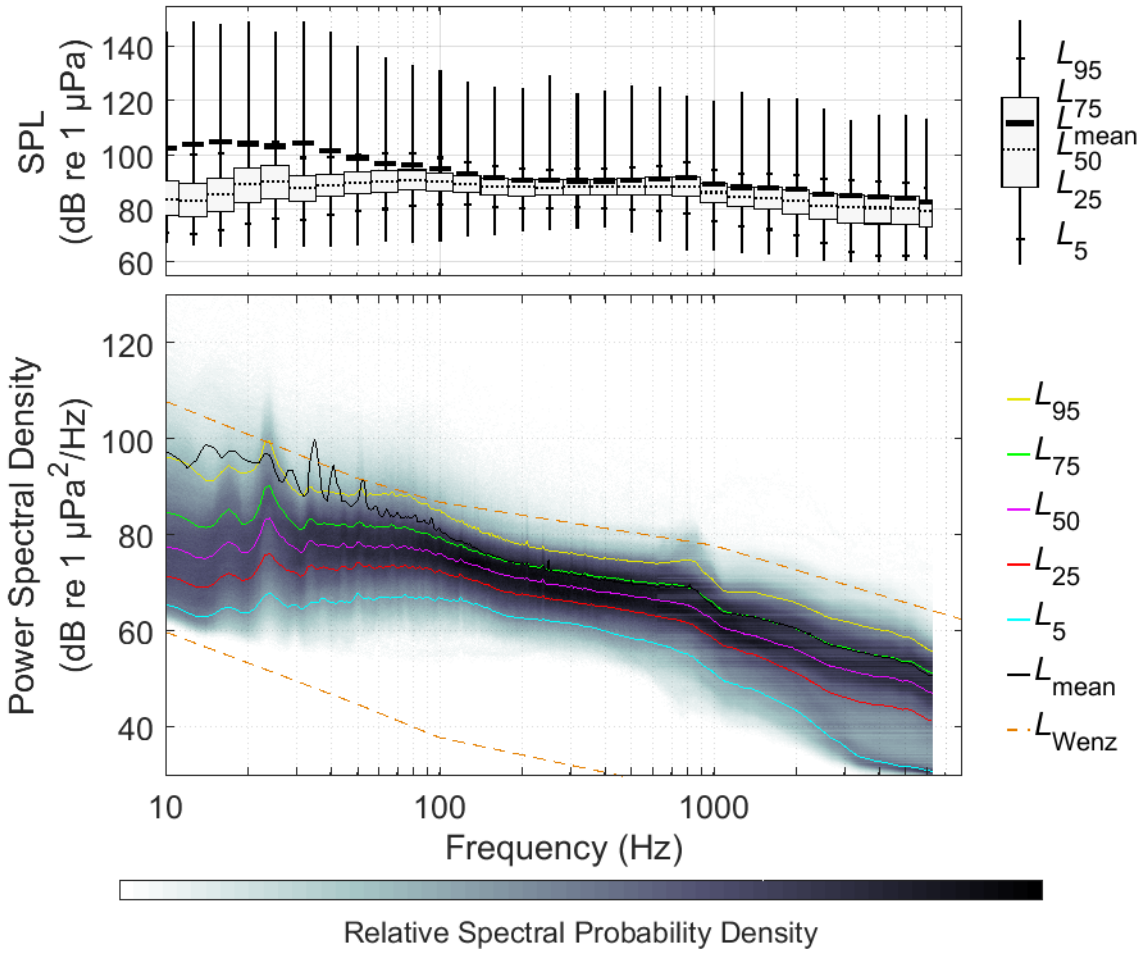

Figure A-3: Station 2, February – August 2017: Percentiles and mean of 1/3-octave-band SPL and (bottom) percentiles and probability density (grayscale) of 1-min PSD levels (Delarue et al. 2017) compared to the limits of prevailing noise (Wenz 1962).

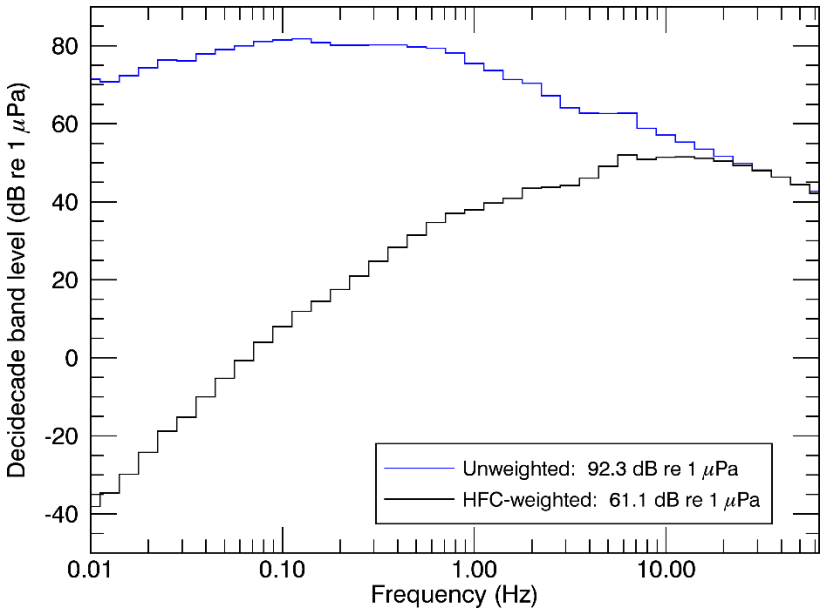

Figure A-4: Ambient noise levels obtained from NIWA Cook Strait Programme. Legend indicates the type of weighting and broadband SEL.

A.5 Model Uncertainty

All modelled assessment approaches contain an inherent level of uncertainty, which results from the individual uncertainty associated to each model input parameter. For some parameters, such as the airgun array sound source, there is little to no uncertainty (McPherson et al. 2018), as the seismic source array is a standard type of airgun array. There is a low-level uncertainty associated with the TGS Northwest Frontier Multiclient 2D MSS which provided all impulse locations, and a slightly increased uncertainty associated with the Todd Energy Trestles 3-D MSS, as impulse locations were approximated using the AIS track lines. On the other hand, uncertainties associated with vessel traffic are expected to be higher due to a larger number of mechanisms associated to vessel noise generation. For example:

- Although a significant number of vessel measurements have been used to determine the source levels for the majority of vessel categories (Appendix C), some vessels might be considered outliers within their category.
- In some cases, noise directivity has been shown to be relevant for noise estimation (Quijano et al. 2018). The model levels considered here are assumed to be isotropic (i.e., not dependent on direction of propagation from the ship).
- The sound levels for the FPSOs and platforms have been conservatively estimated from the literature, and the specific details of those present in New Zealand and operational conditions could result in different source levels, however these are likely be quieter than those included in the modelling.
- Inclusion of vessel traffic on dynamic positioning (information not available at the time of this study) and scaling of dynamic positioning levels based on whether conditions would result in higher accuracy on modelled levels.

The propagation model used in this study is based on an understanding of the physics of sound propagation through the water. This model has been extensively tested during its development and use (Appendix B). Uncertainty in the transmission model arises from the choice of parameter values, such as the sound speed profile and the geoacoustic parameters of the ocean bottom substrate.

9. APPENDIX B TRANSMISSION LOSS MODEL

The propagation of sound through the environment was modelled by predicting the acoustic transmission loss—a measure, in decibels, of the decrease in sound level between a source and a receiver some distance away. Geometric spreading of acoustic waves is the predominant way by which transmission loss occurs. Transmission loss also happens when the sound is absorbed and scattered within seawater, and absorbed scattered, and reflected at the water surface and within the seabed. Transmission loss depends on the acoustic properties of the ocean and seabed; its value changes with frequency.

If the acoustic source level (SL), expressed in dB re 1 μPa^2m^2, and transmission loss (TL), in units of dB, at a given frequency are known, then the received level (RL) at a receiver location can be calculated in dB re 1 μPa by:

$$RL = SL - TL \quad \text{(B-1)}$$

Transmission loss was calculated using JASCO's Marine Operations Noise Model (MONM). MONM computes acoustic propagation via a wide-angle parabolic equation solution to the acoustic wave equation (Collins 1993) based on a version of the U.S. Naval Research Laboratory's Range-dependent Acoustic Model (RAM), which has been modified to account for elastic seabed properties (Zhang & Tindle 1995). The parabolic equation method has been extensively benchmarked and is widely employed in the underwater acoustics community (Collins et al. 1996). MONM incorporates the following site-specific environmental properties: a bathymetric grid of the model area; underwater sound speed as a function of depth; and a geoacoustic profile based on the overall stratified composition of the seafloor.

The study area was divided into 9 zones (Figure B-1) based on water depth ranges (Table B-1). Sediment geoacoustic parameters for each zone were applied based on the water depth (i.e., continental shelf versus continental slope, see Appendix A-1). MONM was used to compute curves of frequency- and range-dependent transmission loss for each zone in 1/3-octave-bands between 10 Hz and 5 kHz, out to a maximum distance of 100 km from the source (Figure B-2). Transmission loss for each zone was modelled assuming uniform bathymetry (i.e., range-independent water depth) for a receiver depth of 10 m. Transmission loss was averaged over five frequencies inside each 1/3-octave-band and the transmission loss compared to range curves are smoothed inside a 200 m window to remove fine-scale interference effects. At high frequencies, mean transmission loss computed by MONM is expected to converge to a high frequency (i.e., ray-theoretical) limit; therefore, transmission loss values for bands above 5 kHz are approximated by adjusting transmission loss at 5 kHz to account for frequency-dependent absorption at higher frequencies (François & Garrison 1982a, 1982b). For each zone, transmission loss was modelled using two different sound speed profiles, representing March and July conditions (Figure A-1), and eleven source depths (1 to 10 m in 1 m step, in addition to 7.5 to model the TGS Northwest Frontier Multiclient 2-D MSS), representing the nominal acoustic emission centres of small and large draft vessels and seismic airgun arrays in this study. Figure B-2 presents plots that help to visualise how the modelled transmission loss varies by distance from the source and frequency, as well as with zones and seasons.

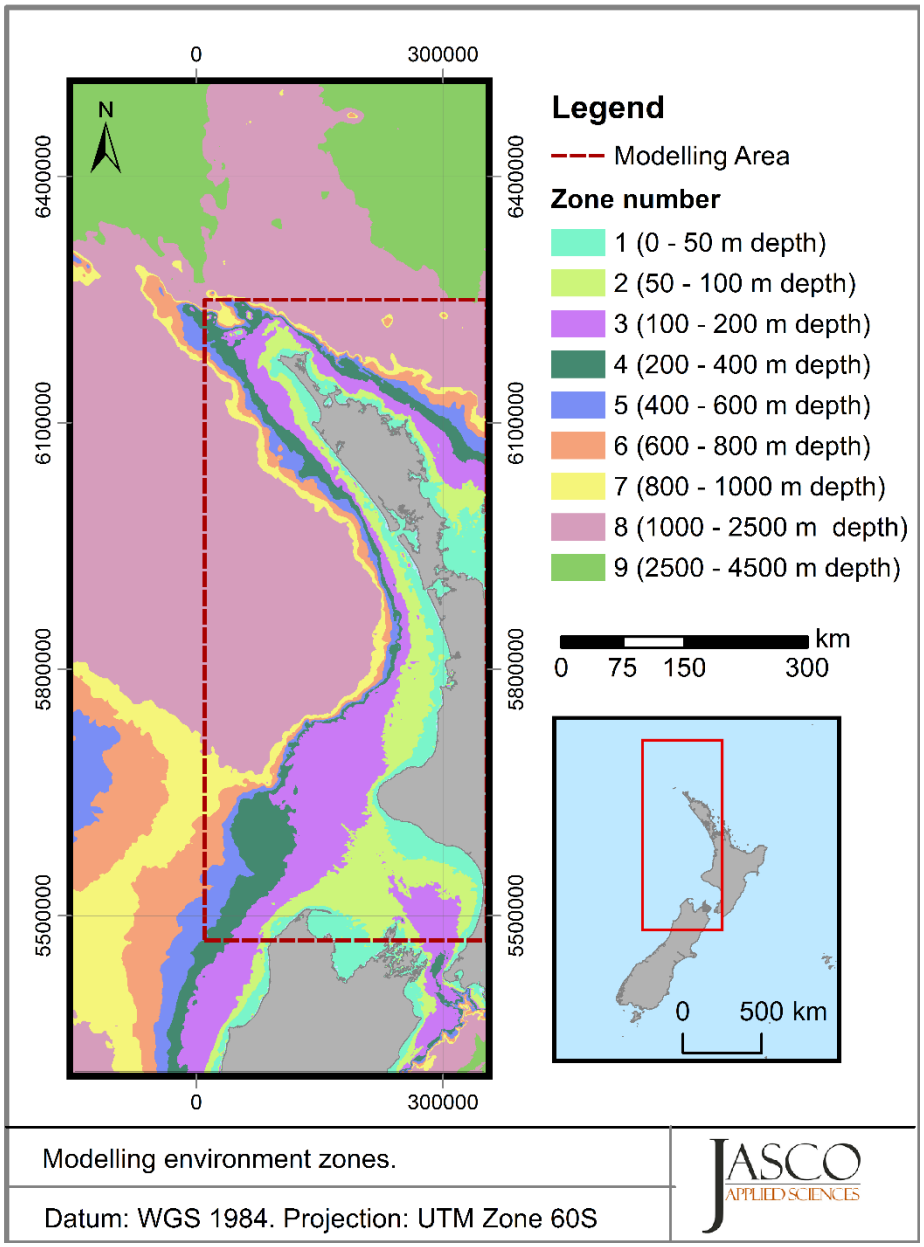

Figure B-1: Map of transmission loss (TL) zones (1–9) used for modelling sound propagation in the study area. Zones 1–4 were modelled using the continental shelf geoacoustic profile (Table A-2), while zones 5–9 were modelled using the continental slope geoacoustic profile (Table A-1).

Table B-1. Description of zone numbers and corresponding geoacoustics and water depths. Geoacoustic profiles of each region are described in Appendix A-1.

Zone	Water depth range (m)	Modelled water depth (m)	Geoacoustic profile
1	0–50	25	
2	50–100	75	Continental shelf
3	100–200	150	
4	200–400	300	
5	400–600	500	
6	600–800	700	
7	800–1000	900	Continental slope
8	1000–2500	1750	
9	2500–4500	3500	

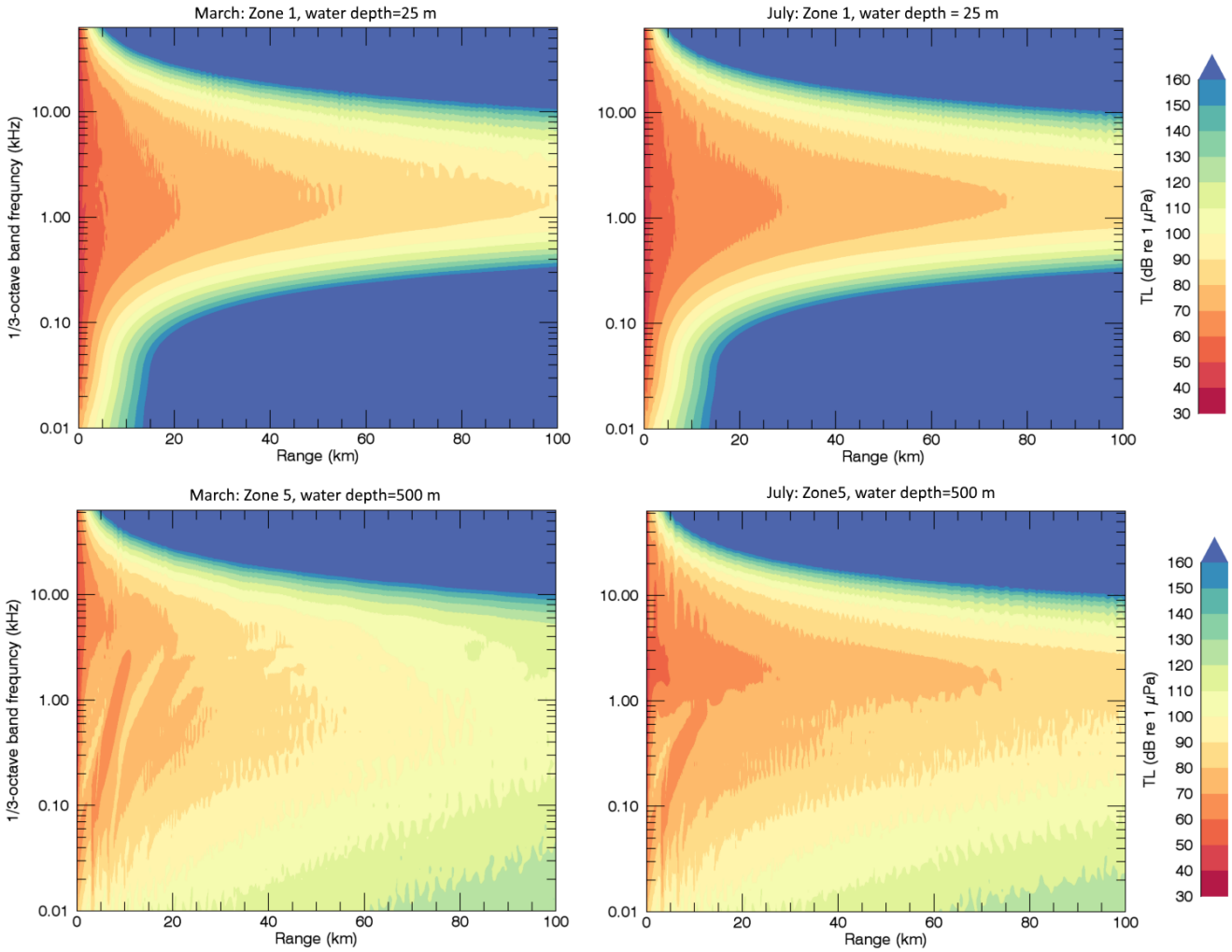

Figure B-2: Example plots of modelled transmission loss as a function of distance from the source and frequency. This example represents the transmission loss in Zone 1(top) and Zone 5 (bottom) seen in Figure B-1, for March (left) and July (right). Source and receiver depths are 7 and 10 m, respectively.

10. APPENDIX C VESSEL SOURCE LEVELS

Since September 2015, JASCO Applied Sciences, in partnership with Ocean Networks Canada (ONC) and the Vancouver Fraser Port Authority's Enhancing Cetacean Habitat and Observation (ECHO) Program, has been collecting measurements of vessel noise emissions (i.e., source levels) on their Underwater Listening Station (ULS) (Hannay et al. 2016), which is a cabled hydrophone system deployed off the coast of British Columbia (Canada). The ULS is situated adjacent to the inbound shipping lanes in the Strait of Georgia and records noise emissions of vessels bound for the Port of Vancouver. Automated processing of vessel source levels is performed by JASCO's ShipSound software, which uses AIS vessel tracking data to detect when vessels transit through the measurement funnel of the ULS. Valid vessel tracks, as selected by automated system, are used for the vessel source level analysis, which conforms approximately to the ANSI standard for ship sound measurements (ANSI/ASA S12.64/Part 1 2009).

ULS source levels for this study were obtained from a publicly available report that presented average source levels for different vessels categories based on an analysis of over 2700 individual ship noise measurements (MacGillivray et al. 2018a). For this study, monopole source levels from the ULS were assigned to nine different categories (Figure C 1, Table C 1), according to vessel category information embedded in the AIS logs: Bulker, Containership, Tug, Tanker, Vehicle Carrier, Fishing, Cruise, Ferry (Ro-Ro passenger), and Government/Research and Naval vessels. Source levels for six additional vessel categories not covered by the ULS data were obtained from other sources: Passenger (less than 100 m)[1]; High-speed craft[2]; Recreational[3]; Other; Floating Production Storage and Offloading (FPSO) facility during dynamic positioning (DP)[4], and jackup platform.

The FPSO facilities operate under DP as required by weather conditions and operational requirements (such as offtake), and as no information was available regarding the use of DP for the modelling study, a conservative approach was taken, which assumes that DP was always operational, and thus is likely to overestimate the contribution over time from these facilities. The locations of the platforms and FPSOs are shown in Figure C 2.

[1] Passenger (< 100 m) source levels were based on whale watching boast source level measurements (Erbe 2002).
[2] Similar to Clipper Ferry jet catamarans included in the slowdown study (MacGillivray et al. 2018a), High-speed craft were based on a vessel source level measurement from Veirs et al. (2016).
[3] Recreational and Other source levels were based on a prior review of published vessel measurements carried out for the Roberts Bank Terminal 2 cumulative modelling assessment (MacGillivray et al. 2014b).
[4] FPSO and Jackup platform source levels based on those presented in McPherson et al. (2016).

Table C-1: Summary of vessel classification.

Category	Length overall (m)	Vessel type
High-speed craft	0–50	Clipper; High Speed Craft; High-Speed Craft
Container	0–1000	Cargo/Containership; Container Ship
Fishing	0–1000	Factory Trawler; Fish Carrier; Fish Factory; Fishing; Fishing Vessel; Trawler
Government/Research	0–1000	Buoy-Laying Vessel; Fishery Patrol Vessel; Fishery Research Vessel; Law Enforce; Patrol Vessel; Replenishment Vessel; Research/Survey Vessel; Fire Fighting Vessel; SAR; Law Enforcement Vessel; Law Enforcement Vessel; Research Vessel; Search And Rescue Vessel; Fisheries Protection
Bulker	0–1000	Bulk Carrier; Cargo; Cargo - Hazard A (Major); General Cargo; LPG Tanker; Rail/Vehicles Carrier; Reefer; Ro-Ro/Container Carrier; Self Discharging Bulk Carrier; Timber Carrier; Wood Chips Carrier; Heavy Lift Vessel; Cement Carrier; General Ship; Not Available Or No Ship (Default); Heavy Load Carrier; Livestock Carrier; Vessel-Reserved For Future Use; Refrigerated Ship
Naval	0–1000	Naval; Naval Auxiliary; Engaged In Military Operations; Logistics Naval Vessel; Military Ops
Other	0–1000	Anti-Pollution; Cable Layer; Dive Vessel; Drill Ship; High Speed Craft; Hopper Dredger; Local Vessel; Other; Pilot Vessel; Port Tender; Reserved; Tender; Unspecified; Wing In Grnd; Anti-Pollution Vessel; Aton; Buoy; Dive Boat; Other Ship; Other Type Of Ship-All Ships Of This Type; Other Vessel; Pilot; Pilot Vessel; Service Ship; Vessel Engaged In Diving Operations; Workboat; Landing Craft; Icebreaker; Harbour Patrol; Unknown
Cruise	100–1000	Passenger; Passengers Ship; Cruise; Cruise Ship; Domestic Passenger; Passenger Ro Ro Ship; Passenger Ship; Passenger-All Ships Of This Type; Passenger-No Additional Information; Passenger-Reserved For Future Use; High-Speed-Craft
Passenger 100 m-	0–100	Passenger; Passengers Ship; Cruise; Cruise Ship; Domestic Passenger; Passenger Ro Ro Ship; Passenger Ship; Passenger-All Ships Of This Type; Passenger-No Additional Information; Passenger-Reserved For Future Use; High-Speed-Craft
Recreational	0–1000	Pleasure Craft; Yacht; Recreational; Sailing; Wig
Tanker	0–1000	Crude Oil Tanker; Tanker; Oil Products Tanker; Oil/Chemical Tanker; Bitumen Tanker; Chemical Oil Products Tanker; Chemical Tanker; LPG Tanker; Molasses Tanker; Fruit

Category	Length overall (m)	Vessel type
Tug and Support Vessels	0–1000	Juice Tanker; Oil And Chemical Tanker; Tankship Anchor Handling Vessel; Dredger; Hopper Dredger; Multi Purpose Offshore Vessel; Offshore Support Vessel; Offshore Tug Supply Ship; Offshore Vessel; Offshore Supply Ship; Pusher Tug; Towing Vessel; Tug; Pollution Control Vessel; Vessel engaged in dredging or underwater operations; Towing;
Vehicle Carrier	0–1000	Vehicle Carrier; Ro-Ro Cargo
FPSO (DP)	NA	Floating production storage and offloading (FPSO) platform during dynamic positioning (DP)
Jackup platform	NA	Oil or gas production facility using jackup legs for support

Figure C-1 shows frequency-dependent source levels by vessel category in 1/3-octave-bands used in this work. The reference for each category is indicated in the legend; scaling of source levels to account for the effect of higher/lower speeds was implemented as described in MacGillivray et al. (2018a). FPSOs and jackup platforms were assumed to be at the locations shown in Figure C-2 for the entire time interval considered in the model.

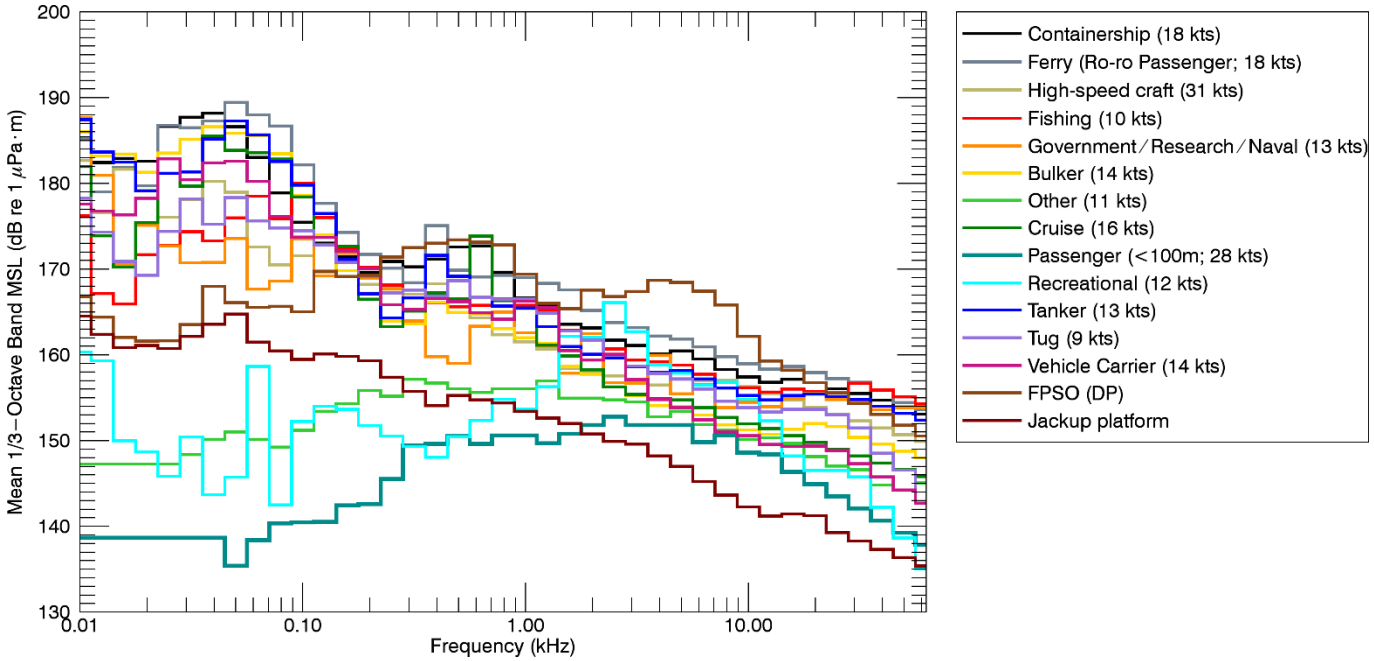

Figure C-1: Frequency-dependent source levels by vessel category, in 1/3-octave-bands (MacGillivray et al. 2018a). The reference speed (average transit speed, in knots) for each category is indicated in the legend. ULS source levels were extrapolated above 31 kHz based on the terminal slope of the 1/3-octave-band level curves.

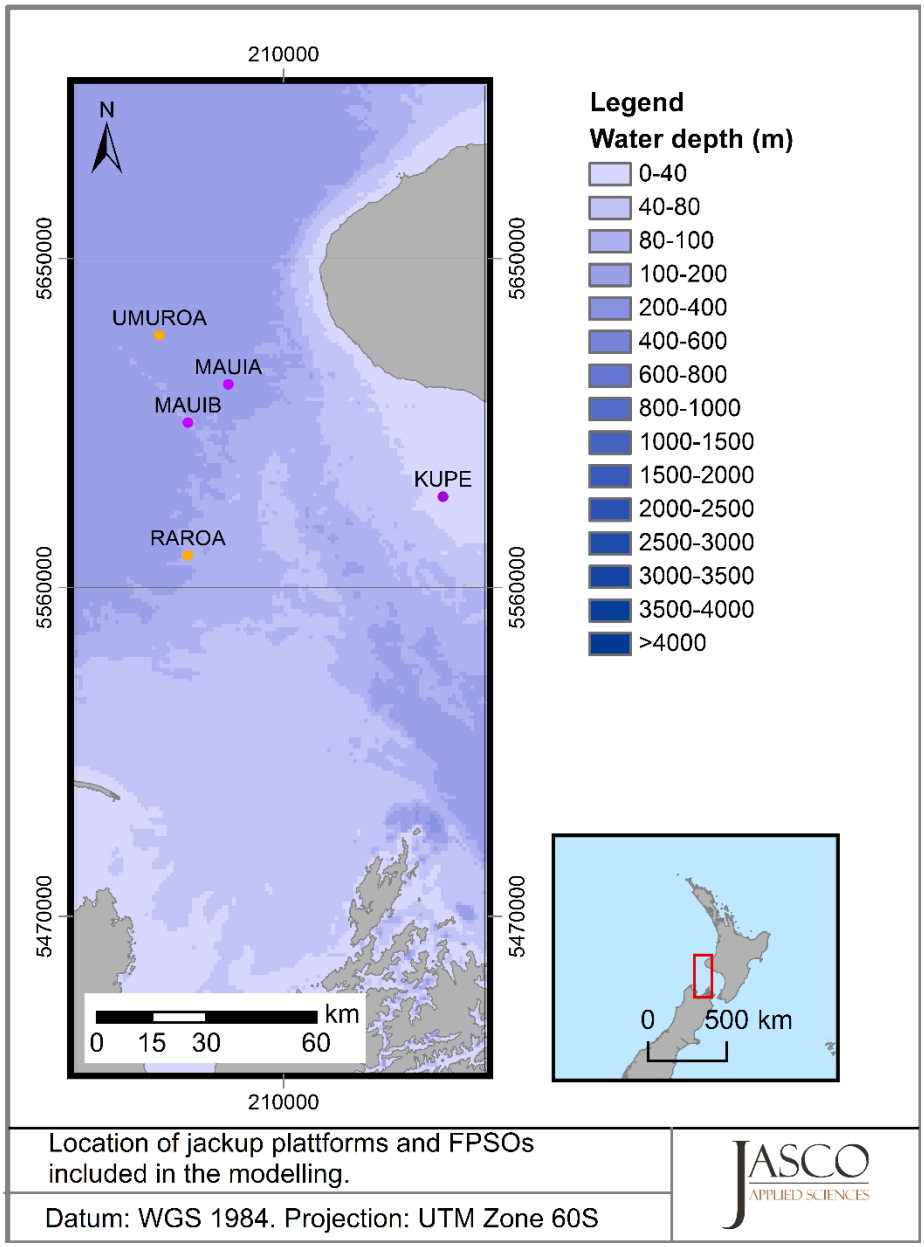

Figure C-2. Locations of the three jackup platforms (MAUIA, MAUIB, and KUPE) and two FPSOs (UMUROA and RAROA) considered in this study.

11. APPENDIX D VESSEL TRAFFIC DATA PRE-PROCESSING

Historical vessel tracking data for the study area, for year of 2014–2015 (excluding half of September), were obtained from the ExactEarth AIS datasets provided by MPI. The raw data consisted of time-stamped position reports as well as other relevant vessel information, such as Maritime Mobile Service Identity (MMSI), speed over ground, and heading. Vessel type was added according to the classification in Table C-1 for each vessel based on the MMSI. Since the AIS data contain temporal gaps, some inconsistent ship tracks, and outlier values, special filtering was applied to remove artefacts that would negatively affect the accuracy of the density/speed predictions. Specifically:

- Vessels with only one entry within any month were removed.
- For any given MMSI, AIS entries separated by more than 10 minutes were assigned separate tracks.

- Speed for all vessels is limited to be greater than 0 m/s, and lower than 20 m/s.
- Platforms and FPSOs on DP were assigned a speed of 0 m/s, and are assumed to be present at all times in the positions indicated in Figure C-2.
- The Polar Duke (MMSI 210582000) and the Aquila Explorer (MMSI 357767000) vessels used to conduct the Todd Energy Trestles 3-D and TGS Northwest Frontier Multiclient 2D MSS respectively, have a dual role in the model: first, they contribute to the transiting vessel noise under the Government/Research category. Second, seismic impulses were included in the modelling. The impulse locations for the Todd Energy Trestles 3-D survey were not provided in time to be included, and instead the vessel AIS track (excluding turns) was used along with the information in the Marine Mammal Impact Assessment (MMIA) (REM 2015) to approximate the impulse locations from the survey. TGS kindly provided track and impulse point data for their Northwest Frontier Multiclient 2-D MSS, also described in an MMIA (SLR Consulting NZ Limited 2014) and thus it was able to be modelled to accurately represent the survey.

12. APPENDIX E AIRGUN ARRAY ACOUSTIC SOURCE MODEL

E.1 Methods

The source levels and directivity of the two airgun arrays considered in this study were predicted with JASCO's Airgun Array Source Model (AASM). AASM includes low- and high-frequency modules for predicting different components of the airgun array spectrum. The low-frequency module is based on the physics of oscillation and radiation of airgun bubbles, as originally described by Ziolkowski (1970), that solves the set of parallel differential equations that govern bubble oscillations. Physical effects accounted for in the simulation include pressure interactions between airguns, port throttling, bubble damping, and generator-injector (GI) gun behaviour discussed by Dragoset (1984), Laws et al. (1990), and Landro (1992). A global optimisation algorithm tunes free parameters in the model to a large library of airgun source signatures.

Whilst airgun signatures are highly repeatable at the low frequencies, which are used for seismic imaging, their sound emissions have a large random component at higher frequencies that cannot be predicted deterministically. Therefore, the high-frequency module of AASM uses a stochastic simulation to predict the sound emissions of individual airguns above 800 Hz, using a multivariate statistical model. The current version of AASM has been tuned to fit a large library of high quality seismic source signature data obtained from the Joint Industry Program (JIP) on Sound and Marine Life (Mattsson & Jenkerson 2008). The stochastic model uses a Monte-Carlo simulation of the random component of the high-frequency spectrum of each airgun in an array. The mean high-frequency spectra from the stochastic model augments the low-frequency signatures from the physical model, allowing AASM to predict airgun source levels at frequencies up to 25 000 Hz.

AASM produces a set of "notional" signatures for each array element based on:

- Array layout
- Volume, tow depth, and firing pressure of each airgun
- Interactions between different airguns in the array

These notional signatures are the pressure waveforms of the individual airguns at a standard reference distance of 1 m; they account for the interactions with the other airguns in the array. The signatures are summed with the appropriate phase delays to obtain the far-field source signature of the entire array in all directions. This far-field array signature is filtered into 1/3-octave-bands to compute the source levels of the array as a function of frequency band and azimuthal angle in the horizontal plane (at the source depth), after which it is considered to be a directional point source in the far field.

A seismic array consists of many sources and the point-source assumption is invalid in the near field where the array elements add incoherently. The maximum extent of the near field of an array (R_{nf}) is:

$$R_{nf} < \frac{l^2}{4\lambda} \quad \text{E-1}$$

where λ is the sound wavelength and l is the longest dimension of the array (Lurton 2002, §5.2.4). For example, an airgun array length of $l = 21$ m yields a near-field range of 147 m at 2 kHz and 7 m at 100 Hz. Beyond this R_{nf} range, the array is assumed to radiate like a directional point source and is treated as such for propagation modelling.

The interactions between individual elements of the array create directionality in the overall acoustic emission. Generally, this directionality is prominent mainly at frequencies in the mid-range between tens of hertz to several hundred hertz. At lower frequencies, with acoustic wavelengths much larger than the inter-airgun separation distances, the directionality is small. At higher frequencies, the pattern of lobes is too finely spaced to be resolved and the effective directivity is less.

E.2 Acoustic Source Levels

Two seismic surveys were considered in summer: The Todd Energy Trestles 3-D MSS (3460 in^3 array) (REM 2015) and the TGS survey (4400 in^3 array) (SLR Consulting NZ Limited 2014). Figure E-1 and Figure E-2 show the broadside (perpendicular to the tow direction), endfire (parallel to the tow direction), and vertical overpressure signatures and corresponding power spectrum levels for the 3460 and 4400 in^3 arrays, respectively. The signatures consist of a strong primary peak, related to the initial release of high-pressure air, followed by a series of pulses associated with bubble oscillations. Most energy is produced at frequencies below 600 Hz. Frequency-dependent peaks and nulls in the spectrum result from interference among airguns in the array, and they correspond with the volumes and relative locations of the airguns to each other.

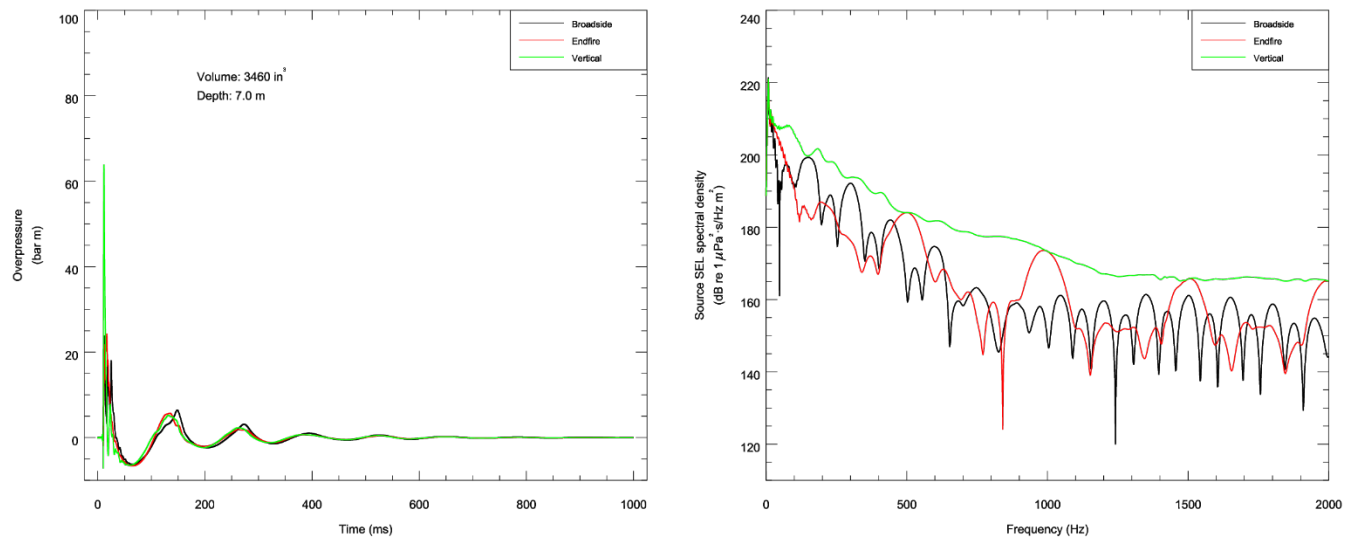

Figure E-1: Predicted source level details for the 3470 in^3 array towed at a depth of 7 m. (Left) the overpressure signature and (right) the power spectrum for broadside (perpendicular to tow direction) and endfire (directly aft of the array) direction, and for vertically down.

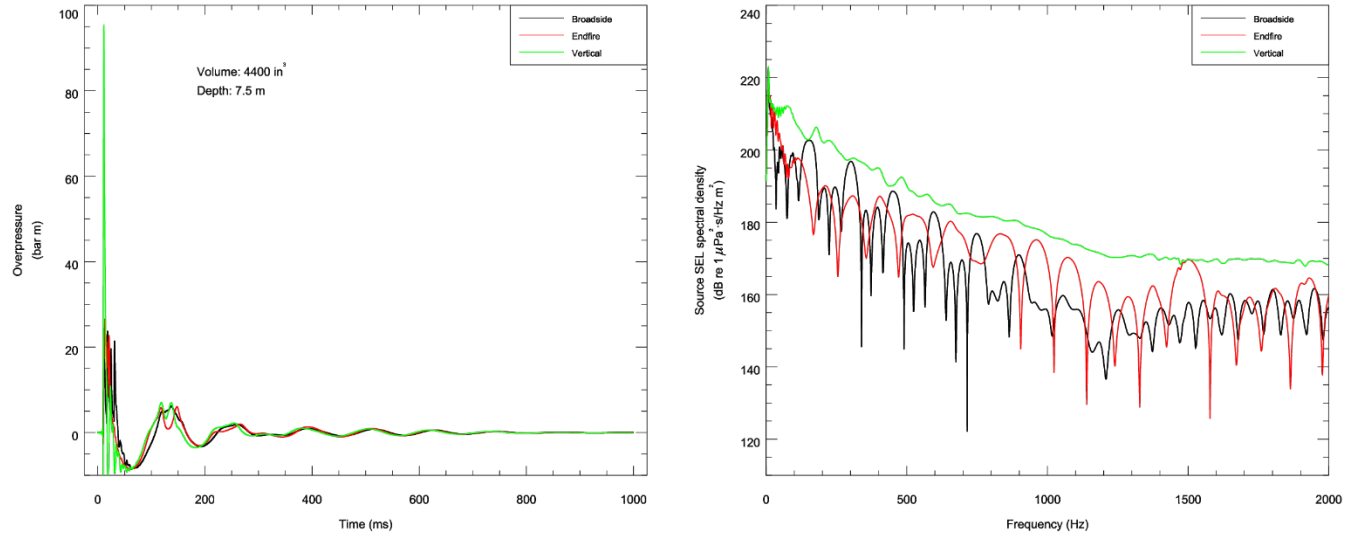

Figure E-2: Predicted source level details for the 4400 in^3 array towed at a depth of 7.5 m. (Left) the overpressure signature and (right) the power spectrum for broadside (perpendicular to tow direction) and endfire (directly aft of the array) directions, and for vertically down.

13. APPENDIX F TERMINOLOGY

F.1 Glossary

1/3-octave
One third of an octave. Note: A one-third octave is approximately equal to one decidecade (1/3 oct ≈ 1.003 ddec) (ISO 2017).

1/3-octave-band
Frequency band whose bandwidth is one one-third octave. Note: The bandwidth of a one-third octave-band increases with increasing centre frequency.

90%-energy time window
The time interval over which the cumulative energy rises from 5 to 95% of the total pulse energy. This interval contains 90% of the total pulse energy. Symbol: T_{90}.

90% sound pressure level (90% SPL)
The root-mean-square sound pressure levels calculated over the 90%-energy time window of a pulse. Used only for pulsed sounds.

A-weighting
Frequency-selective weighting for human hearing in air that is derived from the inverse of the idealized 40-phon equal loudness hearing function across frequencies.

absorption
The reduction of acoustic pressure amplitude due to acoustic particle motion energy converting to heat in the propagation medium.

acoustic impedance
The ratio of the sound pressure in a medium to the rate of alternating flow of the medium through a specified surface due to the sound wave.

AIS
Automatic Identification System is an automatic tracking system used on ships and by vessel traffic services

ambient noise
All-encompassing sound at a given place, usually a composite of sound from many sources near and far (ANSI S1.1-1994 R2004), e.g., shipping vessels, seismic activity, precipitation, sea ice movement, wave action, and biological activity.

attenuation
The gradual loss of acoustic energy from absorption and scattering as sound propagates through a medium.

audiogram
A graph of hearing threshold level (sound pressure levels) as a function of frequency, which describes the hearing sensitivity of an animal over its hearing range.

audiogram weighting
The process of applying an animal's audiogram to sound pressure levels to determine the sound level relative to the animal's hearing threshold (HT). Unit: dB re HT.

Auditory frequency weighting (auditory weighting function, frequency-weighting function)
The process of band-pass filtering sounds to reduce the importance of inaudible or less-audible frequencies for individual species or groups of species of aquatic mammals (ISO 2017). One example is M-weighting introduced by Southall et al. (2007) to describe "Generalized frequency weightings for various functional hearing groups of marine mammals, allowing for their functional bandwidths and appropriate in characterizing auditory effects of strong sounds".

azimuth
A horizontal angle relative to a reference direction, which is often magnetic north or the direction of travel. In navigation it is also called bearing.

background noise
Total of all sources of interference in a system used for the production, detection, measurement, or recording of a signal, independent of the presence of the signal (ANSI S1.1-1994 R2004). Ambient noise detected, measured, or recorded with a signal is part of the background noise.

bandwidth
The range of frequencies over which a sound occurs. Broadband refers to a source that produces sound over a broad range of frequencies (e.g., seismic airguns, vessels) whereas narrowband sources produce sounds over a narrow frequency range (e.g., sonar) (ANSI/ASA S1.13-2005 R2010).

bar
Unit of pressure equal to 100 kPa, which is approximately equal to the atmospheric pressure on Earth at sea level. 1 bar is equal to 10^5 Pa or 10^{11} µPa.

broadband sound level
The total sound pressure level measured over a specified frequency range. If the frequency range is unspecified, it refers to the entire measured frequency range.

broadside direction
Perpendicular to the travel direction of a source. Compare with endfire direction.

cavitation
A rapid formation and collapse of vapour cavities (i.e., bubbles or voids) in water, most often caused by a rapid change in pressure. Fast-spinning vessel propellers typically cause cavitation, which creates a lot of noise.

cetacean
Any animal in the order Cetacea. These are aquatic, mostly marine mammals and include whales, dolphins, and porpoises.

continuous sound
A sound whose sound pressure level remains above ambient sound during the observation period (ANSI/ASA S1.13-2005 R2010). A sound that gradually varies in intensity with time, for example, sound from a marine vessel.

critical ratio
The difference between the sound pressure level of a masked tone, which is barely audible, and the spectrum level of the background noise at similar frequencies. Unit: decibel (dB).

critical band
The auditory bandwidth within which background noise strongly contributes to masking of a single tone. Unit: hertz (Hz).

decade
Logarithmic frequency interval whose upper bound is ten times larger than its lower bound (ISO 2006).

decidecade
One tenth of a decade (ISO 2017). Note: An alternative name for decidecade (symbol ddec) is "one-tenth decade". A decidecade is approximately equal to one third of an octave (1 ddec ≈ 0.3322 oct) and for this reason is sometimes referred to as a "one-third octave".

decidecade band
Frequency band whose bandwidth is one decidecade. Note: The bandwidth of a decidecade band increases with increasing centre frequency.

decibel (dB)
One-tenth of a bel. Unit of level when the base of the logarithm is the tenth root of ten, and the quantities concerned are proportional to power (ANSI S1.1-1994 R2004).

dynamic positioning
A computer-controlled system to automatically maintain a vessel's position and heading through the use of its own propellers and thrusters.

endfire direction
Parallel to the travel direction of a source. See also broadside direction.

ensonified
Exposed to sound.

equivalent level
SPL can also be referred to as L_{eq}, which stands for 'equivalent level'. It is equal to the component of time averaged sound intensity.

far-field
The zone where, to an observer, sound originating from an array of sources (or a spatially-distributed source) appears to radiate from a single point. The distance to the acoustic far-field increases with frequency.

frequency
The rate of oscillation of a periodic function measured in cycles-per-unit-time. The reciprocal of the period. Unit: hertz (Hz). Symbol: *f*. 1 Hz is equal to 1 cycle per second.

hearing group
Groups of marine mammal species with similar hearing ranges. Commonly defined functional hearing groups include low-, mid-, and high-frequency cetaceans, pinnipeds in water, and pinnipeds in air.

geoacoustic
Relating to the acoustic properties of the seabed.

harmonic
A sinusoidal sound component that has a frequency that is an integer multiple of the frequency of a sound to which it is related. For example, the second harmonic of a sound has a frequency that is double the fundamental frequency of the sound.

hearing threshold
The sound pressure level for any frequency of the hearing group that is barely audible for a given individual in the absence of significant background noise during a specific percentage of experimental trials.

hertz (Hz)
A unit of frequency defined as one cycle per second.

high-frequency cetacean (HFC)
The functional cetacean hearing group that represents those odontocetes (toothed whales) specialized for high-frequency hearing.

hydrophone
An underwater sound pressure transducer. A passive electronic device for recording or listening to underwater sound.

intermittent sound
A level of sound that abruptly drops to the background noise level several times during the observation period.

impulsive sound
Sound that is typically brief and intermittent with rapid (within a few seconds) rise time and decay back to ambient levels (NOAA 2013, ANSI S12.7-1986 R2006). For example, seismic airguns and impact pile driving.

low-frequency cetacean (LFC)
The functional cetacean hearing group that represents mysticetes (baleen whales) specialized for low-frequency hearing.

masking
Obscuring of sounds of interest by sounds at similar frequencies.

mean-square sound pressure spectral density
Distribution as a function of frequency of the mean-square sound pressure per unit bandwidth (usually 1 Hz) of a sound having a continuous spectrum (ANSI S1.1-1994 R2004). Unit: $\mu Pa^2/Hz$.

median
The 50th percentile of a statistical distribution.

mid-frequency cetacean (MFC)
The functional cetacean hearing group that represents those odontocetes (toothed whales) specialized for mid-frequency hearing.

MMSI
Maritime Mobile Service Identity is a series of nine digits which uniquely identify ship stations, ship earth stations, coast stations, coast earth stations, and group calls.

mysticete
Mysticeti, a suborder of cetaceans, use their baleen plates, rather than teeth, to filter food from water. They are not known to echolocate, but they use sound for communication. Members of this group include rorquals (Balaenopteridae), right whales (Balaenidae), and grey whales (*Eschrichtius robustus*).

non-impulsive sound
Sound that is broadband, narrowband or tonal, brief or prolonged, continuous or intermittent, and typically does not have a high peak pressure with rapid rise time (typically only small fluctuations in decibel level) that impulsive signals have (ANSI/ASA S3.20-1995 R2008). For example, marine vessels, aircraft, machinery, construction, and vibratory pile driving (NIOSH 1998, NOAA 2015).

octave
The interval between a sound and another sound with double or half the frequency. For example, one octave above 200 Hz is 400 Hz, and one octave below 200 Hz is 100 Hz.

odontocete
The presence of teeth, rather than baleen, characterizes these whales. Members of the Odontoceti are a suborder of cetaceans, a group comprised of whales, dolphins, and porpoises. The skulls of toothed whales are mostly asymmetric, an adaptation for their echolocation. This group includes sperm whales, killer whales, belugas, narwhals, dolphins, and porpoises.

otariid
A common term used to describe members of the Otariidae, eared seals, commonly called sea lions and fur seals. Otariids are adapted to a semi-aquatic life; they use their large fore flippers for propulsion. Their ears distinguish them from phocids. Otariids are one of the three main groups in the superfamily Pinnipedia; the other two groups are phocids and walrus.

otariid pinnipeds in water (OPW)
The functional pinniped hearing group that represents eared seals under water.

pairwise *t*-test
A statistical procedure used to determine whether the means of different groups of observations are different, with corrections for multiple testing.

parabolic equation method
A computationally-efficient solution to the acoustic wave equation that is used to model transmission loss. The parabolic equation approximation omits effects of back-scattered sound, simplifying the computation of transmission loss. The effect of back-scattered sound is negligible for most ocean-acoustic propagation problems.

peak pressure level (PK)
The maximum instantaneous sound pressure level, in a stated frequency band, within a stated period. Also called zero-to-peak pressure level. Unit: decibel (dB).

peak-to-peak pressure level (PK-PK)
The difference between the maximum and minimum instantaneous pressure levels. Unit: decibel (dB).

percentile level, exceedance
The sound level exceeded *n*% of the time during a measurement.

permanent threshold shift (PTS)
A permanent loss of hearing sensitivity caused by excessive noise exposure. PTS is considered auditory injury.

phocid
A common term used to describe all members of the family Phocidae. These true/earless seals are more adapted to in-water life than are otariids, which have more terrestrial adaptations. Phocids use their hind flippers to propel themselves. Phocids are one of the three main groups in the superfamily Pinnipedia; the other two groups are otariids and walrus.

phocid pinnipeds in water (PPW)
The functional pinniped hearing group that represents true/earless seals under water.

pinniped
A common term used to describe all three groups that form the superfamily Pinnipedia: phocids (true seals or earless seals), otariids (eared seals or fur seals and sea lions), and walrus.

point source
A source that radiates sound as if from a single point (ANSI S1.1-1994 R2004).

power spectrum density
Generic term, formally defined as power in W/Hz, but sometimes loosely used to refer to the spectral density of other parameters such as square pressure or time-integrated square pressure.

pressure, acoustic
The deviation from the ambient hydrostatic pressure caused by a sound wave. Also called overpressure. Unit: pascal (Pa). Symbol: *p*.

pressure, hydrostatic
The pressure at any given depth in a static liquid that is the result of the weight of the liquid acting on a unit area at that depth, plus any pressure acting on the surface of the liquid. Unit: pascal (Pa).

received level (RL)
The sound level measured (or that would be measured) at a defined location.

rms
root-mean-square.

signature
Pressure signal generated by a source.

sound
A time-varying pressure disturbance generated by mechanical vibration waves travelling through a fluid medium such as air or water.

sound exposure
Time integral of squared, instantaneous frequency-weighted sound pressure over a stated time interval or event. Unit: pascal-squared second ($Pa^2 \cdot s$) (ANSI S1.1-1994 R2004).

sound exposure level (SEL)
A cumulative measure related to the sound energy in one or more pulses. Unit: dB re 1 $\mu Pa^2 \cdot s$. SEL is expressed over the summation period (e.g., per-pulse SEL [for airguns], single-strike SEL [for pile drivers], 24-hour SEL).

sound exposure spectral density
Distribution as a function of frequency of the time-integrated squared sound pressure per unit bandwidth of a sound having a continuous spectrum (ANSI S1.1-1994 R2004). Unit: $\mu Pa^2 \cdot s/Hz$.

sound field
Region containing sound waves (ANSI S1.1-1994 R2004).

sound intensity
Sound energy flowing through a unit area perpendicular to the direction of propagation per unit time.

sound pressure level (SPL)
The decibel ratio of the time-mean-square sound pressure, in a stated frequency band, to the square of the reference sound pressure (ANSI S1.1-1994 R2004).

For sound in water, the reference sound pressure is one micropascal (p_0 = 1 µPa) and the unit for SPL is dB re 1 µPa^2:

$$L_p = 10 \log_{10}(p^2/p_0^2) = 20 \log_{10}(p/p_0)$$

Unless otherwise stated, SPL refers to the root-mean-square (rms) pressure level. See also 90% sound pressure level and fast-average sound pressure level. Non-rectangular time window functions may be applied during calculation of the rms value, in which case the SPL unit should identify the window type.

sound speed profile
The speed of sound in the water column as a function of depth below the water surface.

source level (SL)
The sound level measured in the far-field and scaled back to a standard reference distance of 1 metre from the acoustic centre of the source. Unit: dB re 1 µPa·m (pressure level) or dB re 1 µPa^2·s·m (exposure level).

spectral density level
The decibel level (10·log$_{10}$) of the spectral density of a given parameter such as SPL or SEL, for which the units are dB re 1 µPa^2/Hz and dB re 1 µPa^2·s/Hz, respectively.

spectrogram
A visual representation of acoustic amplitude compared with time and frequency.

spectrum
An acoustic signal represented in terms of its power, energy, mean-square sound pressure, or sound exposure distribution with frequency.

surface duct
The upper portion of a water column within which the sound speed profile gradient causes sound to refract upward and therefore reflect off the surface resulting in relatively long-range sound propagation with little loss.

temporary threshold shift (TTS)
Temporary loss of hearing sensitivity caused by excessive noise exposure.

thermocline
The depth interval near the ocean surface that experiences temperature gradients due to warming or cooling by heat conduction from the atmosphere and by warming from solar heating.

transmission loss (TL)
The decibel reduction in sound level between two stated points that results from sound spreading away from an acoustic source subject to the influence of the surrounding environment. Also referred to as propagation loss.

underwater listening station (ULS)
A real-time cabled acoustic observatory situated off the coast of British Columbia (Canada), that is operated by JASCO Applied Sciences and Ocean Networks Canada for the Vancouver Fraser Port Authority's Enhancing Cetacean Habitat and Observation (ECHO) Program.

wavelength
Distance over which a wave completes one cycle of oscillation. Unit: metre (m). Symbol: λ.

F.2 Acoustic Metrics

Underwater sound pressure amplitude is measured in decibels (dB) relative to a fixed reference pressure of $p_0 = 1$ µPa. Because the perceived loudness of sound, especially impulsive noise such as from seismic airguns, pile driving, and sonar, is not generally proportional to the instantaneous acoustic pressure, several sound level metrics are commonly used to evaluate noise and its effects on marine life. We provide specific definitions of relevant metrics used in the accompanying report. Where possible we follow the ANSI and ISO standard definitions and symbols for sound metrics, but these standards are not always consistent.

The zero-to-peak sound pressure level (PK; L_{pk}; $L_{p,pk}$; dB re 1 µPa), is the maximum instantaneous sound pressure level in a stated frequency band attained by an acoustic pressure signal, $p(t)$:

$$L_{p,pk} = 20\log_{10}\left[\frac{\max\left(\left|p(t)\right|\right)}{p_0}\right] \quad \text{(F-1)}$$

PK is often included as a criterion for assessing whether a sound is potentially injurious; however, because it does not account for the duration of a noise event, it is generally a poor indicator of perceived loudness.

The peak-to-peak sound pressure level (PK-PK; $L_{pk\text{-}pk}$; $L_{p,pk\text{-}pk}$; dB re 1 µPa) is the difference between the maximum and minimum instantaneous sound pressure levels in a stated frequency band attained by an impulsive sound, $p(t)$:

$$L_{p,pk-pk} = 10\log_{10}\left\{\frac{\left[\max\left(p(t)\right) - \min\left(p(t)\right)\right]^2}{p_0^2}\right\} \quad \text{(F-2)}$$

The sound pressure level (SPL; L_p; dB re 1 µPa) is the root-mean-square (rms) pressure level in a stated frequency band over a specified time window (T, s) containing the acoustic event of interest. It is important to note that SPL always refers to an rms pressure level and therefore not instantaneous pressure:

$$L_p = 10\log_{10}\left(\frac{1}{T}\int_T p^2(t)dt \Big/ p_0^2\right) \quad \text{(F-3)}$$

where $g(t)$ is an optional time weighting function. The SPL represents a nominal effective continuous sound over the duration of an acoustic event, such as the emission of one acoustic pulse, a marine mammal vocalisation, the passage of a vessel, or over a fixed duration. Because the window length, T, is the divisor, events with similar sound exposure level (SEL) but more spread out in time have a lower SPL. SPL can also be referred to as L_{eq}, which stands for 'equivalent level'.

In studies of impulsive noise, the time window function $g(t)$ is often a decaying exponential that emphasizes more recent pressure signals to mimic the leaky integration of the mammalian hearing system. For example, human-based fast time weighting applies an exponential function with time constant 125 ms. Another approach for evaluating L_p of impulsive signals is to set T to the "90% time window" (T_{90}): the period over which cumulative square pressure function passes between 5% and 95% of its full per-pulse value. The SPL computed over this T_{90} interval is commonly called the 90% SPL (SPL(T_{90}); L_{p90}; dB re 1 µPa):

$$L_{p90} = 10\log_{10}\left(\frac{1}{T_{90}}\int_{T_{90}} p^2(t)dt \Big/ p_0^2\right) \quad \text{(F-4)}$$

The sound exposure level (SEL; L_E; $L_{E,p}$; dB re 1 µPa^2·s) is a measure related to the acoustic energy contained in one or more acoustic events (N). The SEL for a single event is computed from the time-integral of the squared pressure over the full event duration (T):

$$L_E = 10\log_{10}\left(\int_T p^2(t)dt \Big/ T_0 p_0^2\right) \quad \text{(F-5)}$$

where T_0 is a reference time interval of 1 s. The SEL continues to increase with time when non-zero pressure signals are present. It therefore can be construed as a dose-type measurement, so the integration time used must be carefully considered in terms of relevance for impact to the exposed recipients.

SEL can be calculated over periods with multiple acoustic events or over a fixed duration. For a fixed duration, the square pressure is integrated over the duration of interest. For multiple events, the SEL can be computed by summing (in linear units) the SEL of the N individual events:

$$L_{E,N} = 10\log_{10}\left(\sum_{i=1}^{N} 10^{\frac{L_{E,i}}{10}}\right). \quad \text{(F-6)}$$

Energy equivalent SPL (dB re 1 µPa) denotes the SPL of a stationary (constant amplitude) sound that generates the same SEL as the signal being examined, $p(t)$, over the same period of time, T:

$$L_{eq} = 10\log_{10}\left(\frac{1}{T}\int_T p^2(t)dt \Big/ p_0^2\right). \quad \text{(F-7)}$$

The equations for SPL and the energy-equivalent SPL are numerically identical; conceptually, the difference between the two metrics is that the former is typically computed over short periods (typically of one second or less) and tracks the fluctuations of a non-steady acoustic signal, whereas the latter reflects the average SPL of an acoustic signal over times typically of one minute to several hours.

If applied, the frequency weighting of an acoustic event should be specified, as in the case of weighted SEL (e.g., $L_{E,LFC,24h}$; Appendix F-3). The use of fast, slow, or impulse exponential-time-averaging or other time-related characteristics should otherwise be specified.

F.3 Marine Mammal Frequency Weighting Functions

In 2015, a U.S. Navy technical report by Finneran (2015) recommended new auditory weighting functions for cetaceans and marine carnivores. The overall shape of the auditory weighting functions is similar to human A-weighting functions, which follows the sensitivity of the human ear at low sound levels. The new frequency-weighting function is expressed as:

$$G(f) = K + 10\log_{10}\left[\left(\frac{(f/f_{lo})^{2a}}{\left[1+(f/f_{lo})^2\right]^a\left[1+(f/f_{hi})^2\right]^b}\right)\right] \quad \text{(F-8)}$$

Finneran (2015) proposed five functional hearing groups for marine mammals in water: low-, mid-, and high-frequency cetaceans, phocid pinnipeds, and otariid pinnipeds. The parameters for these frequency-weighting functions were further modified the following year (Finneran 2016) and were adopted in NOAA's technical guidance that assesses noise impacts on marine mammals (NMFS 2018). Table F-1 lists the frequency-weighting parameters for each hearing group; Figure F-1 shows the resulting frequency-weighting curves.

Table F-1: Parameters for the auditory weighting functions recommended by NMFS (2018).

Hearing group	A	b	f_{lo} (Hz)	f_{hi} (kHz)	K (dB)
Low-frequency cetaceans	1.0	2	200	19 000	0.13
Mid-frequency cetaceans	1.6	2	8 800	110 000	1.20
High-frequency cetaceans	1.8	2	12 000	140 000	1.36
Phocid pinnipeds in water	1.0	2	1 900	30 000	0.75
Otariid pinnipeds in water	2.0	2	940	25 000	0.64

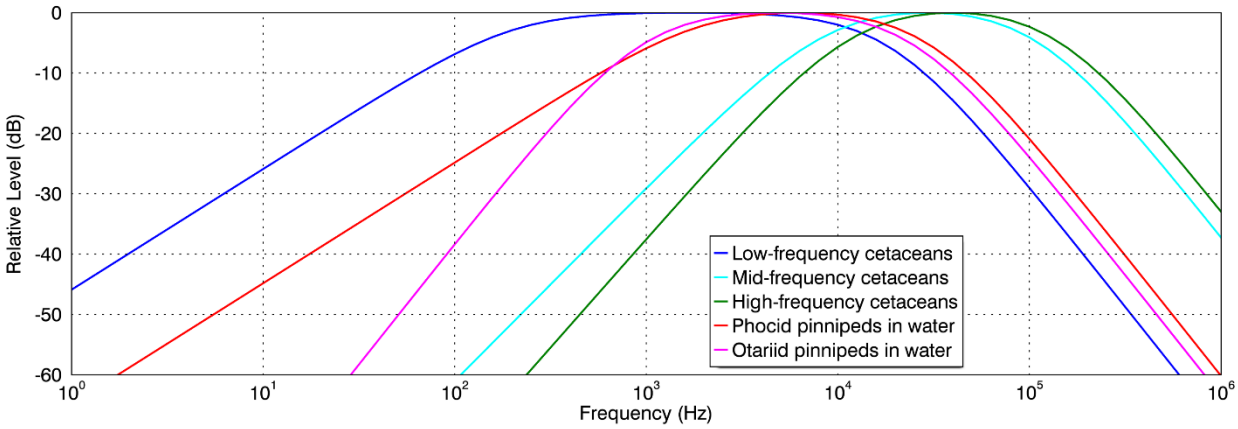

Figure F-1: Auditory weighting functions for functional marine mammal hearing groups as recommended by NMFS (2018).

14. APPENDIX G DATA STORAGE

Data for storage and in addition to what is presented in this report has been supplied to the Ministry as downloaded compressed files for each of the following categories. All files have been named in accordance with the terminology used in the report.

Vessel density and speed grid maps for the periods of full year, summer and winter have been supplied as image files (.png). The file naming format includes:

- The type of map: either 'avg_speed' for speed grid maps or 'sum_dur' for density (summed duration),
- The resolution of the modelling grid: 3000 m,
- The period of interest: FullYear, Summer[Nov-Apr] or Winter[May-Oct]
- The vessel category as listed in Table C-1.
- Examples are:
    - For average speed over a full year for bulker category vessels: avg_speed_3000m_FullYear_Bulker.png
    - For density over a full year for bulker category vessels: avg_speed_3000m_FullYear_Bulker.png

Animations of the SPL and HF-weighted SPL snapshots for the months of March and July are provided as movie files (.mp4). These are provided in two resolutions. The file names are:

- March HFC Weighted low-resolution.mp4
- March HFC Weighted.mp4
- March Unweighted low-resolution.mp4
- March Unweighted.mp4
- July HFC Weighted low-resolution.mp4
- July HFC Weighted.mp4
- July Unweighted low-resolution.mp4
- July Unweighted.mp4

Sound levels at each modelled receiver location are provided as comma separated value files (.csv). These files contain the per-minute sound levels at each receiver location.

- RLvsTime_March_Broadband
- RLvsTime_March_HFC
- RLvsTime_July_Broadband
- RLvsTime_July_HFC

Georeferenced tiff files representing Figures 9–12 are also provided.